INÊS BEATRIZ CASTRO MAIA

OPTIMIZATION OF *EMILIANIA HUXLEYI* GROWTH FOR PRODUCTION OF *n*-3 POLYUNSATURATED FATTY ACIDS AND NOVEL COMPOUNDS WITH OSTEOGENIC ACTIVITY

UAlg FCT
UNIVERSIDADE DO ALGARVE
FACULDADE DE CIÊNCIAS E TECNOLOGIA

2019

INÊS BEATRIZ CASTRO MAIA

OPTIMIZATION OF *EMILIANIA HUXLEYI* GROWTH FOR PRODUCTION OF *n*-3 POLYUNSATURATED FATTY ACIDS AND NOVEL COMPOUNDS WITH OSTEOGENIC ACTIVITY

Mestrado em Biologia Molecular e Microbiana

Trabalho efetuado sob a orientação de:

Professor Doutor João Carlos Serafim Varela

Professora Doutora Luísa Paula Viola Afonso Barreira

2019

Optimization of *Emiliania huxleyi* growth for production of *n*-3 polyunsaturated fatty acids and novel compounds with osteogenic activity.

Declaração de autoria de trabalho

Declaro ser a autora deste trabalho, que é original e inédito. Autores e trabalhos consultados estão devidamente citados no texto e constam da listagem de referências incluída.

ACKNOWLEDGEMENTS

Ao professor João Varela e à professora Luísa Barreira, um muito obrigado por esta oportunidade, por toda a confiança que colocaram em mim e por toda a disponibilidade durante este ano. Sinto-me realmente sortuda.

Ainda ao professor João Varela, por dizer sempre que Sim sempre que lhe bato à porta, várias vezes ao dia, pela (muita) paciência e por todo o excelente trabalho.

Ao Dr. João Navalho da empresa Necton S.A. pela oportunidade, pela confiança e por toda a ajuda e orientação durante o desenvolvimento desta tese.

Ao Hugo, por todo o apoio e ajuda durante este (longo) ano. Por toda a disponibilidade e capacidade de "apaga fogos". Por ter aturado todos os mini ataques de pânico, crises existenciais e stresses que, afinal, não tinham razão de ser. Mas já está mesmo quase a acabar!

À Tamára, por toda a ajuda e tudo o que me ensinou durante este ano. Por se dividir em mil e estar lá sempre para ensinar e para mandar vir quando é preciso, pelos dias bons e pelos de mau humor que depois até passam com a minha simpatia.

A toda a equipa da Necton S.A., em especial à Ana e à Inês, por tudo o que me ensinaram e ainda vão ensinar, por estarem lá para me animarem e me darem alguma perspetiva quando as coisas correram menos bem e por se rirem comigo quando correram muito bem. Mas, principalmente, pela amizade. Essa, levo-a comigo.

Ao grupo BIOSKEL, em especial ao Marco, pela transferência de conhecimento, pela ajuda e paciência no desenvolvimento do trabalho experimental com os peixe-zebra.

Aos meus colegas do grupo MarBiotech, pela amizade, pela ajuda, pela companhia e pelas longas horas. E à Marta porque, afinal, somos o turno da noite!

À Tânia e ao João, pela excelente amizade, pela ajuda, pela paciência… por tudo na verdade! Estamos os três no mesmo barco.

Aos meus amigos, os antigos e os novos que fiz pelo caminho. Por estarem sempre presentes, por todos os momentos e apoio, não só agora, mas sempre.

Ao Bruno, pela imensa paciência com o meu cansaço e mau humor, por todo o carinho e pelas palavras certas nos momentos certos. Por me fazer rir quando estava mesmo a precisar. Por tudo.

E, por último, aos meus pais e à minha irmã. Por todo o esforço que fizeram para eu chegar até aqui. Por todo o gigante e incansável apoio, por acreditarem sempre em mim até mesmo quando eu não acreditei.

Esta tese não é só minha, mas é um bocadinho de cada um de vocês.

Um gigante e sincero Obrigada.

RESUMO

Emiliania huxleyi é uma das mais abundantes espécies de cocolitoforídeos (*Haptophyta*) e é responsável por vastos *blooms* em todo o mundo, sendo até visíveis do espaço. A abundância de *E. huxleyi* nos oceanos sugere fortemente que é uma microalga promissora para a produção industrial de larga escala, com possíveis aplicações biotecnológicas. A sua capacidade de calcificação, devido à produção de placas de calcite, sugere ainda que poderá ser usada para estudos de acidificação dos oceanos, com potencial para mitigação de CO_2.

E. huxleyi é um organismo unicelular com um reduzido tamanho (4-6 µm) que produz cocólitos em vesículas intracelulares especializadas. Possui também um ciclo de vida haplo-diplonte complexo, com 3 tipos celulares diferentes: células portadoras de cocólitos (células C diploides), células nuas não-móveis (células N) e células móveis portadores de escamas (células S haploides). Os diferentes tipos celulares podem ser induzidos durante o ciclo de vida, levando à diferenciação celular. O ciclo de vida haplo-diplonte tem também um papel muito importante para a sobrevivência da espécie.

Esta espécie possui várias caraterísticas com interesse biotecnológico, devido à síntese de ácidos gordos polinsaturados de elevado valor comercial e à produção de pigmentos que poderão servir como substitutos de colorantes artificiais. Além disso, *E. huxleyi* possui ainda uma caraterística diferente de outras espécies de microalgas mais produzidas industrialmente, que é a produção de cocólitos formados por $CaCO_3$. Estes cocólitos demonstram também grande potencial, com aplicações em nanotecnologia ou ainda como substitutos à calcite industrial. A produção de $CaCO_3$ sugere ainda a presença de compostos com atividade osteogénica.

Sete estirpes de *E. huxleyi* foram adquiridas, procedendo-se ao seu crescimento sob condições controladas. Das sete estirpes, a estirpe RCC1250 foi a selecionada, uma vez que foi a que respondeu melhor às condições de *scale-up*. Fatores abióticos importantes – meio de cultura, temperatura e intensidade luminosa – foram otimizados para a estirpe *E. huxleyi* RCC1250 através do uso de fotobiorreatores de escala laboratorial Algem®. Cada ensaio teve a duração de 11 dias, com a monitorização das culturas a cada 2 dias, que incluía: contagens celulares, fluorometria, determinação da concentração de NO_3^- e observações microscópicas. O desempenho de crescimento foi

superior usando Nutribloom® como meio de cultura, quando comparado com o crescimento observado com o meio de cultura K/2, que é considerado o meio de cultura "standard" para esta espécie. A concentração de NO_3^- também mostrou ser crucial para o crescimento, em que o meio de cultura a uma concentração de NO_3^- de 0.6 mM demonstrou ser inibitório, numa fase inicial do crescimento. Com este ensaio, ficou definido que o meio de cultura Nutribloom® a uma concentração de 0.3 mM de NO_3^- seria adicionado no dia 0 e, quando a cultura atingisse uma densidade ótica de 1, esta concentração seria aumentada para 0.6 mM, com adição de meio de cultura a cada 2 dias. A temperatura ótima de crescimento correspondeu a 23 ºC, mas também houve crescimento aos 26 ºC, mostrando um certo nível de adaptação a temperaturas mais altas, o que será vantajoso para uma produção industrial no sul de Portugal. Determinou-se também que 900 µmol fotões/m^2/s corresponde à intensidade luminosa ótima em termos de densidade de fluxo de fotões. Foi ainda possível verificar a inibição da fotossíntese em culturas expostas a intensidades luminosas superiores a 1000 µmol fotões/m^2/s. As condições "standard" (meio de cultura K/2 a uma concentração de NO_3^- de 0.3 mM, posteriormente aumentada para 0.6 mM, 17 ºC e 1219 µmol fotões/m^2/s) foram também comparadas com as condições otimizadas (meio de cultura Nutribloom® a uma concentração de NO_3^- de 0.3 mM, posteriormente aumentada para 0.6 mM, 23 ºC e 900 µmol fotões/m^2/s), resultando num aumento de crescimento significativo. No final dos ensaios nos fotobiorreatores Algem®, a biomassa foi recolhida por centrifugação e liofilizada para a determinação da composição bioquímica de *E. huxleyi*. Determinou-se também o conteúdo proteico e de pigmentos, a percentagem de lípidos totais e o perfil de ácidos gordos.

A biomassa produzida sob as condições standard continha elevadas quantidades de ácidos gordos saturados e monoinsaturados, nomeadamente os ácidos gordos mirístico, palmítico e oleico. No entanto, a biomassa produzida sob as condições otimizadas continha elevadas quantidades de ácidos gordos polinsaturados (PUFA), nomeadamente os ácidos octadecatetrenóico (OTA) e docosahexenóico (DHA), que são conhecidos pelo seu elevado valor comercial. Aumentaram ainda a produção dos PUFAs anteriores em 4 e 5 vezes, respetivamente. O conteúdo proteico foi também significativamente superior nas culturas expostas às condições otimizadas. Elevadas quantidades de 19'-hexanoilofucoxantina e fucoxantina foram também obtidas sob condições otimizadas, com um aumento de 3 e 2 vezes, respetivamente. O potencial osteogénico de vários extratos de *E. huxleyi* (etanol, acetato de etilo e água) foi avaliado em larvas de peixe-

zebra (*Danio rerio*) com 3 dias pós-fertilização, expostas por 3 dias a várias concentrações de cada extrato. Os extratos testados não afetaram a área da cabeça das larvas, sendo este o parâmetro usado para a correção da área do opérculo. Análises morfométricas das larvas coloradas com *alizarin-red* revelaram que o extrato etanólico a 10 µg/mL e 1 µg/mL aumentaram, respetivamente, a área do opérculo em 20 e 11% sobre o controlo (o primeiro tão alto quanto o controlo positivo). A aplicação do extrato de acetato de etilo também levou a um aumento do opérculo em 12% a 100 µg/mL, enquanto o extrato de água não demonstrou nenhum efeito significativo no crescimento do osso. Este ensaio mostrou a presença de compostos pro-osteogénicos, com potencial para desenvolvimento de um novo fármaco.

Em conclusão, o presente estudo revelou uma nova perspetiva no impacto dos fatores abióticos no crescimento de *E. huxleyi* RCC1250. O meio de cultura e a sua concentração de NO_3^- demonstrou ter um papel fundamental no crescimento desta estirpe, assim como a temperatura e a intensidade luminosa. A otimização destes parâmetros levou também a um aumento significativo na produção de compostos de elevado valor comercial, como PUFAs *n*-3, fucoxantina e 19'-hexanoilofucoxantina. Deste modo, este trabalho não só permitiu o estabelecimento de um novo protocolo para o melhoramento do crescimento de *E. huxleyi*, mas também mostrou o seu potencial como uma fonte de compostos de elevado valor comercial e de importantes metabolitos secundários com atividade osteogénica na biomassa produzida.

Palavras-chave:
Microalga marinha; *Emiliania huxleyi*; fotobioreatores Algem®; atividade osteogénica; *Danio rerio*.

ABSTRACT

Emiliania huxleyi is one of the most abundant species of coccolithophores (*Haptophyta*) and is responsible for extensive blooms worldwide. The widespread abundance of *E. huxleyi* suggests that it may be a promising species for industrial production with high potential for biotechnological applications. Important abiotic factors – culture media, temperature and light intensity – were optimized for *E. huxleyi* RCC1250 using lab-scale Algem® photobioreactors. Growth performance was higher using Nutribloom® as culture medium as compared to K/2, which is the considered to be the "standard" medium for this species. Optimal temperature and light intensity were, respectively, 23ºC and 900 µmol photons/m^2/s in Nutribloom® growth medium. The biomass produced contained high amounts of polyunsaturated fatty acids (PUFA), in particular octadecatetraenoic (OTA) and docosahexaenoic acids (DHA), which are known to have high market value. Optimized conditions increased the production of these PUFAs by 5- and 4-fold, respectively. High amounts of 19'-hexanoyloxyfucoxanthin and fucoxanthin were also achieved under optimized conditions with an increase of 2- and 3-fold. The osteogenic potential of several *E. huxleyi* extracts (i.e., ethanol, ethyl acetate and water) was assessed in zebrafish (*Danio rerio*) larvae at 3 days post-fertilization exposed for 3 days to a range of concentrations of each extract. Morphometric analysis of alizarin red-stained larvae revealed that the ethanolic extract at 10 µg/mL and 1 µg/mL increased, respectively, the operculum area by 20 and 11% over the control (the former as high as the positive control). Ethyl acetate extract also induced an operculum increase of 12% at 100 µg/mL, whereas water extract did not show any significant effect on bone growth. In conclusion, this work has not only established a new protocol to improve *E. huxleyi* growth performance but has shown the presence of high-value compounds and important secondary metabolites with osteogenic activity in the produced biomass.

Keywords:

Marine microalgae; *Emiliania huxleyi*; Algem® photobioreactors; osteogenic activity; *Danio rerio*.

INDEX

INDEX - FIGURES

INDEX - TABLES

GLOSSARY

A_0 – Area above the fluorescence curve between F_0 and F_m

AA – Amino acids

AL – Actinic light

ALA – α-linolenic

CC – Cellular concentration

CCHO – Carbohydrates

CP – Coccolith polysaccharide

*d*CHO – Dissolved carbohydrates

*p*CHO – Particulate carbohydrates

DHA – Docosahexaenoic acid

DIC – Dissolved inorganic carbon

dpf – Days post-fertilization

DOC – Dissolved organic carbon

DW – Dry weight

EA – Ethyl acetate

EPA – Eicosapentaenoic acid

E_{PAR} – Photosynthetically active radiation

FA – Fatty acids

FAME – Fatty acid methyl esters

F_m – Maximum fluorescence

F_0 – Basal fluorescence

hpf – Hours post-fertilization

LA – Linoleic acid

LC – Light-response curves

L:D – light:dark

LEDs – Light-emitted diodes

LOD – Limit of detection

LOQ – Limit of quantification

ML – Measuring light

MUFA – Monounsaturated fatty acid

n.a. – Not available

n.d. – Not detected

NB^+ - Nutribloom Plus

NPQ – Non-photochemical quenching

OD – Optical density

ODA – Oleic acid

OJIP – Chlorophyll fluorescence induction kinetics

OPA – Octadecapentaenoic acid

OTA – Octadecatetraenoic acid

PBR – Photobioreactors

PFD – Photon flux density

PIC – Particulate inorganic carbon

POC – Particulate organic carbon

PSII – Photosystem II

PQ - Polyquinone

PUFA – Polyunsaturated fatty acids

QY – Quantum yield

RCC – Roscoff Culture Collection

RCII – Reaction center II

rETR – Relative electron transport rate

SFA – Saturated fatty acid

TAG – Triacylglycerols

1.1. MICROALGAE

Microalgae are key organisms due to their role as primary producers (Custódio et al. 2012; Promdaen et al. 2014). They are a diverse group of photosynthetic microorganisms (Pulz & Gross 2004) with different sizes and morphotypes (Mendes et al. 2003; Drews-Jr et al. 2013; Pereira et al. 2013). These organisms are able to convert carbon dioxide into oxygen and other metabolites that can be used as food, feed and high value biochemicals (Walker et al. 2005; Spolaore et al. 2006; Pereira et al. 2011). Because of their higher photosynthetic rates resulting in higher efficiency in terms of CO_2 fixation, microalgae are also a very promising model for CO_2 sequestration and mitigation and could be an effective resource for applications with important environmental impact such as wastewater treatment, energy production (Hu et al. 2012; Hussain et al. 2017; Schulze et al. 2017), bioremediation, and nitrogen fixation (Malik 2002; Kalin et al. 2005; Muñoz & Guieysse 2006). Furthermore, the presence of important biomolecules in different microalgal strains reveal that these organisms are a good source of compounds that can be used in several areas, namely fatty acids, proteins, carotenoids, vitamins, phycobilins, sterols, polysaccharides, lipids (mainly triacylglycerols) and phenolics (Pulz & Gross 2004; Hu et al. 2008; Plaza et al. 2009; Guedes et al. 2011; Hemaiswarya et al. 2013; Pereira et al. 2015). When exposed to abiotic stress, microalgae can accumulate specific bioactive compounds as, for example, the production of high-value carotenoids (Coesel et al. 2008). The presence of compounds in the microalgal biomass that are responsible for various biological activities (e.g., cytotoxic, anticancer, antitumor, antibiotic, antioxidant, anti-inflammatory, antifungal, antiviral, anticholesterol, immuno-suppressive, hepatoprotective and neuroprotective activities) have also been described, underlining the importance of these microorganisms (Gouveia et al. 2008; Plaza et al. 2009; Patil et al. 2011; Pereira et al. 2011).

Even though they are microscopic, most microalgae possess some characteristics in common with higher plants (e.g., efficient oxygenic photosynthesis and simple nutritional requirements), having also other properties similar to those of bacterial cells, such as fast growth in liquid medium and accumulation and secretion of metabolites (Custódio et al. 2012). Industrial production of microalgal biomass is commonly achieved

in open (e.g., raceways) or closed (e.g., photobioreactors or fermenters) systems (Chisti 2007; Custódio et al. 2014; Pereira et al. 2015), thus enabling the production of large quantities of biomass and biomolecules (Sánchez et al. 2008). They are also very promising candidates in the process of CO_2 mitigation (Thawechai et al. 2016; Yun et al. 2016; Hussain et al. 2017) and production of important bioproducts (Pereira et al. 2016). This is due to their high photosynthetic and growth rates and their ability to be cultivated on non-arable land (e.g., deserts; Haiduc et al. 2009; Mutanda et al. 2011). Moreover, they are able to grow at high biomass concentrations per unit area (25-30 t/ha/year in open ponds and 50-150 t/ha/year in photobioreactors; Haiduc et al. 2009), using non-potable water (sea- or wastewater; Thomas et al. 2016). In addition, some microalgae are able to grow at very high CO_2 concentrations. In general, concentrations of 10-15% CO_2 can be used. However, *Scenedesmus obliquus*, *Chlorella kessleri* and *Arthrospira* sp. can grow at up to 18% CO_2 and *Chlorella* sp. can withstand concentrations of 70-100% CO_2 (Zhao & Su 2014; Thawechai et al. 2016). Some microalgae are capable of tolerating extreme environmental conditions such as hypersaline environments, brackish water and a wide thermal range (Mutanda et al. 2011). Last but not least, they are able to produce several metabolites that can be used in different biotechnological fields: lipids for biodiesel (Chisti 2007; Pereira et al. 2016), biomass and pigments such as chlorophyll and carotenoids (Thawechai et al. 2016) for colouring scales of ornamental fish and the yolk of chicken eggs; and protective agents against sunburns (Varela et al. 2015). All these applications have the possibility of implementing zero-waste methodologies (Thomas et al. 2016) by means of the establishment of biorefineries.

To achieve a high growth rate in photoautotrophic microalgae, specific culture parameters must be controlled, namely CO_2, nitrogen, phosphorus, iron and trace metals, temperature, pH and a light source, which can be natural (sunlight) or artificial (e.g., light-emitting diodes; Chandra et al. 2011; Schulze et al. 2014).

Because microalgae are highly biodiverse, they are classified into different taxonomic groups according to their evolutionary history (Drews-Jr et al. 2013). The taxonomic classification of algae is based on their phylogenetic relationships that usually coincides with the classes of pigments they can biosynthesize. Some very important taxa include the *Chlorophyta* (green algae), *Rhodophyta* (red algae), *Bacillariophyceae* (diatoms), *Dinoflagellata* (dinoflagellates) and *Haptophyta* (haptophytes). Specifically, the coccolithophores such as *Emiliania huxleyi*, are classified in the phylum *Haptophyta* (Adl et al. 2012; Keeling 2013; Burki et al. 2016).

1.2. HAPTOPHYTA

The phylum *Haptophyta* is now recognized as belonging to the *Haptista* super-group (Burki et al. 2016) and includes two classes: *Pavlovophyceae* and *Prymnesiophyceae* (Adl et al. 2012). Haptophytes are abundant primary producers in marine and freshwater environments (Andersen 2004; Keeling 2009), representing an important component of the ocean's phytoplankton (Zapata et al. 2004). Nearly all known haptophytes are photosynthetic organisms that usually possess a haptonema, some of them forming large blooms (Andersen 2004; Keeling 2009). The haptonema is a microtubular appendix located between two closely equal flagella that serves the purpose of collecting food particles and/or attaching to surfaces. The haptonema is unique to the haptophytes, being often a feature used to diagnose their taxonomical classification (Kawachi et al. 1991; Andersen 2004; Billard and Inouye 2004).

The plastids of haptophytes were acquired through secondary endosymbiosis, and belong to the "red plastid lineage", being surrounded by four membranes (Keeling 2010; Keeling 2013). The primary function of their chloroplasts is to carry out photosynthesis, having a wide range of light-harvesting pigments, including one or more types of chlorophyll *c*. To aid the microalgae to carry out photosynthesis, the flagella have autofluorescent substances (e.g., flavin and pterin) that have an important role in phototaxis (Jeffrey 1976; Kawai & Inouye 1989; Andersen 2004).

Haptophytes can show absence (naked cells) or presence of several types of cell coverings, with some having mineralized scales, others having only organic scales and some of them being surrounded by gelatinous material. Haptophytes that are able to produce calcified scales covering their cell body are called **coccolithophores** (Andersen 2004). These coccolithophores have an important role as a long-term sink of inorganic carbon and thus CO_2 sequestration (Van Der Wal et al. 1995; Jordan & Chamberlain 1997; Zapata et al. 2004).

1.3. COCCOLITHOPHORES

Coccolithophores are haptophytes belonging to the class *Prymnesiophyceae* (Billard & Inouye 2004; Adl et al. 2012). They have a very important role in the ocean, estimated to be responsible for half of the precipitation of $CaCO_3$, which becomes part of the deep sea sediment in the form of calcified cell coverings (Milliman 1993; Richier & Fiorini 2011). Even though coccolithophores are able to export carbon as organic matter and calcite, they also release CO_2 in the process of calcification (Read et al. 2013). These

microorganisms are able to produce mass blooms under certain environmental conditions (Tyrrell & Merico 2004; Poulton et al. 2010).

They are known for producing $CaCO_3$ plates (coccoliths) that form their exoskeleton (coccosphere), covering the cell surface (Müller et al. 2008; Read et al. 2013). Coccoliths can become detached from the cells when they are exposed to stress or even from healthy cells as they grow and age (Balch et al. 1996). However, high detachment rates often occur under nutrient stress (Balch et al. 1993; Poulton et al. 2010). The cell coverings of coccolithophores consist of several layers of organic scales (i.e., the coccoliths) that are connected together through fibrillary material with adhesive properties, calcifying the distal scales of the periplast (Billard & Inouye 2004). Coccolithophores can produce different types of coccoliths that are divided into two groups with different morphologies and origin: heterococcoliths and holococcoliths. Heterococcoliths are assembled from two different crystal units of variable size and shape. They are intracellularly produced, and later mineralized in the dictyosome-derived vesicles. Holococcoliths are formed from one single type of crystal that is smaller than the ones present in the heterococcoliths. It has been proposed that the organic base of these coccoliths develops in dictyosomes, but mineralization occurs outside the plasma membrane (Young et al. 1999; Billard & Inouye 2004; Dashiell 2010).

Even though the haptonema is a feature of haptophytes, it is often vestigial in various groups of coccolithophores or is even absent, as is in the case of *Emiliania huxleyi* (Billard & Inouye 2004). Regarding chloroplasts, coccolithophores normally have two golden-brown chloroplasts with chlorophylls *a* and *c*. In addition, each chloroplast contains a pyrenoid with 1,3-β-glucan (chrysolaminarin) as the main product of photosynthesis (Billard & Inouye 2004; Van Lenning et al. 2004).

1.4. COCCOLITHOPHORES AND THE GLOBAL CARBON CYCLE

Coccolithophores have a global impact in the geochemical surface-ocean processes, mainly due to the blooms produced by them (Tyrrell & Merico 2004; Poulton et al. 2010) that extend for several square kilometres and are visible from space (Holligan et al. 1993; Merico et al. 2003). They actively participate in gas exchange between the ocean and the atmosphere (CO_2, O_2 and dimethyl sulphide (DMS)) and in the export of carbonate and organic matter to deep oceanic layers or even deep-sea floor (Fig. 1). They, along with the foraminifera, are responsible for the calcification that happens in the oceans (Rost & Riebesell 2004; Engel et al. 2009; Balch 2018), due to the production of

exoskeletons that act on an extensive range of geological and ecological time scales (de Vargas et al. 2007). Because coccolithophores are calcifying primary producers, they contribute to the biological carbon pump, to the carbonate counter-pump and to the global carbon cycle (Fig. 1; Rost & Riebesell 2004; de Vargas et al. 2007; Taylor et al. 2017) Because of their blooms, they are also responsible for half of the precipitation of CaCO3 in the oceans (Milliman 1993; de Vargas et al. 2007; Richier & Fiorini 2011).

The process of biomineralization carried out by coccolithophores has a great impact on the alkalinity and carbonate chemistry in the photic zone of the world's oceans. The formation of $CaCO_3$ in the form of calcite is frequently named as particulate inorganic carbon (PIC) and it is thought that they contribute significantly for the decrease of atmospheric CO_2 by two ways: 1) absorption of dissolved inorganic carbon (DIC) in the form of HCO_3^- and 2) in the sedimentation of organic matter in the bottom of the oceans due to cell death or coccolith release (de Vargas 2007; Balch 2018).

However, there has been some disagreement among authors on whether coccolithophores are the ideal microalgae for biotechnological processes of mitigation/sequestration of CO_2 due to the release of CO_2 in the precipitation process of $CaCO_3$:

$$Ca^{2+} + 2HCO_3^- \leftrightarrow CaCO_3 + CO_2 + H_2O \qquad \text{(Urey, 1952)}$$

It is evident that, for each two moles of consumed bicarbonate, one mole of $CaCO_3$ is produced along with a mole of CO_2. This shows that they also have an important role in the ocean alkalinity pump (Balch 2018). Even though there is the consumption of an atom of carbon, this process will result in a short-term local source of atmospheric CO_2 (de Vargas et al. 2007). Yet, it is known that this temporary increase is frequently compensated by the processes of sedimentation of organic material to the bottom of the ocean (Fig. 1; Rost & Riebesell 2004).

The biogenic carbonate produced constitutes an optimal material for aggregation of particulate organic carbon (POC) created by photosynthesis. Coccolithophores also contribute to the formation of organic debris in the form of dissolved organic carbon (DOC) or through the formation of POC as suspended cells in the water column or coccoliths (Engel et al. 2009; Taylor et al. 2017). The accumulation of coccoliths into marine snow ballasts organic matter and other debris—which would not sink to deep oceanic layers or to the deep-sea floor any other way—is a main driver of the organic carbon pump. Therefore, coccolithophores are an important factor for the removal of CO_2 from the atmosphere (de Vargas et al. 2007).

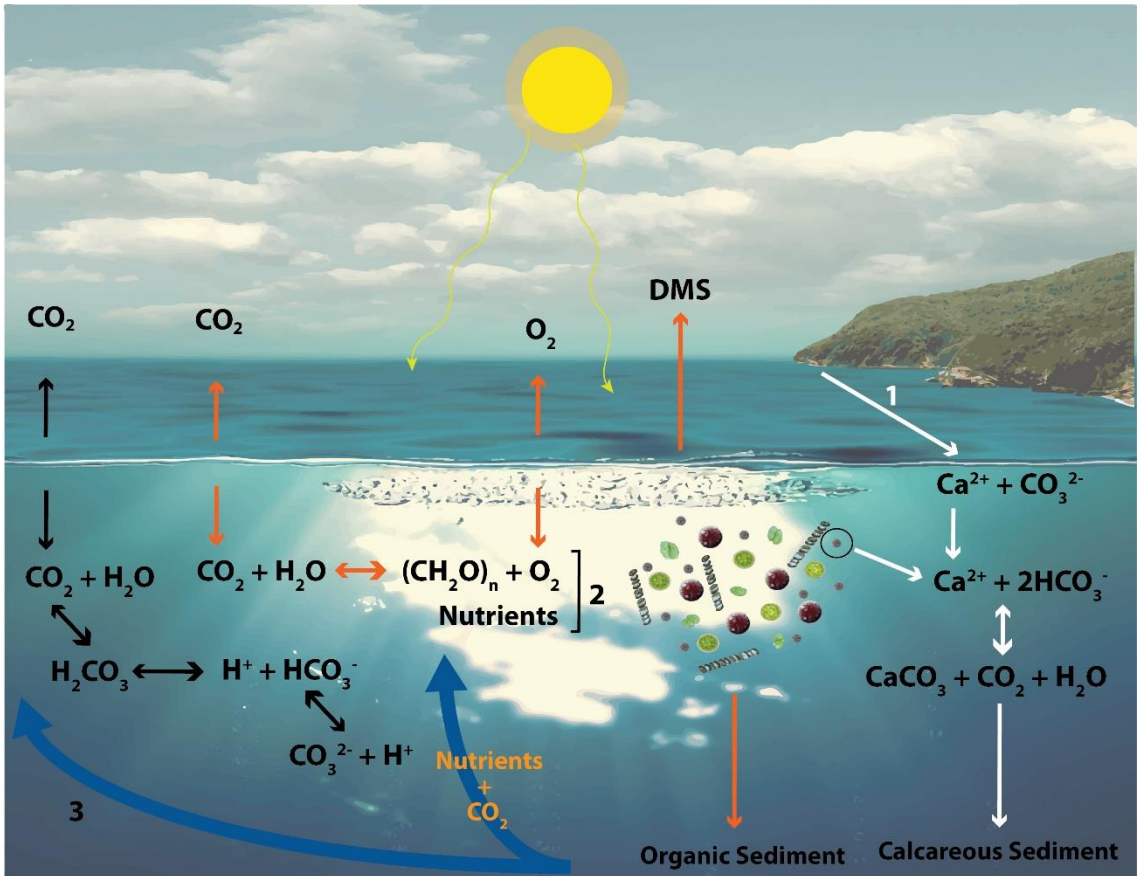

Figure 1 – Schematic representation of the biological carbon pump, carbonate counter-pump and carbon cycle. CO_2 can enter the ocean through the atmosphere or through the (1) weathering of calcite rock. Part of the atmospheric CO_2 that enters the ocean - carbon cycle (black arrows) - is converted into H_2CO_3 which, in turn, dissociates into protons and HCO_3^- that can be, again, dissociated into protons and CO_3^{2-}. However, the atmospheric CO_2 can also enter the biological carbon pump (orange arrows). CO_2, water and light are used in photosynthesis, originating oxygen, DMS and (2) phytoplankton growth that represent the primary producers. A group of these producers (coccolithophores) can also fix carbon (carbonate counter-pump; white arrows), as they use Ca^{2+} and $2HCO_3^-$ to produce $CaCO_3$. During this process, there is the release of CO_2 and water, resulting in a local increase of CO_2. However, part of the biomass produced will result in organic sediment and the coccoliths produced will result in calcareous sediment. These sediments can later be remobilized due to the action of upwelling currents (3, orange text), providing more nutrients and CO_2 for phytoplankton growth.

The biotechnological processes proposed for coccolithophores mimic not only the formation of calcite in the form of coccoliths but also the sequestration of carbon in organic material, since the biomass of the microalga is collected, having a high commercial value.

This group – coccolithophores - has been widely studied to understand their biochemical processes and role in the carbon cycle of the ocean, mainly the coccolithophore *Emiliania huxleyi* that serves as a model due to their high abundance in blooms occurring in the world's oceans.

Emiliania huxleyi (Lohmann) Hay and Mohler represents one of the most abundant calcifying planktonic microalgae (Richier & Fiorini 2011) and one of the most productive coccolithophores (Barcelos e Ramos et al. 2010; Jakob et al. 2017), accounting for up to 20-50% of the total coccolithophore community present in oceanic blooms (Westbroek et al. 1993). These can occupy areas greater than 100,000 km^2 (Brown & Yoder 1994; Laguna et al. 2001), being visible in satellite images (Holligan et al. 1993), which detect the shedding of highly reflective coccoliths produced by them (Poulton et al. 2013). The widespread abundance of *E. huxleyi* and its ability to calcify body scales strongly suggests that this is a promising species to study ocean acidification (Young et al. 2014) with potential for CO_2 mitigation and sequestration (Riebesell 2004; Young et al. 2014). The physiology and molecular ecology of this species has been studied extensively (Paasche 2002; von Dassow et al. 2009; Rokitta et al. 2011), because of its impact on the biosphere, enhancing the fluxes of several important elements (oxygen, carbon and sulphur) between the atmosphere, the ocean and the ocean floor (Westbroek et al. 1993; Rost & Riebesell 2004; Frada et al. 2012). *E. huxleyi* is capable of carbon fixation on a global scale due to its widespread distribution, ability to carry out photosynthesis and body scale calcification (Linschooten et al. 1991).

2.1. MORPHOLOGY OF *EMILIANIA HUXLEYI*

Morphologically, *E. huxleyi* is a unicellular organism with a small cell body size (4-6 µm; Klaveness 1972a, Paasche 2002) and relatively low amounts of chlorophyll *a* (Haxo 1985). The coccoliths (Jong et al. 1976; Laguna et al. 2001; Jakob et al. 2017) are formed intracellularly in a specialized vesicle (Klaveness 1972b; Borman et al. 1982), via controlled crystal growth, being excreted and assembled to form the coccosphere at a later stage. Each cell can produce between 10 to 15 coccoliths (Jakob et al. 2017). So far, eight morphotypes of *E. huxleyi* (Fig. 2) have been described (Paasche 2002; Beaufort et al. 2011; Cook et al. 2011; Hagino et al. 2011; Read et al. 2013). These differ in their genetic makeup, cell size, distribution, and coccolith morphology (Cook et al. 2011; Müller et al. 2017). Type A (Fig. 2A) and type B (Fig. 2E) are the best characterized. Type A is the most common and widespread morphotype and type B is distinctly less calcified than the former, but tend to produce more coccoliths per cell, though irregular ones (Paasche 2002;

Schroeder et al. 2005; Young et al. 2014). Type C (Fig. 2G) resembles type B, but cells are lighter and have smaller coccoliths with the central area open or covered with a delicate plate (Young & Westbroek 1991; Beaufort et al. 2011). Type B/C (Fig. 2F) is similar to both type B and C but have an intermediate size with delicate coccoliths (Young et al. 2003). Type O (Fig. 2H) is similar to type B but the coccoliths always have an open central-area (Hagino et al. 2011). Type R (Fig. 2C) presents extremely thick coccoliths similar to the ones produced by *Reticulofenestra parvula* (Paasche 2002; Cook et al. 2011). Type *corona* (Fig. 2D) is very similar to type A, however, they have a projection formed from inner elements protruding from the centre (Young & Westbroek 1991).

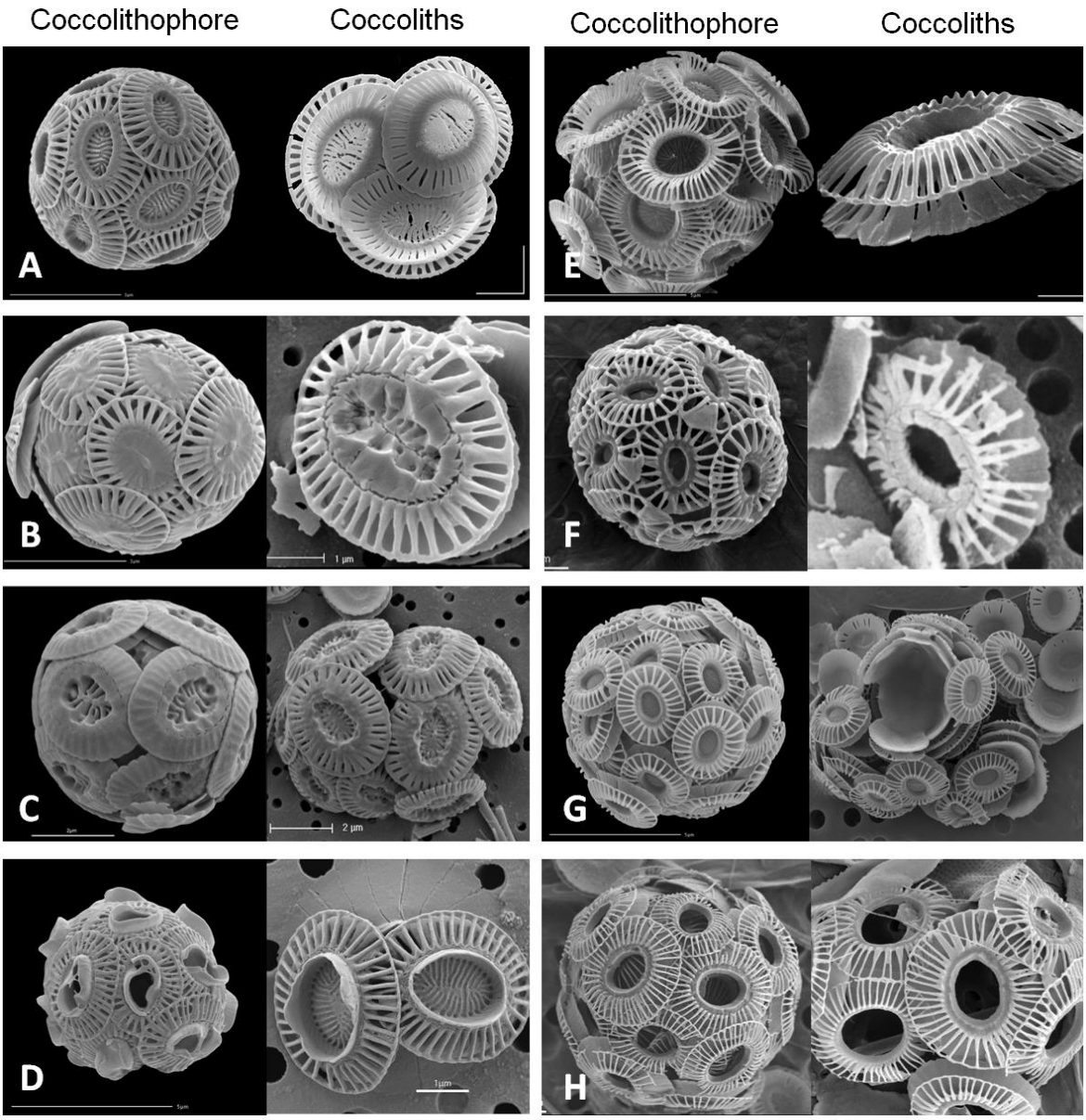

Figure 2 - Scanning electron microscopy of the different morphotypes and coccoliths present in *Emiliania huxleyi*. (A) morphotype A; (B) morphotype A overcalcified; (C) morphotype R; (D) morphotype *corona*; (E) morphotype B; (F) morphotype B/C; (G) morphotype C; (H) morphotype O. Adapted from Wei & Wise (1992) and Young et al. (2003).

Recently, an overcalcified morphotype (Type A overcalcified; Fig. 2B) was described where the relative abundance of individuals with this morphotype increases in acidic waters (Beaufort et al. 2011).

2.2. LIFE CYCLE OF *EMILIANIA HUXLEYI*

With a complex life cycle, *E. huxleyi* presents different cell types that include: i) C cells (coccolith-bearing coccolithophores) usually found in nature; ii) N cells (non-motile naked cells) that appear spontaneously in C cell cultures and iii) S cells (scale-bearing motile cells) with flagella that also appear spontaneously in cultures (Figure 3). Each cell type is capable of vegetative reproduction, with reports of C cells resulting in both N and S cells (Klaveness 1972b; Green et al. 1996; Laguna et al. 2001). Cell division within the C cell type can occur in two ways: i) after the cell contents escape from the coccosphere in the form of a naked cell where the daughter cells gradually produce coccoliths; or ii) it can happen via simple fission, where the original coccoliths are retained by the daughter cells (Paasche 1968). N cells do not form coccoliths and have a slower reproduction rate due to smaller chloroplasts. They are not part of the normal life cycle of *E. huxleyi*, but the appearance of C cells can be induced upon depletion of sodium nitrate (Wilbur & Watabe 1963; Paasche & Klaveness 1970). S cells differ from the N and C cells, primarily because they exhibit flagella. They also possess a single external layer of organic scales different from the scales produced by C cells (Klaveness 1972a). Beside these different cell types, *E. huxleyi* also presents a haplo-diplontic life cycle, with diploid C cells and the haploid S cells (Frada et al. 2008) playing an important role in the ecology of the species (Rokitta & Rost 2012). Haploid individuals are able to survive to

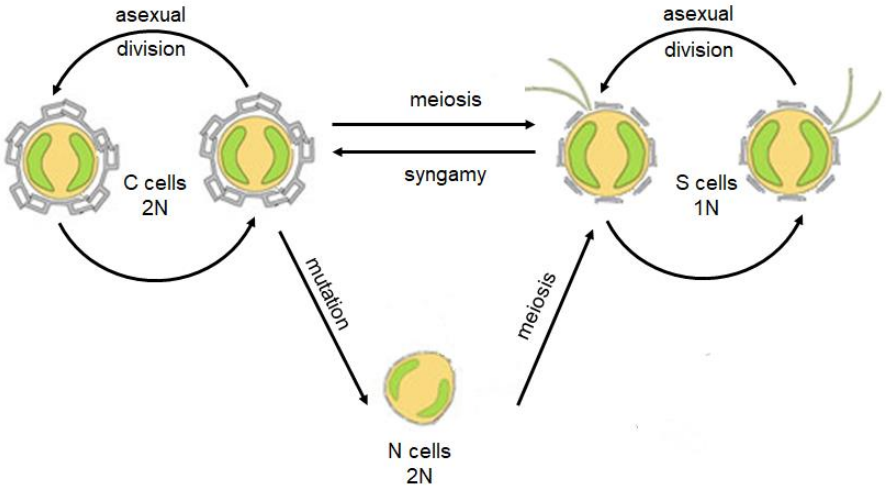

Figure 3 – Life cycle of the coccolithophore *Emiliania huxleyi*. Diploid cells are represented by C (coccolith-bearing cells) and N cells (non-motile naked cells) and haploid cells by S cells (scale-bearing motile cells). Adapted from Paasche (2001).

stage-specific viruses that destroy blooms of diploid individuals. The endocytic vesicles, present only in diploid cells, might be the structures targeted by virus when under limiting bloom conditions. The virus infects the diploid cells and forces the termination of the bloom (Rokitta et al. 2011) through the up-regulation activity of the host metacaspase (Bidle et al. 2007). This action causes caspase-dependent programmed cell death, leading to population collapse (Mayers et al. 2016). On the other hand, haploid cells are apparently not affected by the virus. Thus, it has been suggested that meiosis might act as an escape strategy (Frada et al. 2008) to viral infection. This strategy has been named as "The Cheshire cat escape strategy". Haploid cells are also likely to act as sexual gametes (Frada et al. 2012), possibly justifying the metabolic differences between haploid and diploid cells (Rokitta & Rost 2012). Even though they are the same species, the haploid form of *E. huxleyi* expresses different classes of genes as compared to those of the diploid form (Rokitta et al. 2011).

2.3. GROWTH PERFORMANCE AND CULTURE CONDITIONS

Because *E. huxleyi* is an interesting species from a biotechnological point of view, it was necessary to understand which strain was more appropriate to "domesticate" and grow, being able to withstand the climate in southern Portugal upon scale-up in outdoor pilot- and industrial-scale facilities. For this purpose, data was gathered about the available strains and it was possible to analyse how these strains were grown and which were better adapted to be cultivated in Portugal due to the information about the site and temperature from where they were isolated. A comprehensive literature review of growth experiments carried out in different *E. huxleyi* strains and the culture conditions used are presented in Table I.

The *E. huxleyi* strains used in most works were obtained from the National Center for Marine Algae and Microbiota (NCMA; formerly known as CCMP) and from the Roscoff Culture Collection (RCC). Guillard´s f/2 and K were the most used growth media to culture this microalga. Both of them were used in diluted form in some works (e.g., f/10 or K/2 media). In addition, the culture medium was often adjusted or supplemented, in particular when nutrient limitation experiments were carried out. Nitrate and phosphate were among the nutrients whose concentrations were frequently modified (e.g., Riegman et al. 2000; Stolte et al. 2000; Eltgroth et al. 2005; McKew et al. 2015; Skau et al. 2017). The temperature at which cultures were grown ranged between 13 and 25 ºC, with 15 ºC as the most reported temperature. Nevertheless, the highest growth rates were obtained in

experiments where cultures were grown between 20-21 ºC (Paasche & Klaveness 1970; Conte et al. 1998; Muller et al. 2008; Moheimani et al. 2011; Bartal et al. 2015; Hariskos et al. 2015; Jakob et al. 2018). The pH of most experiments varied between 7.5 and 8.7. Salinities above 30 were most frequently reported; however, salinities ranging from 23.7 to 38 can be found in the literature. The most frequent photoperiod chosen was a 16:8 light:dark (L:D) cycle followed by 12:12 and 24:0 L:D cycles. Upon comparison of the 24:0 and 12:12 L:D cycles, higher cell concentrations were obtained under the latter condition (Laguna et al. 2001). When comparing 24:0 and 16:8 L:D cycles, cultures under the former photoperiod showed a higher production of POC and PIC, but cultures under the 16:8 L:D photoperiod showed a higher ratio of PIC/POC (Zondervan et al. 2002). The photon flux density (PFD) ranged from 10 to 1500 µmol photons/m^2/s. However, it has been shown that PFD above 500 µmol photons/m^2/s causes photoinhibition in calcifying strains. PFD at lower levels also gives rise to higher chlorophyll *a* content (Hariskos et al. 2015).

The initial cell concentration of inoculum cultures is of the outmost importance. A culture with a concentration of 10^5 cells/mL seemed to be the most commonly used as an initial inoculum for batch cultures of about 15 days. Samples were usually taken during exponential growth phase and growth rates ranged from 0.13 to 2.8/day.

Concerning the volume of the culture, successful growth of *E. huxleyi* in 6-L flat-plate photobioreactors (PBR), 10-L carboy and 20-L custom made bag PBRs have been reported. In the 10-L carboy PBR, however, *E. huxleyi* showed a slower growth rate (Moheimani et al. 2011). *E. huxleyi* cultures were also produced in raceway ponds (200 L), but after two weeks the culture deteriorated due to contamination by ciliates and other microalgae (Moheimani 2005). For coccolith production, Jakob et al. (2018) achieved 5 g/L in a 2-L stirred PBR under low carbon conditions. Aeration was not used since it causes cell damage caused by air bubble burst-associated shear stress (Chisti 2001; Moheimani et al. 2011; Jakob et al. 2018).

More information is available in Supplementary Data 1.

Table I: Compilation of experimental data from research made on Emiliania huxleyi, including strains used, culture medium, growth temperature, pH, light cycle, irradiance, salinity, duration and sampling and growth rate.

Species and strain	Culture medium	Growth temperature (ºC)	pH	Light cycle (L:D)	PFD (µmol photons/m^2/s)	Salinity	Growth rate (d^{-1})	References
Emiliania huxleyi	f/2	20	n.a.	n.a.	56-70	n.a.	n.a.	(Sumitra-Vijayaraghavan 1976)
Emiliania huxley AC481	Surface post-bloom SW	13 and 18	n.a.	14:10	150	35.6	Higher growth rate at 18ºC and present CO_2: 0.15	(De Bodt et al. 2010)
Emiliania huxleyi BOF92	Eppley and f/25	18	n.a.	15:9	45	n.a.	n.a.	(Nanninga et al. 1996)
Emiliania huxleyi BOF92	Eppley and f/25	18	8.1	24:0	200	n.a.	2.6 and 2.8	(Nanninga & Tyrrell 1996)
Emiliania huxleyi B11	f/2	15	n.a.	14:10	30 and 300	n.a.	0.11 - 0.45	(Ragni et al. 2008)
Emiliania huxleyi B92/21, G1779Ga, M181[b], S.Africa, Van556	f/2	6, 9, 12, 15, 18, 21, 24, 27 and 30	n.a.	16:8	100-200	n.a.	1.75 at 21ºC	(Conte et al. 1998)
Emiliania huxleyi BT_6	D	n.a.	n.a.	n.a.	12	n.a.	n.a.	(Haxo 1985)
Emiliania huxleyi CCAP 920/2	ASW supplemented	18	n.a.	12:12	80	n.a.	2.6 days (doubling time)	(Flynn 1990)
Emiliania huxleyi CCMP 370	L1	15	n.a.	12:12	130	n.a.	n.a.	(Garrido et al. 2016)
Emiliania huxleyi CCMP 370, 373, 374, 379	f/2 (-Si)	15	n.a.	14:10	100	n.a.	n.a.	(Strom et al. 2003)
Emiliania huxleyi CCMP 371	f/2	23	n.a.	12:12 and 18:6	300; 350; 320 and 120-130	n.a.	0.99±0.06; dry weight productivity: 0.47±0.022 g/L/day	(Moheimani et al. 2011)
Emiliania huxleyi CCMP 371	f/50	21	n.a.	12:12	300	n.a.	From 1.05 to 1.08	(Muller et al. 2008)
Emiliania huxleyi CCMP 371 and CS-369	Pacific ASW in modified f/50 (CCMP371) and GSe/2 (CS-369)	18, 20 and 25	7.7-7.9 and 8.1-8.3	12:12	150-300	23.7-33.1	0.17±0.09 - 1.19±0.03; 1.38±0.09 at 23.7 ppt; 0.99±0.06 in plate PBR	(Moheimani, 2005)
Emiliania huxleyi CCMP 371 and RCC 1216	ESW	21	n.a.	24:0	10, 20, 50, 100, 300, 400, 500, 800, 1500	n.a.	1.1	(Hariskos et al. 2015)
Emiliania huxleyi CCMP 373	f/2 (-Si)	23	n.a.	14:10	900	n.a.	n.a.	(Aluwihare & Repeta 1999)
Emiliania huxleyi CCMP 373 and CCMP 370	f/2	15	n.a.	16:8	80-100	n.a.	0.47-0.70; no production of coccoliths	(Wolfe & Steinke 1996)

Emiliania huxleyi CCMP 373 and CCMP 374	f/2 (-Si)	18	n.a.	14:10	450	n.a.	0.9	(Bidle et al. 2007)
Emiliania huxleyi CCMP 1516	SW with f/2 metals and vitamins	20	n.a.	16:8	150	n.a.	From 0.67±0.05 to 1.25±0.04	(Bartal et al. 2015)
Emiliania huxleyi CCMP 1516	f/2	15	n.a.	14:10	250	n.a.	n.a.	(Evans et al. 2009)
Emiliania huxleyi CCMP 1516	ASW supplemented with Erd-Schreiber's SW	25	n.a.	24:0	100	n.a.	(cell density on day 6 at 25ºC) $8.6\pm1.8 \times 10^6$ cells/mL	(Kotajima et al. 2014)
Emiliania huxleyi CCMP 1516	f/50 or f/2	17-18	n.a.	24:0 or 12:12	600	n.a.	n.a.	(Laguna et al. 2001)
Emiliania huxleyi CCMP 1516	ASW with f/8 trace metals and vitamins	18	n.a.	16:8	300	n.a.	n.a.	(McKew et al. 2015)
Emiliania huxleyi CCMP 1516	f/2 (-Si)	18	n.a.	14:10	200	n.a.	2.5×10^6 cells/ml (only cell abundance)	(Rose et al. 2014)
Emiliania huxleyi CCMP 1742, 1516, 370, 374	f/2 or f/20	16	n.a.	16:8	80	n.a.	n.a.	(Eltgroth et al. 2005)
Emiliania huxleyi CCMP 2090	K/2	18	n.a.	16:8	100	n.a.	n.a.	(Shemi et al. 2016)
Emiliania huxleyi CCMP 3266, CCMP 3268 and CCMP 2090	L1 (-Si)	18	n.a.	16:8	n.a.	n.a.	n.a.	(Mayers et al. 2016)
Emiliania huxleyi Ch24-90 and Ch25-90	f/2	10 and 15	7.98 - 8	16:8	70-155	n.a.	0.8-0.9	(van Bleijswijk et al. 1994)
Emiliania huxleyi CS-57	f/2	20	n.a.	16:8	80	n.a.	n.a.	(Rontani et al. 2007)
Emiliania huxleyi DWN 61/81/5	f/2	15	n.a.	12:12	100	n.a.	n.a.	(Bell & Pond 1996)
Emiliania huxleyi EHSO 5.14	f/20 or f/80	14	7.48-8.06	24:0	100-115	35	0.2	(Müller et al. 2017)
Emiliania huxleyi EHSO 5.30, 5.25, 5.28, 5.11, 6.17, 8.15	K	16	n.a.	12:12	70	n.a.	1.04 and 0.86	(Cook et al. 2011)
Emiliania huxleyi F	Eppley (-Si)	21	n.a.	24:0	196	30	1.42 (C-cells) and 1.68 (N-cells)	(Paasche & Klaveness 1970)
Emiliania huxleyi	IMR/2	17	n.a.	n.a.	42 or 196	30	n.a.	(Klaveness 1972)

F61, F63, G4								
Emiliania huxleyi F61 and 92	Droop and Eppley (-Si)	19	n.a.	n.a.	70	n.a.	n.a.	(Jong et al. 1976)
Emiliania huxleyi isolated	f/2 pre-culture and f/20 for experiment	15	7.47 - 8.36	14:10	150	34	1.01	(Barcelos e Ramos et al. 2010)
Emiliania huxleyi isolated	MNK	18	n.a.	18:6	n.a.	n.a.	n.a.	(Hagino et al. 2011)
Emiliania huxleyi isolated	IMR ½	13 and 19	n.a.	14:10	170	30	Higher growth rate at high P: 0.855-1.045	(Skau et al. 2017)
Emiliania huxleyi L	f/50 or Eppley's	18	8	16:8	90	n.a.	0.8 - 1.1 div/cell/4h (0.034 - 1.1)	(Linschooten et al. 1991)
Emiliania huxleyi L	Prepared from SSW	15	8	24:0	200	n.a.	0.14 - 0.63	(Riegman et al. 2000)
Emiliania huxleyi L and CCMP 370, 373, 374, 379 and 1516	f/2 (-Si)	15	n.a.	18:6	40	30	0.62 - 0.82	(Steinke et al. 1998)
Emiliania huxleyi L, 92, 92D and MCH	f/50	19	n.a.	16:8	n.a.	n.a.	n.a.	(Young & Westbroek 1991)
Emiliania huxleyi NIES-837	MNK	20	n.a.	12:12	20-30	n.a.	n.a.	(Mizoguchi et al. 2011)
Emiliania huxleyi NIES 873	Erd-Schreiber	20	n.a.	24:0	100	n.a.	n.a.	(Obata & Shiraiwa 2005)
Emiliania huxleyi PCC 92 and 92d	ESW	18	n.a.	24:0	n.a.	n.a.	n.a.	(Vasconcelos et al. 2002)
Emiliania huxleyi PCC 92 and 92d	f/10	18	8	24:0	n.a.	35	From 0.72 to 0.83	(Vasconcelos & Leal 2001)
Emiliania huxleyi PML B92/11	Treated and supplemented SW with f/2 metals	14 and 18	7.97	16:8	300	32	0.1 and 0.3	(Borchard & Engel 2012)
Emiliania huxleyi PML B92/11	f/2	14	8.24	16:8	19	33	0.2	(Borchard & Engel 2015)
Emiliania huxleyi PML B92/11	f/2	15	7.8 – 8.6	24:0 and 16:8	15, 30 and 80	n.a.	1.11 (high [CO2])	(Zondervan et al. 2002)
Emiliania huxleyi RCC 1216	ESAW	21	n.a.	n.a.	350	n.a.	1.06 ± 0.01	(Jakob et al. 2018)
Emiliania huxleyi RCC 1216 and RCC 1217	K/2 (-Tris, -Si)	17	n.a.	14:10	80	n.a.	0.843 ± 0.028 and 0.851 ± 0.004	(Dassow et al. 2009)

Emiliania huxleyi RCC 1216 and RCC 1217	K/2 (-Tris, -Si)	17	n.a.	14:10	150	38	control: 0.79±0.02; elevated pCO2: 0.76±0.02	(Richier & Fiorini 2011)
Emiliania huxleyi RCC 1216 and RCC 1217	North Sea SW with f/2 vitamins and trace metals	15	7.7 – 8.2	18:6	50 and 300	32	From 0.63±0.14 to 1.18±0.20	(Rokitta & Rost 2012)
Emiliania huxleyi RCC 1216 and RCC 1217	f/2	15	8.1 – 8.2	16:8	50 and 300	32.2	From 0.87±0.12 to 1.18±0.20	(Rokitta et al. 2011)
Emiliania huxleyi RCC 1216, 1249 and 1213	K/2 (-Tris, -Si)	18	n.a.	12:12	85	n.a.	n.a.	(Frada et al. 2008)
Emiliania huxleyi RCC 1266	Oligotrophic SSW	16	n.a.	14:10	60	n.a.	diploid: 0.75±0.03 (axenic) and 0.76±0.01 (non-axenic); haploid: 0.98±0.05	(Van Oostende et al. 2012)
Emiliania huxleyi RuG collection	f/2	16	n.a.	16:8	75	35	0.34±0.08	(Boelen et al. 2013)
Emiliania huxleyi 88E	K	19	n.a.	14:10	51	n.a.	n.a.	(Balch et al. 1993)
Emiliania huxleyi 88E	K	17	7.93 - 8.74	n.a.	75	n.a.	From 0.24 to 0.99	(Balch et al. 1996)
Emiliania huxleyi 88E	K	16	n.a.	16:8	200	n.a.	0.49±0.01 for low irradiance and 0.81±0.04 for high irradiance	(Fernandez et al. 1994)
Emiliania huxleyi 92D	f/2	15	n.a.	12:12	50-100	n.a.	0.9	(Harris 1994)
Emiliania huxleyi 92d	1:1:1 Erd-Schreiber, ASP2 and Miquel-Allen	15	n.a.	12:12	n.a.	n.a.	n.a.	(Marlowe et al. 1984)
Emiliania huxleyi (several strains)	f/2	15	n.a.	12:12	100	n.a.	n.a.	(Pond & Harris 1996)
*Emiliania huxleyi (*16 different strains)	Nutrients added to nutrient-poor SW	15	n.a.	16:8	70	n.a.	From 0.13 to 0.70	(Stolte et al. 2000)
Emiliania huxleyi (34 different strains)	f/2	15	n.a.	14:10	200	n.a.	n.a.	(Iglesias-Rodriguez et al. 2006)

Table I Glossary: ASW - Artificial seawater; ESW - Enriched seawater; L:D - Light:Dark; n.a. - Not available; PBR – Photobioreactor; PFD - Photon flux density; SW - Seawater; SSW - Synthetic seawater.

2.4. BIOCHEMICAL COMPOSITION

2.4.1. PROTEINS

In order to grow and bloom, *E. huxleyi* has various proteins that help cells adapt to different environments such as: a) several photoreceptors and proteins involved in the assemblage and repair of said photoreceptors that help withstand photoinhibition; b) inorganic phosphate transporters, alkaline phosphatases, purple acid phosphatases and other enzymes that hydrolyse organic phosphorus compounds, thus being able to thrive in low phosphorus conditions; c) transporters used in the uptake and assimilation of inorganic nitrogen, in particular in the form of ammonium transporters; d) resistance-associated macrophage protein class of metal transporters, multi-copper oxidases, ferric reductases and siderophores that allow for growth in surface waters with low iron concentration; e) presence of selenoproteins, usually found in mammals and green algae, that promote the use of selenium for growth (Obata & Shiraiwa 2005; Read et al. 2013). Overall, the protein content in *E. huxleyi* is around 6.7 pg/cell for coccolith-forming cells and 6.6 pg/cell for naked cells (Paasche & Klaveness 1970).

2.4.2. AMINOACIDS

Because of their role in the structure of proteins, amino acids (AA) are of extreme importance. With *E. huxleyi*, that is no exception. During the life cycle of *E. huxleyi*, the transport and metabolism of AA varies, with higher expression during the haploid phase, showing specific transcriptomes for each of their life cycle phases (Rokitta et al. 2011). It has also been shown that *E. huxleyi* can grow well in a medium with free AA that are used as a nitrogen source (Ietswaart et al. 1994; McKew et al. 2015). Considerable growth of axenic cultures in growth medium containing alanine and leucine has been described. In the presence of bacteria, *E. huxleyi* is able to grow at a higher rate when in the presence of glutamine and glycine (Ietswaart et al. 1994; Bruhn et al. 2010). In 100 g of total AA obtained from the biomass of this haptophyte, the most abundant AA are glutamic acid (12.4 g), alanine (11.6 g), leucine (9.3 g), aspartic acid (7.6 g) and lysine (7.6 g; Chau et al. 1967).

2.4.3. LIPIDS

Lipids are formed primarily of carbon, hydrogen and oxygen and represent an important class of compounds for microalgal metabolism (Babayan 1987). In *E. huxleyi*, only small amounts of neutral lipids are stored, usually in the form of triacylglycerols

(TAG), while polyunsaturated long-chain alkenes, alkenones and alkenoates, are produced in higher amounts (Volkman et al. 1980, Marlowe et al. 1984; Eltgroth et al. 2005). These compounds are connected to structures such as the endoplasmic reticulum and the coccolith-producing compartment (Evans et al. 2009). The production of ketones suggests that these compounds act as storage lipids, replacing the role of TAG (Bell & Pond 1996). Their sphingolipids are primarily glucosylceramides with a C9-methyl chain that are usually found only in fungi and some animals (Oura & Kajiwara 2010; Read et al. 2013). Sulpholipids are used as partial replacements for cellular phospholipids (Van Mooy et al. 2009; Read et al. 2013). In terms of glycerolipids, *E. huxleyi* has high contents of phosphatidylcholine, monogalctosyldiacylglycerols, and sulpho-quinovosylglycerol. It also contains significant amounts of hydrocarbons, methyl and ethyl ketones and sterol esters (Pond & Harris 1996).

2.4.4. FATTY ACIDS

In the marine environment, fatty acids (FA) are usually provided by microalgae to other organisms in the food web, playing a vital role in terms of energy storage, somatic growth and reproduction (Evans et al. 2009). Docosahexaenoic acid (DHA) and eicosapentaenoic acid (EPA) are considered to be extremely important for human nutrition, being used in food and feed supplements (Boelen et al. 2013; Read et al. 2013). *E. huxleyi* lipids are predominantly rich in (*n*-3) polyunsaturated fatty acids (PUFA; Conte et al. 1994). Different types of FA are present in this species, such as tetradecanoic (14:0), hexadecenoic (16:0) and oleic (ODA; 18:1*n*-9) acids. Regarding PUFA, DHA (22:6*n*-3), octadecapentaenoic (OPA; 18:5*n*-3), α-linolenic (ALA; 18:3*n*-3) and octadecatetraenoic (OTA; 18:4*n*-3) acids are frequently present in higher abundances (33, 20, 5 and 10%, respectively). Docosapentaenoic acid (DPA; 22:5*n*-3) and EPA (20:5*n*-3) are also present; however, smaller proportions (0.8 and 0.9%, respectively) are commonly detected (Conte et al. 1994, Bell & Pond 1996, Pond & Harris 1996; Evans et al. 2009, Khozin-Goldberg et al. 2011, Boelen et al. 2013).

2.4.5. CARBOHYDRATES

Carbohydrates (CHO) are molecules often released as a part of dissolved organic matter, making up a big part of the DOC present in the ocean (Pakulski & Benner 1994; Myklestad 2000; Van Oostende et al. 2012). A major percentage of CHO in seawater comes from either phytoplankton biomass (Pakulski & Benner 1994; Børsheim et al. 1999) or extracellular CHO (Biersmith & Benner 1998; Aluwihare & Repeta 1999) that

are released from the cells after hydrolysis of the polymer chains (Borchard & Engel 2015). Usually, extracellular CHO in seawater is composed of neutral hexoses, pentoses and deoxy sugars like galactose or mannose; of amino sugars and uronic acids (Aluwihare et al. 1997; Biersmith & Benner 1998; Engel et al. 2011; Borchard & Engel 2012;).

In *E. huxleyi*, there are two types of CHO present: dissolved (*d*CHO) and particulate (*p*CHO). The *d*CHO form is released by these cells and has arabinose and glucose as the most abundant sugars. In the *p*CHO form, glucose and rhamnose are the most abundant sugars. This variation among different forms of CHO may be related with ecological and physiological functions (Borchard & Engel 2015). Total CHO yield in *E. huxleyi* is 49.1% (in 100% organic carbon) with the most abundant polysaccharides being glucose, galactose, xylose and mannose (Nanninga et al. 1996; Biersmith & Benner 1998).

Accumulation of *d*CHO happens at a late stage in the growth rate of *E. huxleyi*, mainly when they reach stationary and declining phases. The amount of *d*CHO varies between 0.4 and 3.5 µg/mL throughout their growth, with the higher amount when cell number is declining (Sumitra-Vijayaraghavan 1976).

Differently from plants and green algae, *E. huxleyi* produces β-D-glucan that is a water soluble neutral polysaccharide and storage compound, instead of the water insoluble α-glucan (Vrum et al. 1986; Ball et al. 2011; Tsuji et al. 2015). These molecules, known as chrysolaminarin, are (1→6)-linked β-D-glucan with branches in the position 3 and (1→6) linkages in the side chains (Beattie et al. 1961; Vrum et al. 1986) and are composed of more than 99% glucose (Obata et al. 2013). *E. huxleyi* also produces an acid polysaccharide known as "Coccolith Polysaccharide" (CP; Kayano & Shiraiwa 2009; Tsuji et al. 2015). CP consists of a mannose polymer as the main chain and xylose, galacturonic acid and rhamnose with sulphate ester groups as side chains (Fichtinger-Schepman et al. 1981; Tsuji et al. 2015). CP is able to bind to calcium ions (De Jong et al. 1976) and to the surface of $CaCO_3$ crystals (Henriksen et al. 2004), where they can inhibit (Borman et al. 1982) and modify (Didymus et al. 1993) crystal formation. It has been proposed that CP is produced in intracellular coccolith vesicles coming from dictyosomes, being deposited on the cell surface, integrated in $CaCO_3$ crystals and then transported to the cell surface with the coccoliths (van Emburg et al. 1986). CP might also aid the formation of extremely elaborate structures of coccoliths (Kayano et al. 2011), therefore being considered to be a structural component (Tsuji et al. 2015).

2.4.6. PIGMENT AND CAROTENOID COMPOSITION

The main pigment of all oxygenic phototrophs is chlorophyll *a* (Stolte et al. 2000; Mizoguchi et al. 2011). *E. huxleyi* cells absorb mainly between 400-450 nm and 620-700 nm (blue and red ranges of the absorption spectrum; Zapata et al. 2004; McKew et al. 2015). *E. huxleyi* has also chlorophyll c_1, chlorophyll c_2 and chlorophyll c_3, pigments usually found in heterokonts, dinoflagellates, cryptophytes and haptophytes, which have an intense absorption at 400 nm (Bachvaroff et al. 2005; Zapata et al. 2006; Mizoguchi et al. 2011; Adl et al. 2012). Beside chlorophyll pigments, this species also has other light-harvesting pigments related to the carotenoid fucoxanthin, namely 19'-hexanoyloxyfucoxanthin, which is present at a higher percentage when compared with other carotenoids and chlorophylls, and acts as an antenna pigment. In addition, it contains the photoprotective xanthophyll cycle pigment diadinoxanthin, which is the precursor for diatoxanthin, a xanthophyll that protects cells from the damaging effects caused by saturating light (Haxo 1985; Kooistra et al. 2007; Cook et al. 2011; Garrido et al. 2016).

2.4.7. VITAMINS

E. huxleyi growth depends on several vitamins, which they are able to synthesize *de novo*, such as pro-vitamin A, and vitamins C, D, E, B_6 and biotin (Carlucci & Bowes 1970; Read et al. 2013). However, *E. huxleyi* lacks the ability to synthesize B_{12} vitamin, which is essential to their growth, but it is able to survive in a growth medium lacking this vitamin as long as the cultures are not axenic and contain bacteria able to secrete this essential metabolite (Helliwell et al. 2011; Read et al. 2013; Mayers et al. 2016).

2.5. BIOTECHNOLOGICAL APLICATIONS OF *EMILIANIA HUXLYEI*

Emiliania huxleyi has several characteristics with biotechnological interest. The biomass itself can be used in animal and, potentially, human nutrition. Their biochemical composition has also increased in significance: they synthesize unusual lipids and fatty acids with high commercial value that can be incorporated as nutritional or feedstock supplements (Pond & Harris 1996; Boelen et al. 2013; Read et al. 2013) and they have pigments of interest, mainly 19'-hexanoyloxy-4-ketofucoxanthin, which can be used as a replacement for food colourants (Wördenweber et al. 2018).

Because of the production of coccoliths, *E. huxleyi* has an added component that it is not found on other groups. These coccoliths have shown great potential in different fields because of their nanoscale architecture (Read et al. 2013). There have been reports

of using coccoliths in light scattering (Gordon & Du 2001) and nanotechnological applications (Skeffington & Scheffel 2018), and as a substitute for industrial calcite (Jakob et al. 2017).

Apart from these properties, *E. huxleyi* has also a group of secondary metabolites known as polyketides (Jones et al. 2011) that present antibiotic, antifungal, anticancer and immunosuppressive properties (Staunton & Weissman 2001). Because of the presence of these secondary metabolites and calcium carbonate, it is possible that this species presents molecules with osteogenic activity as well.

2.5.1. OSTEOGENIC ACTIVITY

The human skeleton represents the most common organ to be affected by diseases that cause great morbidity (Coleman et al. 2006), with osteoporosis in the list of the most common bone diseases (U.S. Department of Health and Human Services 2004; Pisani 2013). Some of these diseases are characterized by low bone mass and deterioration of bone tissue, which causes fragility and increased susceptibility to fractures (Pisani 2013).

In aquaculture, skeletal deformities represent one of the factors affecting this industry, in terms of economical loss and fish welfare. Several types of deformities have been reported. Scoliosis, lordosis, mandibular deformities, semi-opened or short operculum, double fins, vertebrae fusion, neck-bend are an example of the most common deformities (Cunningham et al. 2005; Eissa et al. 2009; Berillis 2017). These deformities are known to affect the economic value of the produced fish in the aquaculture market due to the rejection of these individuals by consumers (Boglione et al. 2001; Berillis 2017).

Fish deformities are a result of infectious diseases, nutritional imbalance, environmental pollution, genetic factors (for example inbreeding), management issues (such as overcrowding) and environmental factors (Brown and Nunez 1998; Eissa et al. 2009; Berillis 2017). When fish are exposed to these elements during their early growth stages (Vogel 2000), they are more likely to develop skeletal deformities from what is thought to be linked to the disruption of early development processes (Longwell et al. 1992; Eissa et al. 2009). A great part of the occurred deformities has been linked to vitamin C deficiency (Lim & Lovell 1978; Dabrowski et al. 1988), presence of heavy metals (Bengtsson & Larsson 1986), genetics (Mair 1992), strong water currents in early development stages (Backiel et al. 1984), parasites (Stevens et al. 2001), bacterial

infections (Pasnik et al. 2007), among others (Andrades et al. 1996; Eissa et al. 2009; Berillis 2017).

Although there are several drugs available in the pharmaceutic market to prevent or limit the effects of these diseases (Miller 2009; Feng & McDonald 2011; McClung et al. 2013), undesirable side effects may arise from their use, such as esophageal cancer or acute phase response (Bernabei et al. 2014; Khan et al. 2017). Thus, it is important to find novel molecules with anabolic properties with the capacity to counter the effects of said diseases for new osteogenic treatments, while having minor- or non-side effects (Laizé et al. 2014; Tarasco et al. 2017).

A potential source of new compounds with osteogenic activity could be microalgae, mainly coccolithophores because of their production of calcium carbonate. There have been reports of extracts of macroalgae with bioactive compounds that demonstrate mineralogenic (Surget et al. 2017) and osteogenic (Carson et al. 2018) activities, therefore, demonstrating promising therapeutic applications.

To test the effect of new molecules on bone development, several *in vivo* systems of zebrafish (*Danio rerio*, Hamilton, 1922) have been developed (Laizé et al. 2014; Tarasco et al. 2017). Compounds are added directly into the water (Tarasco et al. 2017) in which the zebrafish grow, representing an easy way for drug delivery (Wilkinson & Pritchard 2015). The analysis of the operculum system has been chosen for its simplicity and for the low amount of compound required. The operculum is one of the first dermal bones to ossify, has a high growth rate during early larval development and is easy to observe through staining; it is therefore a bone structure of choice to screen the effects of osteogenic compounds and to evaluate bone morphogenetic variations in zebrafish larvae (Huycke et al. 2012; Tarasco et al. 2017).

III OBJECTIVES

Emiliania huxleyi is a microalgal species that shows great potential for industrial production. In the open ocean, it can form km-long blooms and is able to synthesise high-interest compounds such as *n*-3 PUFAs or fucoxanthin. Moreover, because it produces calcium carbonate, this species contributes greatly to the sinking of carbon, which can be used as a CO_2 mitigation feedstock.

This thesis aimed to establish the optimal culture conditions for the bloom-forming coccolithophore *E. huxleyi*, mainly focusing on the production of high-value biocompounds (e.g., *n*-3 PUFA). To achieve this goal, the most important growth parameters (culture media, temperature and light) were tested independently under laboratory conditions using Algem® PBRs. In addition, the effect of the different parameters on the growth performance and biochemical composition was also investigated.

Another objective of the present thesis was to determine whether the biomass market value could be further upgraded by screening for specific bioactive properties. For this purpose, different extracts of *E. huxleyi* biomass were tested for the presence of compounds with osteogenic activity in zebrafish larvae.

4.1. SCALE-UP PROCESS

Several European culture collections were searched for the selection of *E. huxleyi* strains appropriate for cultivation and scale-up (Supplementary Data 2). Using the data collected, the criteria for selecting a given strain was its immediate availability, growth temperature (at least 22ºC), and ability to produce coccoliths. From the available strains, seven cultures met the aforementioned criteria and were thus selected: RCC 1250, RCC 1821, RCC 3485, RCC 3498 and RCC 4537, RCC CL14-1 and RCC C5.

Prior to inoculation, all the material was sterilized in an autoclave at 121ºC to prevent contaminations.

Upon the arrival of the seven purchased strains (30 mL), the scale-up process began. From the purchased strains, 15 mL of culture were transferred to 50 mL Erlenmeyers that were supplemented with K/2 media (Keller et al. 1987) modified by Ian Probert, according to the specifications sent by the RCC. The cultures were supplemented with concentrated culture medium to reach a final concentration of 0.3 mM of nitrates. Upon seven days of cultivation, each culture was transferred to 250-mL Erlenmeyers and thereafter scaled up to 1-L Erlenmeyers. The remaining cultures were regrown upon the addition of culture medium, to keep stock cultures of different volumes.

Upon the unsuccessful attempts at growing several *E. huxleyi* strains, the process was repeated. However, instead of using K/2 media, Nutribloom® Plus (NB^+) was selected as the growth medium of choice. The cultures were supplemented with this concentrated culture medium to reach a final concentration of 0.4 mM of nitrates.

All the Erlenmeyer flasks were kept in a Panasonic MLR-253-PE growth chamber (MarBioTech, CCMAR) at 22ºC with a light cycle of 12:12 light:dark (L:D) and under low light intensity (40 µmol photons/m/s). Every flask was daily shaken to homogenize the cultures.

4.1.1. LAB-SCALE ALGEM® PHOTOBIOREACTORS

To understand the growth and response of the fastest growing *E. huxleyi* isolate, the strain RCC 1250 was selected to inoculate the Algem® PBRs (Algenuity, Bedfordshire, UK; Fig. 4). These lab-scale PBRs are composed of two units. Each unit is fully enclosed and has a panel of light-emitted diodes (LEDs) at the bottom (Fig. 4C), a

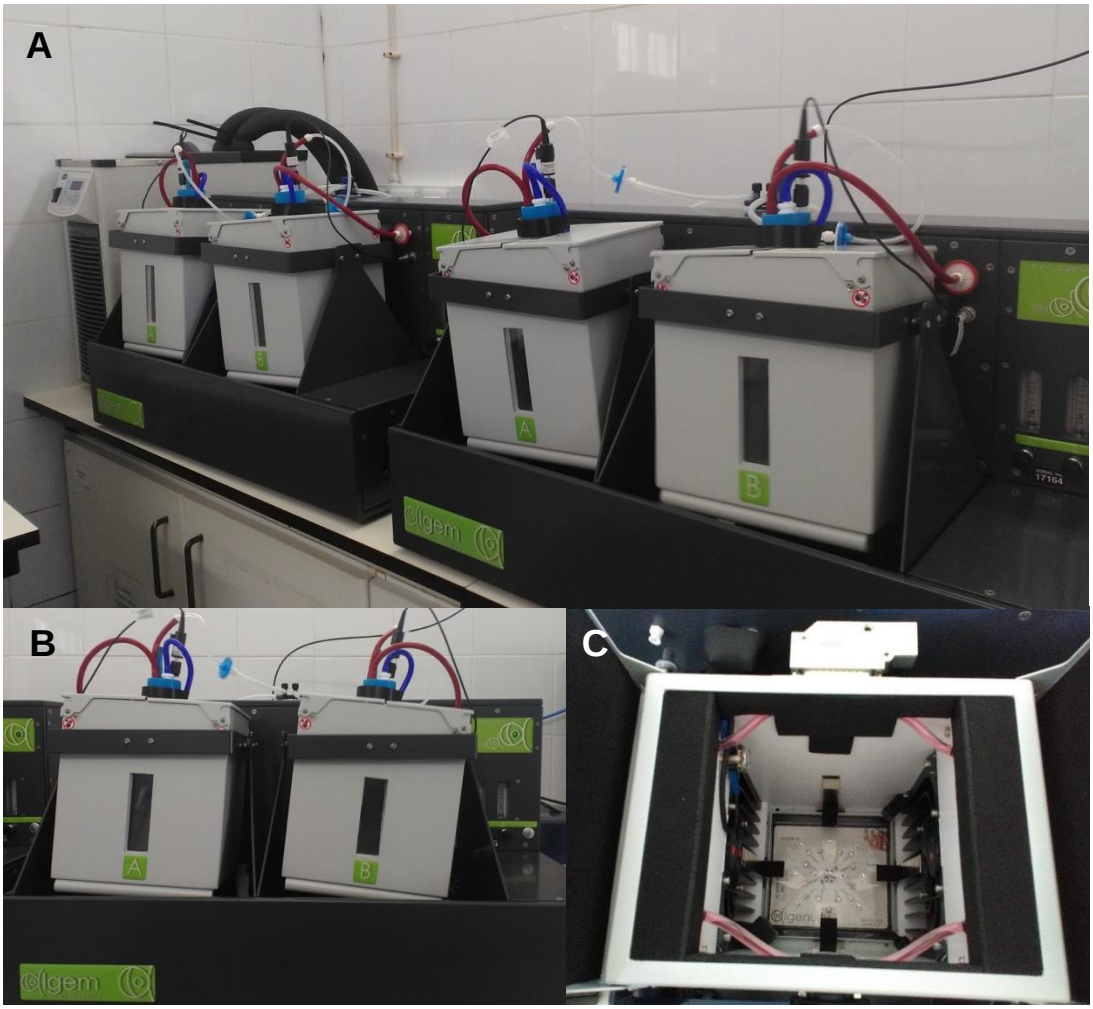

Figure 4 - Algem® PBR array at Necton's facility. General view of the equipment, composed of two systems, each with two PBR units (A); one system of Algem® comprising two oscillatory PBR units (B); and the interior view of the chamber (C).

heating and cooling system, a mixing system that prevents sedimentation and a spectrophotometer (λ = 740 nm) for real-time growth monitoring. For each experiment, each unit is inoculated with a flask equipped with a specialized cap that provides a gas and aeration delivery system, a tube for air exhaustion and a pH probe.

The Algem® is also equipped with a software with 80 years of averaged meteorological data that models light and temperature profiles for a specific location anywhere in the world. This software can independently control a LED panel for attaining specific photoperiods, light intensities and flashing light duty cycles as well as independent control of the red, blue and white LEDs. Temperature profiles, pH set-points with CO_2 injection, mixing rates and the recording of the optical density (OD) of the cultures can also be automatically set using the aforementioned software.

4.1.2. PARAMETERS FOR GROWTH OPTIMIZATION

To evaluate the growth response of *E. huxleyi* RCC 1250 strain to different conditions, several parameters were tested using the Algem® PBRs:

1) Culture media with different nitrate concentrations: 0.3 M (K/2 0.3 mM NO_3^-, NB^+ 0.3 mM) or 0.6 M (K/2 0.6 mM NO_3^-, NO_3^- and NB^+ 0.6 mM NO_3^-);
2) Temperature: 17, 20, 23 and 26ºC;
3) Irradiance measured in terms of photon flux density (PFD): 600, 900, 1200 and 1500 µmol photons/m^2/s;
4) Standard *vs.* optimized conditions.

Using the software equipped with the Algem®, it was possible to simulate the environmental conditions at the location of Necton facilities (37º 1' 31" N, -7º 52' 8" W)

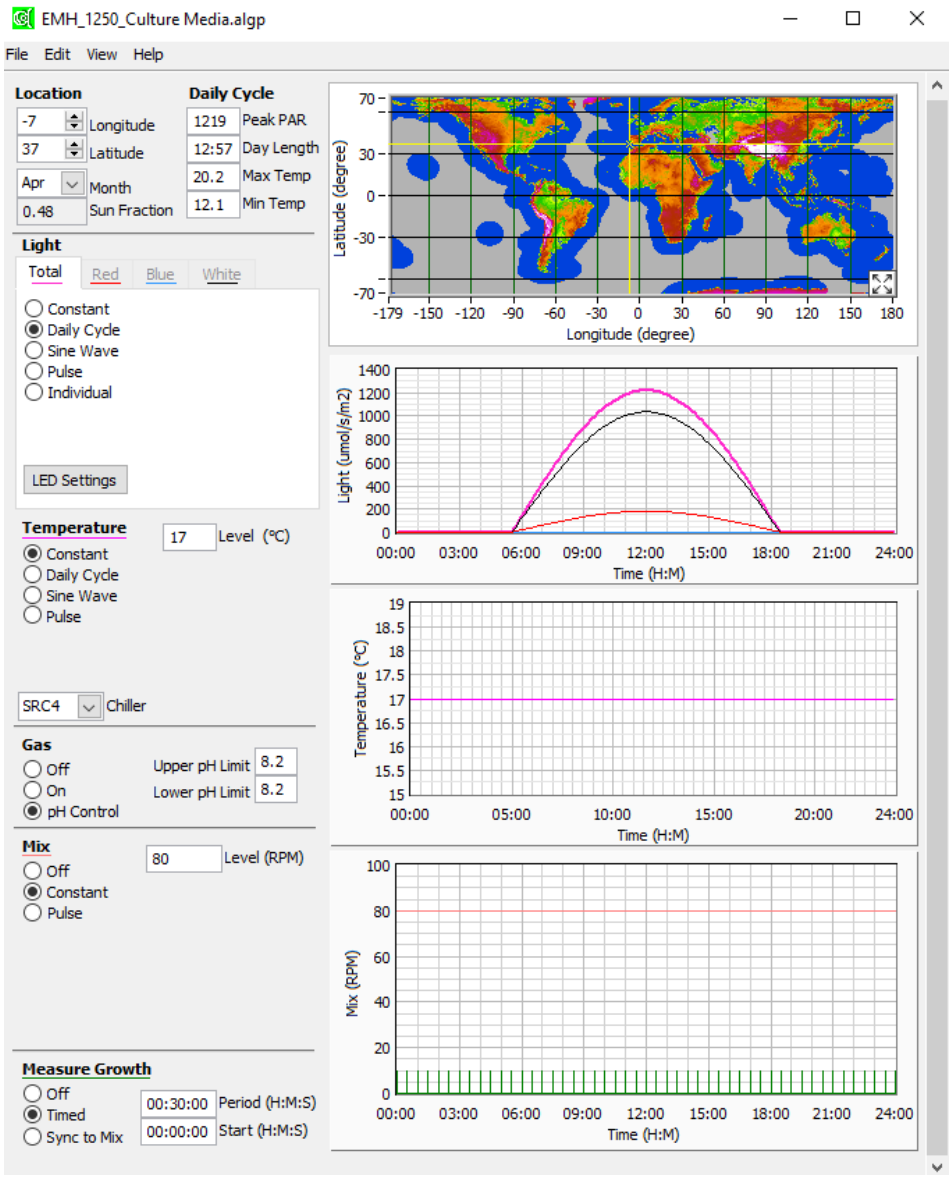

Figure 5– Example of a profile used in a trial using the Algem® software.

during April. Therefore, a set of parameters were fixed for each test with following profile (Fig. 5): 12:57h of light with a PFD peak of 1219 µmol photons m^{-2} s^{-1}; a light profile composed of 15% red light, 0% blue light and 85% white light; temperature set at 17ºC; pH set-point at 8.2; and the mixing rate set at 80 rpm.

4.1.3. ALGEM® INOCULATION

For the inoculation of the PBRs, a concentrated inoculum was brought from the growth chamber at CCMAR to Necton's facilities. Firstly, the OD was measured at 740 nm using an UVmin-240 spectrophotometer. Afterwards, the culture was diluted 1:5 (v/v) to make up an initial OD of 0.2 with a final volume of 500 mL per Erlenmeyer. To each flask, NB^+ growth medium was added, so that the final concentration of NO_3^- was 0.3 mM. $NaHCO_3$ was also added at a concentration of 0.087 g L^{-1} to supplement the growth medium with an additional carbon source.

Finally, every Erlenmeyer was prepared with their respective pH probe and specialized cap and placed inside the PBRs. The environmental settings for each chamber were uploaded for the respective chamber using the provided software.

4.1.4. CULTURE MONITORING

In each trial, samples were collected at days 0, 2, 4, 7, 9 and 11 to monitor the growth of the cultures for each condition. Culture growth was monitored by measuring:

- **Optical density**

To determine the OD of the cultures, a sample of 3 mL was collected from each flask and transferred to a plastic cuvette. Every sample was measured at 540, 680, 720 and 740 nm in a UVmin-240 spectrophotometer. Samples were diluted when the OD measured was higher than 1.0.

- **Dry weight**

Dry weight (DW) was determined using a protocol designed by Necton. Firstly, 0.7-µm filters were washed in a vacuum filtration system with 10 mL of distilled water and 2 mL of 31.5 g L^{-1} ammonium formate to dissolve seawater salts. The filters were then transferred to an aluminium box and moved to an incubator at 60ºC for 24h to dry. Once dried, the filters were put in a desiccator and, upon reaching room temperature, were weighed together with their respective box.

From each culture growing in the Algem® PBRs, a sample of 10 mL was collected and was filtered using the previously washed filters. After the filtration, the filters were washed with 10 mL of ammonium formate. The pH of this solution was adjusted to 8.0

to prevent the dissolution of coccoliths from the cells. The filters were then transferred to their corresponding box and put in the incubator for 24h and were again weighed when dried.

The DW in g/L was calculated using the following formula:

$$\text{DW (g/L)} = \frac{(\text{final weight (g)} - \text{initial weight (g)})}{\text{volume (L)}}$$

- **Cellular concentration**

Cellular concentration (CC) was obtained by cell counts using a Neubauer chamber according to the manufacturer's procedure. Dilutions were carried out as necessary in order to have between 30 and 300 cells per field. The CC was obtained with the following formula:

$$\text{CC (cells/mL)} = \text{number of counted cells} \times 10^4 \times \text{dilution}$$

- **Fluorometry**

For chlorophyll *a* fluorescence monitoring, samples of 3 mL were collected from each culture to determine the OJIP test, non-photochemical quenching (NPQ) as well as to produce rapid light-curves (Malapascua et al. 2014). For these determinations, a cuvette-based fluorometer AquaPen 110-C (Photon Systems Instruments, Czech Republic) was used. After the collection of the samples, these were adapted to dark conditions for 10 minutes, so that the photosystems II (PSII) were fully "open".

For the **OJIP test**, the samples were transferred into the equipment after the dark adaptation of the cells and the desired measurement was selected. Firstly, a weak modulated measuring light (ML) was activated to make sure that there was fluorescence emission but was not strong enough to begin photosynthesis, providing the value for the basal fluorescence (F_0). After this, a pulse of actinic light (AL) was activated for one second providing the response of the cells when exposed to light and providing the value for maximum fluorescence (F_m).

With these parameters, the variable fluorescence was calculated using the following formula:

$$F_v = F_m - F_0$$

The maximum quantum yield (QY) of the cells was also possible to determine, which represents the efficiency of the PSII and it was calculated using the following formula (Malapascua et al. 2014):

$$QY = F_v/F_m = \frac{F_m - F_0}{F_m}$$

To determine **NPQ**, which represents the energy dissipation via heat release of the cells in response to excess light, a comparison is made between the maximal fluorescence emitted of a dark-adapted sample measured during the first short saturation flash of light (F_m) and the following PSII fluorescence intensity of light-adapted cells (F_m'). Firstly, the sample was transferred into the equipment and the NPQ protocol was selected. Like the OJIP test, a ML was activated to provide F_0. Afterwards, a short saturating flash of light is then applied to reduce the PQ pool and measure F_m. After a short dark relaxation, the sample is exposed to AL and a set of five saturating flashes with intervals of 12 seconds were applied on top of that to achieve steady state. This provided the necessary information to obtain NPQ and QY values in the light-adapted state. The NPQ was calculated using the following formula:

$$NPQ = \frac{F_m - F_m'}{F_m'}$$

- **Nutrient consumption**

To analyse the consumption of nutrients, a sample from each culture of 10 mL was collected and centrifuged at 2700g for 10 minutes. After centrifugation, the supernatant was removed and stored in the freezer for a multi-parametric analysis of the nutrients present therein. From the supernatant, 1 mL was collected for the determination of nitrate concentration.

- **Nitrate concentration**

For the determination of nitrate concentration, Falcon tubes were prepared with a stock solution with 9.8 mL of NaCl (35 g/L) and 0.2 mL of HCl. For each sample, duplicates were prepared with 9.3 mL of NaCl, 0.2 mL of HCl and 0.5 mL of supernatant. Absorbance was read in quartz cuvettes at 220 and 275 nm. The reading at the latter wavelength is required to detect whether organic matter is also present, which might interfere with the correct determination of the nitrate concentration (APHA 2000). NO_3^- concentration was calculated using a previously established calibration curve between known concentrations of this ion and respective absorbance values.

- **Microscopy**

To determine the status of the culture, microscopic observations were made in a Zeiss Axioimager Scope A1 with a Nikon Eclipse Ni-U camera, using differential interference contrast (DIC). Images of the culture were obtained with a 100 × lens with an additional amplification of 1.6 × using an Optovar. All images were treated with AxioVision SE64 4.9.1 software.

4.2. BIOCHEMICAL COMPOSITION OF *E. HUXLEYI*

4.2.1. PROTEINS

Protein content was determined using elemental analysis through the measurement of total nitrogen. For this purpose, 1 mg of lyophilized biomass was weighed and encapsulated in small aluminium caps. These caps were transferred to a 96-well plate and the samples were analysed using a Vario EL III (Elementar Analysensysteme GmbH, Germany). The total nitrogen content was multiplied by 6.25 to obtain the total protein content of the biomass (Barreira et al. 2017).

4.2.2. LIPIDS

Total lipids were determined using a modified protocol of the Bligh & Dyer (1959) method (Pereira et al. 2011). The lipid tubes were dried at 60ºC for at least 3 hours and then put on the desiccator until cooled. After this, they were weighed in a precision scale and stored in the desiccator.

Lyophilized biomass was weighed into the tubes for lipid extraction and 0.8 mL of distilled water were added to it. To each sample, 2 mL of methanol and 1 mL of chloroform was added and homogenised using an IKA T18 Ultra Turrax disperser at 25000 rpm for 60 seconds, on ice. Afterwards, 1 mL of chloroform was added, and the samples were homogenised for 30 seconds, on ice. Finally, upon the addition of 1 mL of distilled water, the samples were homogenised for 30 seconds (Fig. 6A). All the samples were then centrifuged for 10 minutes at 685*g* at room temperature (Fig. 6B). Using a Pasteur pipette, the organic phase (chloroform) was transferred into new tubes. From these, 0.7 mL of chloroform were pipetted to the previously weighed tubes. The tubes were put in a dry bath at 60ºC until the chloroform was evaporated completely. After this, the lipid tubes were put in the desiccator until cooled and later weighed in the precision scale (Fig. 6C).

The percentage of total lipids was calculated using the following formula:

$$\% \text{ total lipids} = \frac{\left[\frac{[(\text{FW} - \text{IW}) \times \text{total volume of chloroform}]}{\text{evaporated volume of chloroform}}\right]}{\text{Sample weight}} \times 100$$

FW: final weight; IW: initial weight

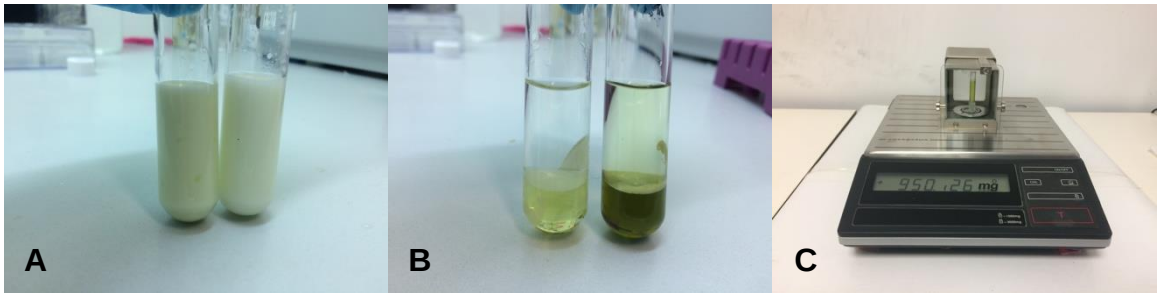

Figure 6– Some of the steps of total lipid quantification. Lipid samples after extraction on the Ultra Thurrax and before centrifugation (A), extracted lipids with phase separation after centrifugation (B) and lipid mass measurements after dried (C).

4.2.3. PIGMENTS

For the determination of carotenoids by HPLC, the procedure for carotenoid extraction was performed. First, 3 mg of dried biomass were weighed and 0.7 g of glass beads (425-600 µm) were added to the sample. After this, 3 mL of 100% acetone were also added and vortexed for 2 min at maximum speed. The samples were centrifuged at 7012*g* for 5 minutes. Later, the supernatant was transferred into dark glass vials to prevent pigment degradation and the above-mentioned procedure was repeated until the supernatant was colourless. After the centrifugation, the acetone was evaporated under nitrogen flow and resuspended in 600 µL of HPLC-grade methanol. Finally, the sample was filtered through 0.22-µm PTFE filter into amber HPLC glass vials.

The carotenoids extracts were analysed in a Dionex 580 HPLC System (DIONEX Corporation, United States) equipped with a PDA 100 Photodiode-array detector, P680 Pump, ASI 100 Automated Injector and STH 585 column oven, using a LiChroCART® RP-18 (5µm, 250x4 mm, LiChrospher®) column and Chromeleon® software. The mobile phase consisted of 9:1 (v/v) acetonitrile:water (solvent A) and ethyl acetate (solvent B). The gradient program applied was as follows: 0–16 min, 0–60% B; 16–30 min, 60% B; 30–32 min 100% B and 32-35 min 100% A at a flow rate of 1 mL/min. The temperature was maintained at 20ºC and the injection volume was 100 µL. The carotenoids were detected at 450 nm and quantified using a calibration curve for fucoxanthin.

4.2.4. FATTY ACIDS

- **FAME Preparation**

Fatty acid profile was determined using a modified protocol of Lepage & Roy (1984), as described in Pereira et al. (2012). This is a method based on direct transesterification and later extraction of the lipidic phase.

Firstly, lyophilized biomass was weighed into derivatization vessels (reaction tubes) and treated with 1.5 mL of methanol/acetyl chloride (derivatization solution, 20:1, v/v). To disrupt the biomass, an IKA T18 Ultra Turrax disperser was used to homogenise the samples at 25000 rpm during two 60- and 30-s periods, on ice. The samples were then put on a water bath at 70ºC for 60 minutes (Fig. 7A). After this, the derivatization vessels were put on ice to decrease their temperature. The samples were then transferred into centrifugation tubes by means of a Pasteur pipette. Distilled water (1 mL) and *n*-hexane (4 mL) were added and the samples were vortexed at maximum speed for two cycles of 30 seconds. Samples were then centrifuged at 438*g* for 5 minutes, at room temperature (Fig. 7B). Using a Pasteur pipette, the hexane fraction was transferred to new glass tubes. The centrifugation process was repeated until the hexane fraction was colourless. Anhydrous sodium sulphate was added in excess to precipitate any water that could be present in the latter fraction, being later filtered using 0.22-µm PTFE filters (Fig. 7C and 7D). The hexane was evaporated under nitrogen gas flow until fully dried (Fig. 7E) and was again resuspended in 500 µL of chromatography-grade hexane. The extract was transferred to small vials and stored at -20ºC for further analysis.

- **Determination of FAME Profile by GC-MS**

FAME were analysed on a Bruker GC-MS (Bruker SCION 456-GC, SCION TQ MS) equipped with a ZB-5MS capillary column (30 × 0.25 mm of internal diameter with 0.25 µm film thickness; Phenomenex) using helium as carrier gas. The temperature program was as follows: 60ºC for 1 minute, 30ºC/min to 120º C, 5ºC/min to 250ºC and 20ºC/min to 300ºC, with an injection temperature of 300ºC for 2 minutes. For the identification of FAME, a Supelco® 37 component FAME Mix (Sigma-Aldrich, Sintra, Portugal) was used as a standard, with five different dilutions (1:10, 1:25, 1:50, 1:72 and 1:100). Separate calibration curves were made for each of the 37 FAME found in the commercial standard used. For identified FAME not present in the standard, the response

factor of the most similar FAME was used. The results are expressed as a percentage of total FAME content (Pereira et al. 2016).

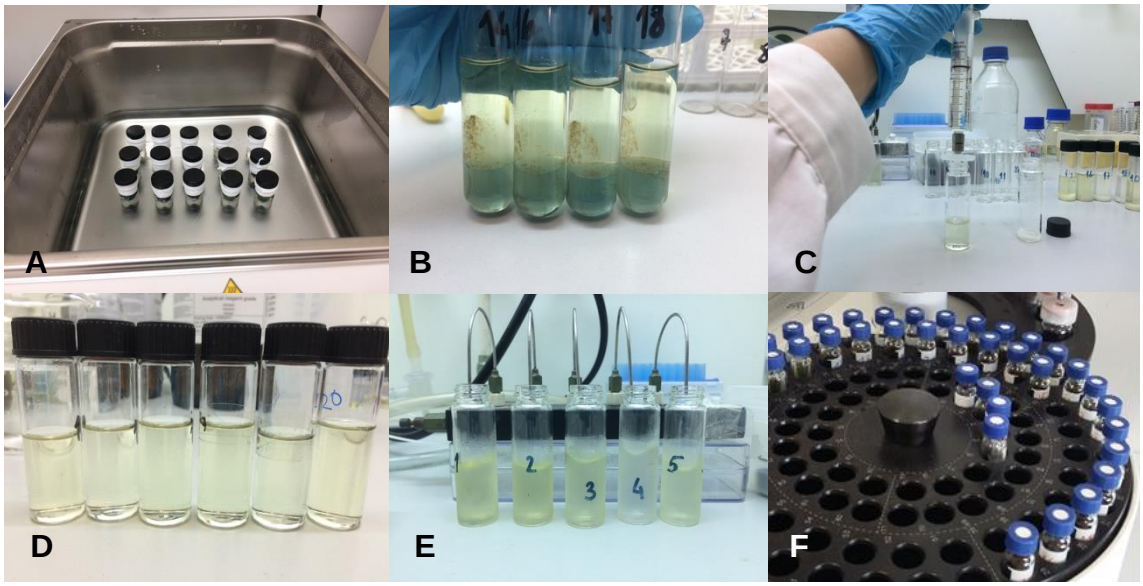

Figure 7 – Some of the steps of the fatty acids samples. Samples during the heat treatment, in a water bath of 70ºC (A), fatty acids samples after centrifugation (B), filtration of the hexane fraction through 0.22-µm PTFE filters (C), samples after filtration (D), hexane evaporation under a nitrogen flow (E) and display of the fatty acid samples in the GC-MS chromatograph analyser (F).

4.3. OSTEOGENIC BIOACTIVITY USING ZEBRAFISH AS A MODEL

4.3.1. BIOMASS PRODUCTION AND COLLECTION

In order to obtain *E. huxleyi* biomass, the scale-up process was continued at Necton using several 5-L balloons with the RCC1250 strain (Fig. 8) that were supplemented with $NaHCO_3$ (0.087 g/L) and NB^+ to a final concentration of 0.4 mM of nitrates. The cultures were kept in the inocula room of the facility at a temperature of 22 ± 2ºC with natural light. Every flask was daily shaken to homogenize the cultures.

When the cultures reached a high cellular concentration, they were collected and concentrated by centrifugation (1670*g* for 30 minutes). The pellets were then stored at -20ºC until lyophilization.

4.3.2. EXTRACTS PREPARATION

After the process of lyophilization, the dried microalgae biomass was weighed and transferred into an Erlenmeyer flask with each solvent (ethanol, ethyl acetate (EA) and distilled water; Table II). The extractions were performed for 16 ± 1h under continuous stirring at room temperature. The flasks were covered with aluminium foil to prevent the degradation of photosensitive molecules. At a later stage, each extract was filtered through 0.22-µm filters and the supernatant was dried on a rotary evaporator (120 rpm at 45ºC; Table II) under vacuum. The dried extracts were later resuspended in

Figure 8 – Production of biomass of *E. huxleyi* strain RCC 1250 at Necton's facilities.

ethanol, DMSO and distilled water, respectively, to make up a final concentration of 100 mg/mL and stored at -4ºC.

4.3.3. ETHICS STATEMENT ON ANIMAL EXPERIMENTS

All the experimental procedures involving animals followed the EU Directive 2010/63/EU and National Decreto-Lei 113/2013 legislation for animal experimentation and welfare. Animal handling and experiments were performed by qualified operators accredited by the Portuguese Direção-Geral de Alimentação e Veterinária (DGAV).

4.3.4. ZEBRAFISH LARVAE PRODUCTION

Zebrafish larvae were obtained through the mating of sexually mature zebrafish (AB wild-type line) using an in-house breeding program. Fertilized eggs were transferred into a 1-L breeding tank containing fish water (pH 7.5 ± 0.1, conductivity 700 ± 50 µS, NH_3 and NO_2 < 0.1 mg/L and NO_3 at 5 mg/L; Tarasco et al. 2017) and incubated at 28ºC ± 0.1ºC. The tank was also supplemented with methylene blue (0.0002% w/v) to inhibit fungal growth.

4.3.5. EXPOSURE TO DIFFERENT EXTRACTS

The zebrafish larvae were placed in a 6-well plate with 10 mL of fish water and 15 larvae per well at three days post-fertilization (dpf; Fig. 9), as described by Tarasco et al. (2017). They were exposed to different concentrations of ethanol, EA and distilled water extracts (0.1, 1, 10 and 100 µg/mL), as well as to calcitriol (1,25-dihydroxyvitamin D_3, Sigma-Aldrich), ethanol and the solvent used for extraction as controls. Vitamin D was used as a positive control and the other two as negative controls. Water renewal (70% of total volume) was renewed every day until the larvae reached six dpf.

At the end of the treatment, the larvae were transferred to a 24-well plate where they were exposed to alizarin red S (0.01%) for 15 minutes at room temperature for bone staining. After this, they were washed twice with MilliQ water for five minutes (Tarasco et al. 2017, adapted from Bensimon-Brito et al. 2016). Euthanasia was then performed using a lethal dose of Phenoxyethanol (0.6 mM, pH 7, Sigma-Aldrich) and the larvae were imaged immediately after.

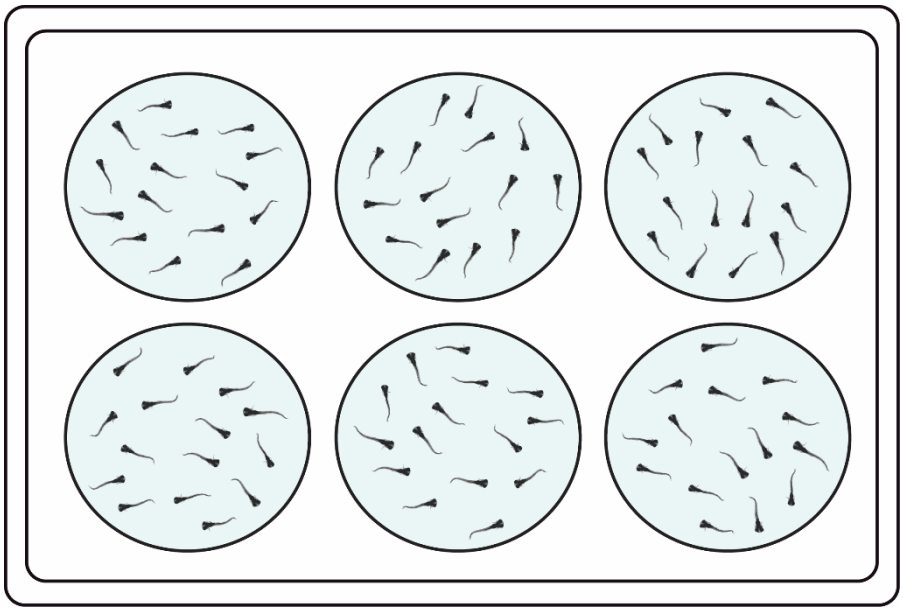

Figure 9 – Schematic representation of the experimental setup.

4.3.6. IMAGE ACQUISITION

Alizarin red S stained larvae were placed in a lateral plane onto a 2% agarose plate and observed using a MZ 7.5 fluorescence stereomicroscope (Leica, Wetzlar, Germany) equipped with a green filter (λ_{ex} = 530-560 nm and λ_{em} = 580 nm) and a black and white F-View II camera (Olympus, Hamburg, Germany). Images (Fig. 10A) were taken using the following parameters: exposure time of one second, gamma 1.00, image format 1376 × 1032 pixels, binning 1×1 (Tarasco et al. 2017).

4.3.7. MORPHOMETRIC ANALYSIS

The fluorescence images were processed using ImageJ 1.52a software. Brightness and contrast of the red channel were adjusted to enhance the visibility of the operculum

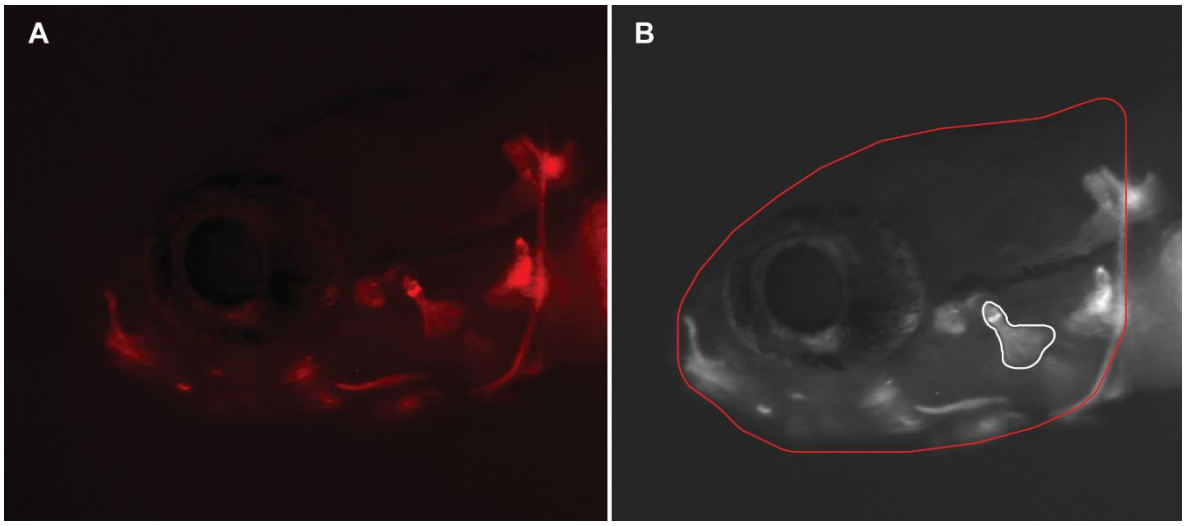

Figure 10 – Observations of zebrafish larvae (*Danio rerio*) using a MZ 7.5 fluorescence stereomicroscope (A) with a green filter (λ_{ex} = 530-560 nm and λ_{em} = 580 nm) and (B) optimized image using the ImageJ software to measure the head area (red line) and the operculum area (white line).

and maximum displayed pixel values were set to 0 and 69, respectively (Tarasco et al. 2017). The area of the head and of the operculum was determined using built-in tools (Fig. 10B).

4.3.8. STATISTICAL ANALYSIS

Statistical analyses were performed using Prism version 6 (GraphPad Software, Inc. La Jolla, CA). Statistical differences were determined through one-way ANOVA followed by Dunnett's multiple comparison test (****$p < 0.05$ and **$p < 0.1$).

V RESULTS AND DISCUSSION

5.1. GROWTH OPTIMIZATON

In order to optimize the growth conditions of *E. huxleyi*, the strain RCC1250 was selected. This decision was made according to the fact that it responded better to the growth conditions upon scale-up as compared to other inocula purchased at RCC. Several abiotic factors were tested, namely culture media and nutrient concentration, temperature and light intensity in Algem® PBRs.

5.1.1. CULTURE MEDIA OPTIMIZATION

In the first trial, two different culture media (K/2 and NB^+) were used containing two different NO_3^- concentrations (0.3 and 0.6 mM). All cultures were supplemented with $NaHCO_3$, as previously described in the literature (Jakob et al. 2018).

During the first 7 days, cultures grown with culture media containing the lowest NO_3^- concentration (0.3 mM) showed better growth performance (Fig. 11). However, after this time period, *E. huxleyi* cells ceased growth in both growth media, whereas they continued growing at 0.6 mM in both media, reaching the highest cell concentrations at the end of the trial. In fact, the culture grown in NB^+ at 0.6 mM of NO_3^- was the one that showed the best growth performance (Fig. 11).

These results suggest that a concentration of NO_3^- of 0.6 mM was inhibitory for the growth of *E. huxleyi*, because of the low CC at the beginning of the experiment (Fig. 11 and Fig. 13). Accordingly, *E. huxleyi* is known to bloom in surface waters that contain low amounts of inorganic nutrients (McKew et al. 2015). However, as the culture achieved a higher CC at day 9, before the onset of culture decline (Fig. 11), higher nutrient concentration seemed to be the most adequate one for optimal growth.

At the end of the experiment, the cultures exposed to the culture media at a NO_3^- concentration of 0.3 mM presented a decrease in growth, resulting in cultures with a whitish colour (Fig. 12). This decrease affected not only the OD but the CC as well (Fig. 13).

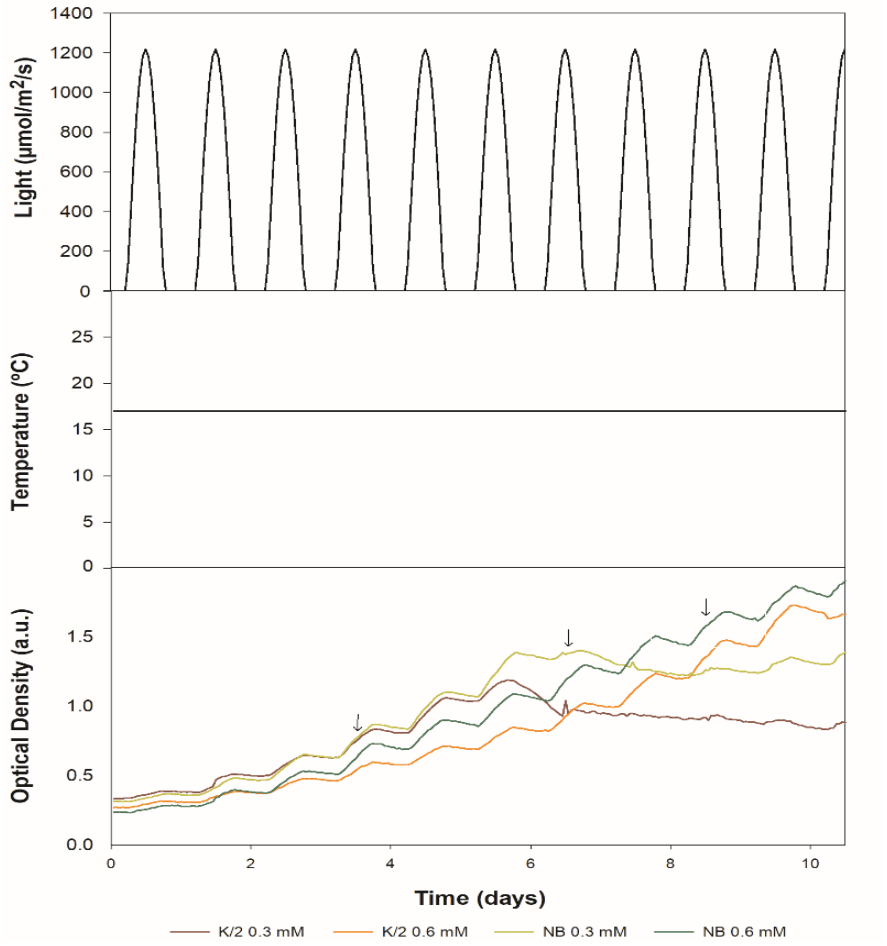

Figure 11– Growth performance of *Emiliania huxleyi* when exposed to different culture media and at different concentrations. Arrows represent the replenishment of culture media.

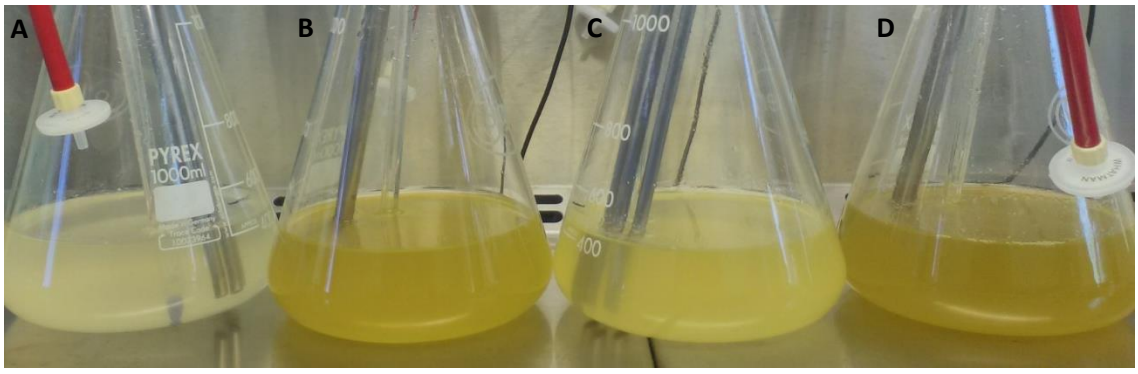

Figure 12 - Cultures at the end of the experiment grown in K/2 with 0.3 mM NO_3^- (A); K/2 with 0.6 mM NO_3^- (B); NB^+ with 0.3 mM NO_3^- (C) and NB^+ with 0.6 mM NO_3^- (D).

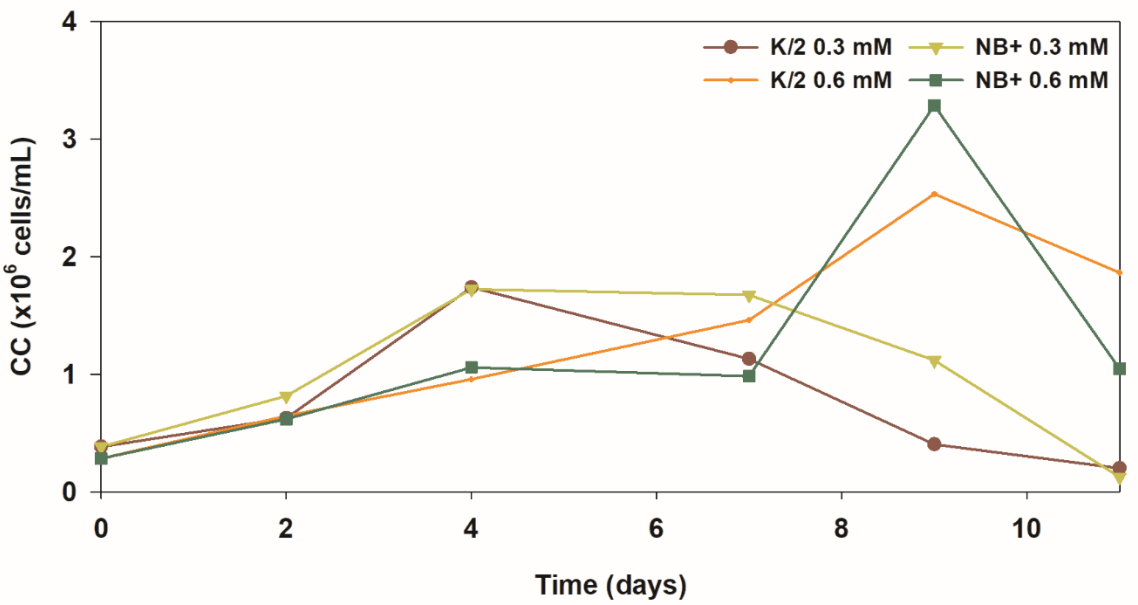

Figure 13 – Cellular concentration of the cultures exposed to different culture media at different concentrations.

To evaluate the status of the culture and understand the transfer efficiency and the status of reduction of the electron acceptors of PSII through the cell, the chlorophyll fluorescence induction kinetics (OJIP) was recorded after dark adaptation of the sample. On day 0, the OJIP curve had J and I inflections, which represents the state of reduction of the Q_A and Q_B acceptors (Fig. 14A). On day 2, it is possible to see that the OJIP curves maintained their typical polyphasic rise and that there was a decrease on the overall area above the fluorescence curve between F_0 and F_m (Table II; Fig. 14B). This area above the OJIP transients (A_0) is related to the number of electrons that are transported through the electron transport chain before F_m is reached (Kalaji et al. 2014).

At this point, the cultures exposed to NB^+ had a higher A_0, which indicates that the cultures were not under stress. Finally, at day 9, the cultures exposed to 0.3 mM of NO_3^- had a smaller A_0 (Table II), most probably due to the fact that the culture collapsed (Fig. 13). At day 9, the OJIP did not maintain its polyphasic rise. This could be explained by the calcification initiated by the cells, a process which is thought to be dependent on the availability of nutrients in the culture media. Jakob et al. (2018) showed that the calcification process is related to the concentration of several trace elements (e.g., Sr).

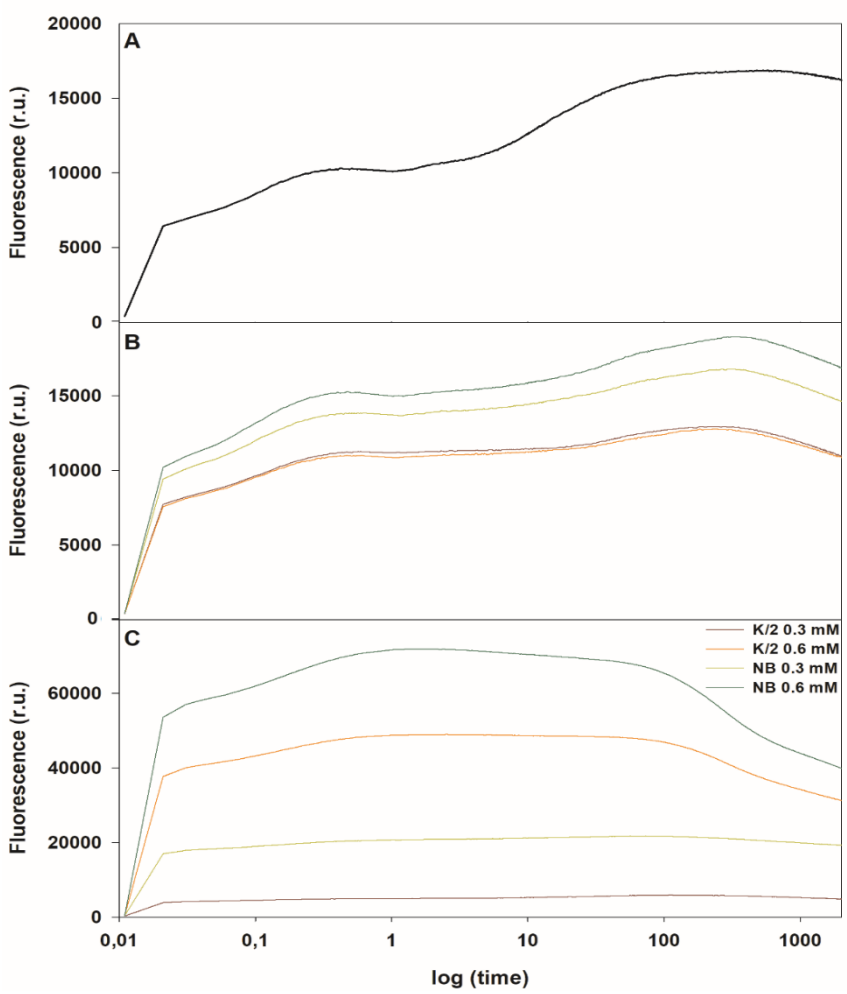

Figure 14 – Rapid fluorescence induction kinetics (OJIP test) of *Emiliania huxleyi* cultures in the trial for culture media optimization, at mid-day (12:00h) at day 0 (A), day 2 (B) and day 9 (C).

Table II: Areas (A_0) between the fluorescence curve and F_m of the OJIP test performed in the culture media optimization trial.

	K/2 at 0.3 mM of NO_3^-	K/2 at 0.6 mM of NO_3^-	NB^+ at 0.3 mM of NO_3^-	NB^+ at 0.6 mM of NO_3^-
Day 0	7.72×10^6	7.72×10^6	7.72×10^6	7.72×10^6
Day 4	2.19×10^6	2.14×10^6	4.11×10^6	5.17×10^6
Day 9	6.02×10^5	4.83×10^6	2.15×10^6	2.88×10^6

The cultures supplemented with 0.6 mM of NO_3^- presented a higher area than the ones supplemented with 0.3 mM of NO_3^- . However, the unusual shape of the curve and the decline at the end may have been caused by lower amounts of available PSII donor sites due to partial damage of the photosynthetic apparatus (Kalaji et al. 2014). This might explain why the cultures rapidly lost cell counts on day 11 (Fig. 13), showing early signs of physiological stress caused most probably by nutrient depletion.

From these results, NB^+ was defined as the optimal culture medium. The ideal concentration of NO_3^- was defined as 0.3 mM until the culture reached an OD of 1 and, after that, the cultures were supplemented with 0.6 mM of NO_3^- every 2 days, allowing for a decrease of the impact of nutrient limitation on growth (Müller et al. 2017).

5.1.2. TEMPERATURE OPTIMIZATION

In order to understand the optimal range of temperatures, a trial using four different temperatures was performed: 17ºC, 20ºC, 23ºC and 26ºC. In this trial, NB^+ was supplemented at 0.3 mM of NO_3^- and when the cultures reached an OD of 1, the concentration of NO_3^- was increased to 0.6 mM, as defined in the previous trial. Thereafter, NB^+ was added every two days, along with $NaHCO_3^-$.

Out of the four tested temperatures, the culture that showed the best growth performance was the one exposed to 23 ºC, followed by those at 20, 17 and 26 ºC (Fig. 15). Unlike the previous trial, none of the cultures reached the white phase at day 11, but the cultures at 17º, 20º and 23ºC apparently started the calcification process (Fig. 16). However, the estimation of CC showed a different result (Fig. 17), with a higher CC at

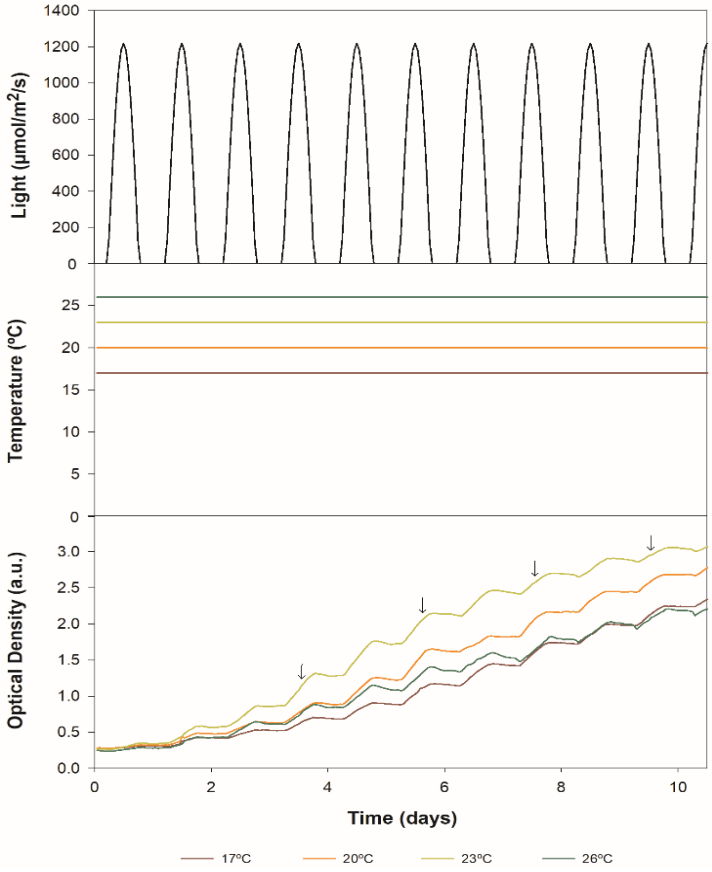

Figure 15 – Growth performance of *Emiliania huxleyi* when exposed to different temperatures. Arrows represent the replenishment of culture media.

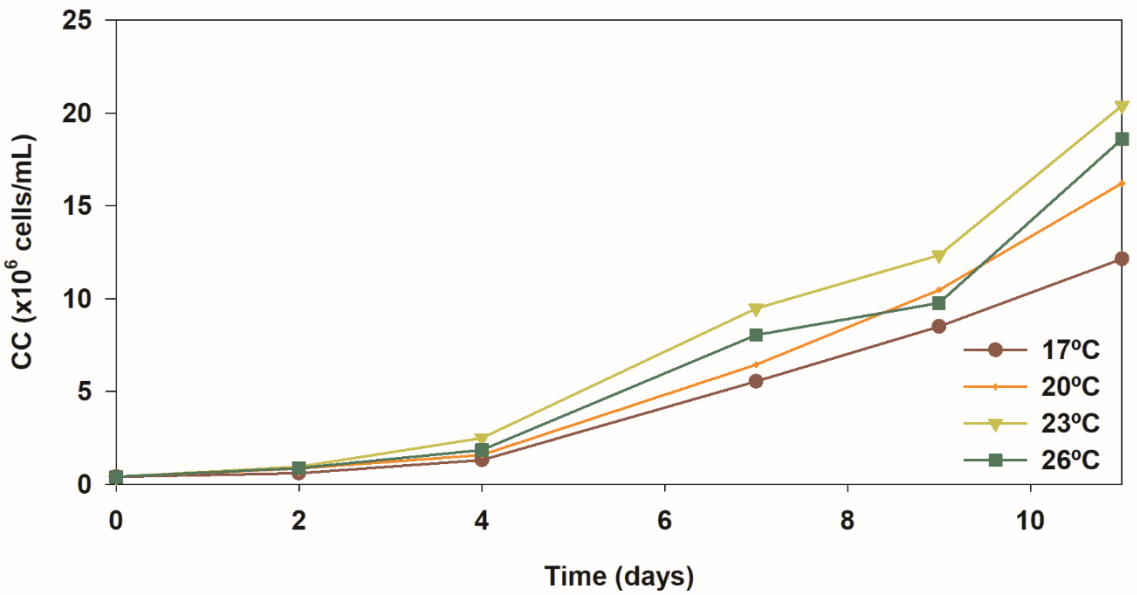

Figure 16 – Cellular concentration of the cultures exposed to different temperatures.

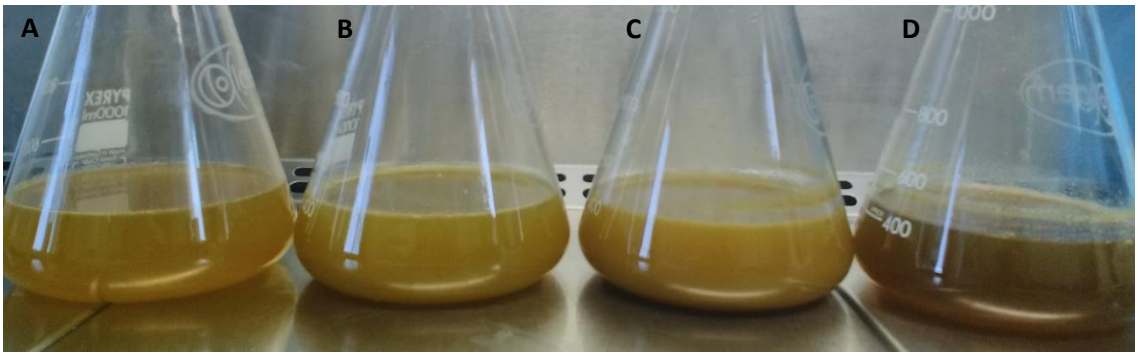

Figure 17 – Cultures at the end of the experiment, exposed to: 17º (A); 20º (B); 23º (C) and 26ºC (D).

23º and 26ºC. This difference may be related with the detached coccoliths produced by the cells that may have influenced the OD in the cultures exposed to 17º and 20ºC. The ability of this *E. huxleyi* strain to grow at these temperatures is probably consistent with its origin of isolation (Conte et al. 1998), which also prevented it from growing at higher temperatures (results not shown). When temperature is elevated towards the optimal range for growth, processes like protein synthesis, light saturated photosynthesis and cell division increase (Skau et al. 2017). Elemental production (PIC, POC) have also been defined as positively correlated with temperatures over the sub-optimal to optimal temperature of growth (Rosas-Navarro et al. 2016).

Regarding fluorescence monitoring, the OJIP curve presented a similar response at day 0 as in the previous trial, maintaining the polyphasic rise (Fig. 18A). At day 2, the fluorescence response by the cultures increased due to a correspondent increase in CC (Fig. 18B). The cultures exposed to 23ºC and 26ºC presented a higher A_0 than the cultures grown at 17ºC and 20ºC, with their OJIP curve not presenting the typical polyphasic rise (Table III; Fig. 18B), which may be related to a slower growth rate (Malapascua et al. 2014). At day 4, that pattern remains. Nonetheless, the fluorescence response increased, most probably because the CC was higher (Fig. 18C). The cultures at 23ºC and 26ºC maintained the higher A_0 with slight J and I inflections, representing the reduced state of

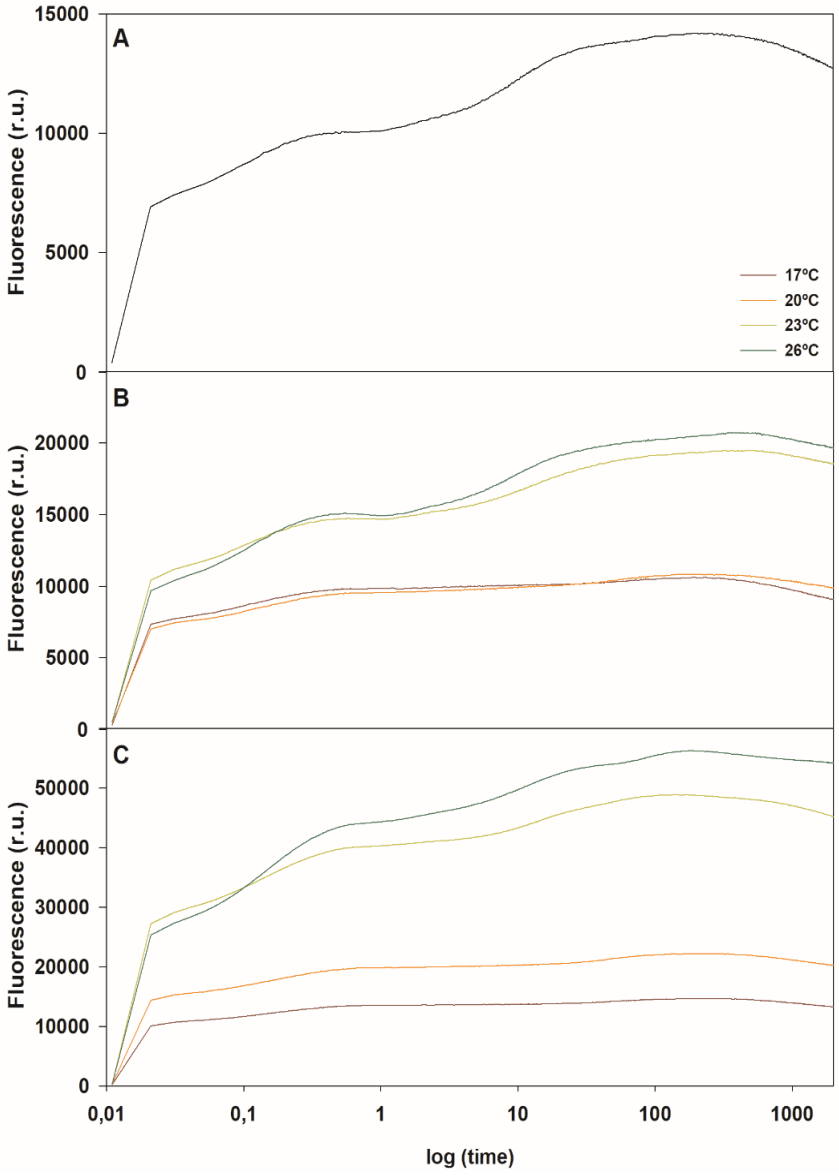

Figure 18 – Rapid fluorescence induction kinetics (OJIP test) of *Emiliania huxleyi* cultures in the trial for temperature optimization, at mid-day (12:00h) at day 0 (A), day 2 (B) and day 4 (C).

Table III: Areas (A_0) between the fluorescence curve and F_m of the OJIP test performed in the temperature optimization trial.

	17ºC	20ºC	23ºC	26ºC
Day 0	2.56×10^6	2.56×10^6	2.56×10^6	2.56×10^6
Day 2	1.93×10^6	2.45×10^6	6.71×10^6	6.71×10^6
Day 4	$2{,}84\times10^6$	3.86×10^6	6.66×10^6	9.81×10^6

the PSII acceptors and the transport of electrons through the photosystem (Malapascua et al. 2014). Because of the increase in CC in this trial, samples analysed after day 4 were very dense and the equipment was not able to make proper readings.

E. huxleyi is normally grown at a temperature of 18 ºC (Hagino et al. 2011; Mayers et al. 2016; Shemi et al. 2016). The highest growth temperatures previously reported for *E. huxleyi* were 25ºC (Moheimani 2005; Kotajima et al. 2014) and 27-30ºC (Conte et al. 1998). In this trial, *E. huxleyi* was also able to grow at 26ºC, showing an adaptation to higher temperatures, which is a requirement for industrial production in the south of Portugal. However, optimal temperature conditions should be determined for each strain due to strain-specific characteristics (Jakob et al. 2018).

From these results, 23ºC was selected as the optimal temperature for growth due to the highest OD and CC achieved at the end of the trial.

5.1.3. LIGHT INTENSITY OPTIMIZATION

In order to select the optimal light intensity for *E. huxleyi* growth, a trial using four different light intensities was performed. Cultures were exposed to PFDs of 600, 900, 1200 and 1500 µmol photons/m^2/s. Nutrient supplementation was equally done as in the previous trial and the temperature selected for growth was 23ºC.

Throughout the experiment, all four cultures presented a similar growth response to different light intensities (Fig. 19), not presenting any significant differences. As previously observed in the temperature trial, none of the cultures reached the white phase (Fig. 20), but the cultures exposed to 900, 1200 and 1500 µmol/m^2/s seemed to have started the calcification process. CC is also in accordance to the growth performance shown previously (Fig. 17 and 21), with no significant differences between the different treatments.

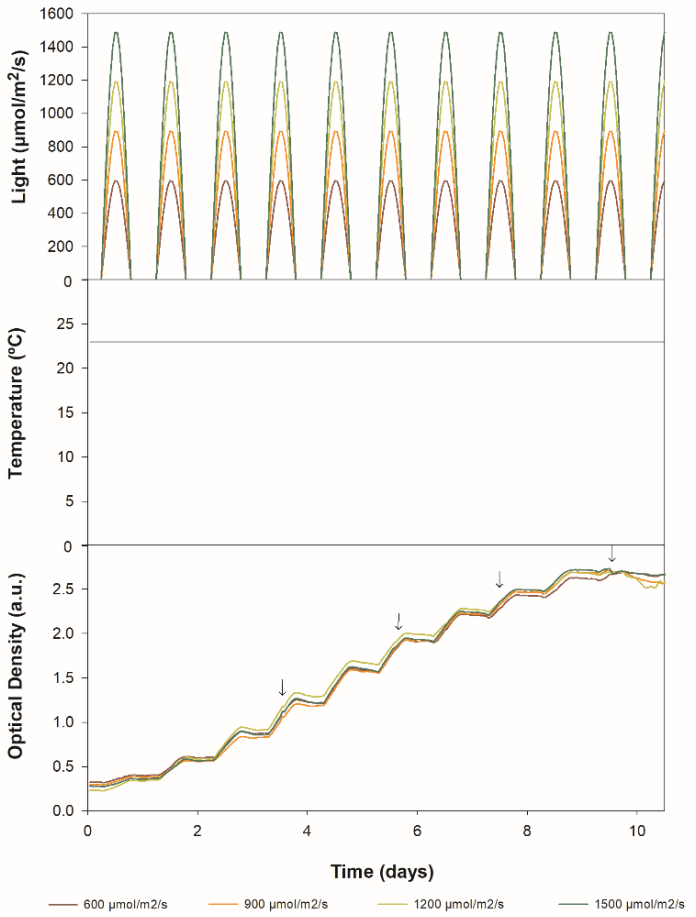

Figure 19 – Growth performance of *Emiliania huxleyi* when exposed to different light intensities. Arrows represent the replenishment of culture media.

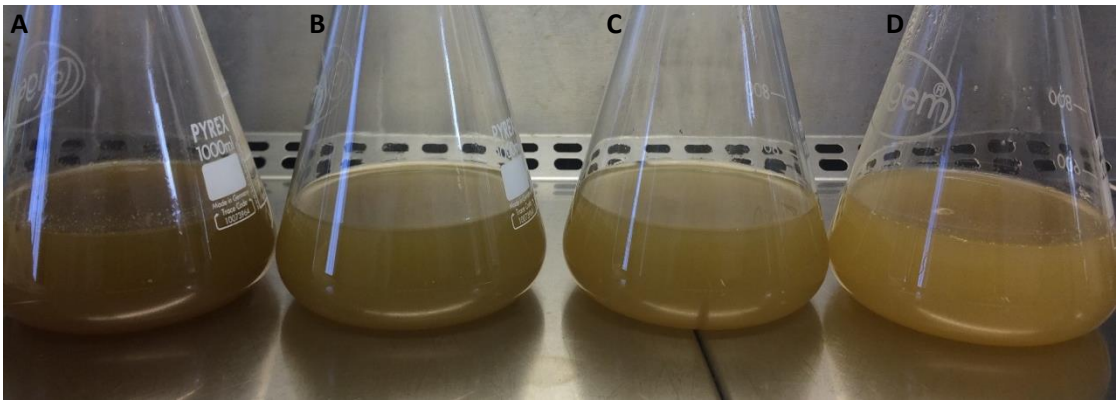

Figure 20– Cultures at the end of the experiment, exposed to: 600 (A); 900 (B); 1200 (C) and 1500 µmol photons/m^2/s (D).

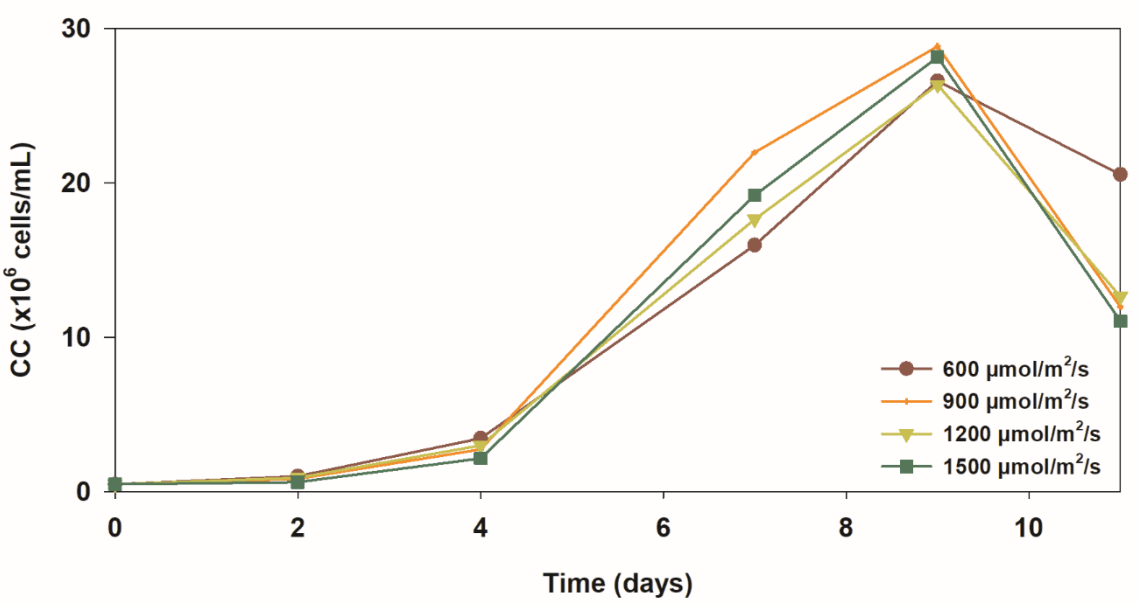

Figure 21 – Cellular concentration of the cultures exposed to different light intensities.

Regarding fluorescence monitoring, at day 0, it is possible to see that the culture is apparently not adapted to high light intensities (Fig. 22A), because the curve does not show the J and I inflections. At day 2 (Fig. 22B), the cultures exposed to 600 and 900 µmol/m^2/s showed a higher A_0 (Table IV), suggesting that these cultures were better adapted to these two light intensities, whereas those exposed to higher PFDs seemed to have undergone some degree of photoinhibition. However, the correspondent OJIP curves

Table IV: Averaged areas (A_0) between the fluorescence curve and F_m of the OJIP test performed at different light intensities.

	600 µmol photons/m^2/s	900 µmol photons/m^2/s	1200 µmol photons/m^2/s	1500 µmol photons/m^2/s
Day 0	1.79×10^6	1.79×10^6	1.79×10^6	1.79×10^6
Day 2	2.69×10^6	1.14×10^6	5.45×10^5	9.81×10^4
Day 9	6.72×10^6	3.70×10^6	1.18×10^6	5.29×10^5

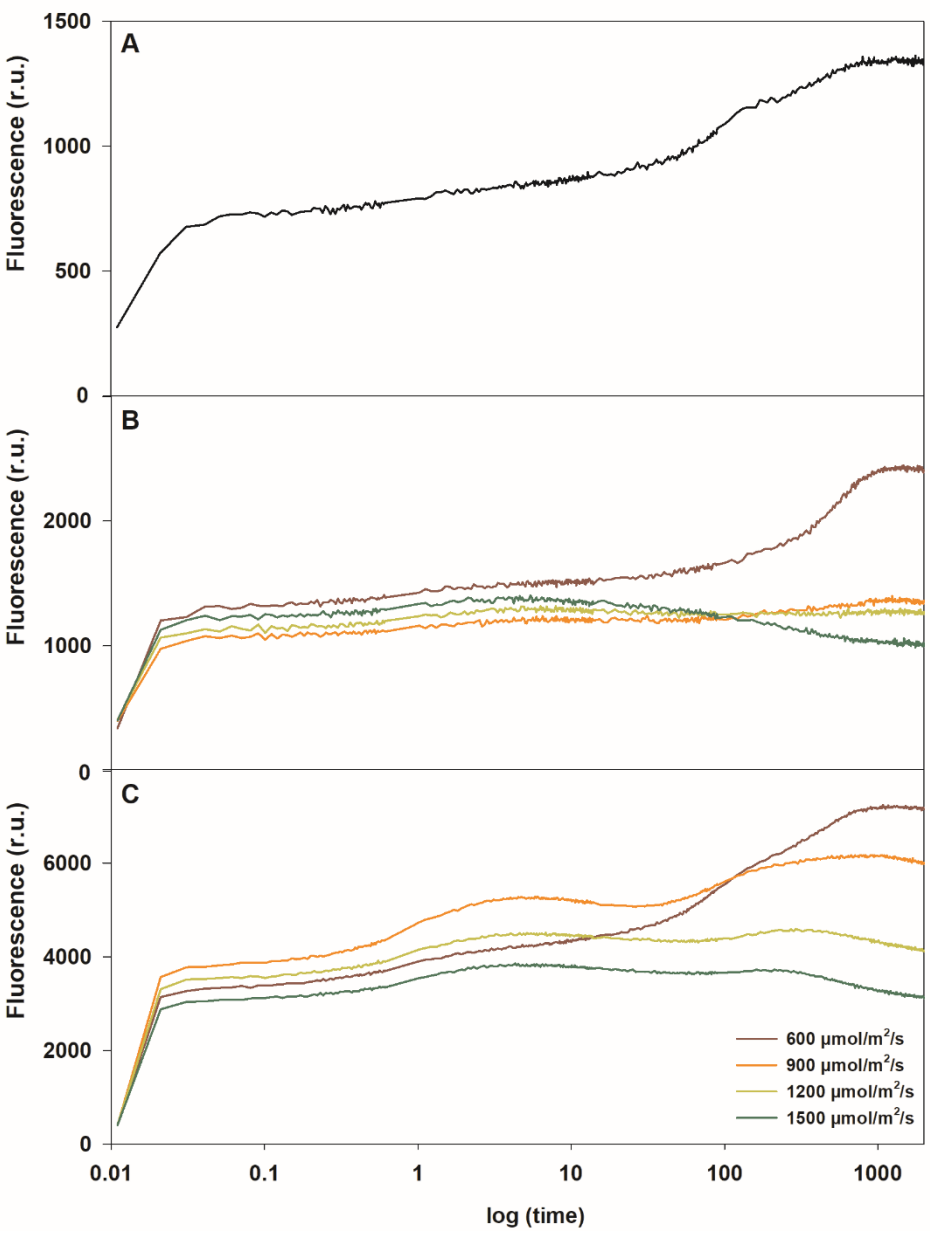

Figure 22 - Rapid fluorescence induction kinetics (OJIP test) of Emiliania huxleyi cultures in the trial for light intensity optimization, at mid-day (12:00h) at day 0 (A), day 2 (B) and day 7 (C).

on this day (Fig. 22B) shows very little difference, while the contrary happens on A_0 (Table IV). Because the time is represented in logarithmic scale, it is possible that the fluorescence values for $t > 100$ have a higher importance. At day 9 (Fig. 22C), the culture exposed to 600 and 900 µmol/m^2/s presented the typical polyphasic rise of the OJIP curve with a high I inflection that represents slow electron transport beyond the P maximum, which is probably explained by the slow growth rate of this species (Malapascua et al. 2014). The cultures under 1200 and 1500 µmol/m^2/s had a smaller A_0 (Table IV) and no

J and I inflection in their OJIP curves, once again suggesting that these cultures were partially photoinhibited (Hariskos et al. 2015).

These results are in accordance with Perrin et al. (2016), who showed a higher CC under low light conditions. Nanninga & Tyrrell (1996) demonstrated that photoinhibition occurs at PFDs higher than 1000 µmol/m^2/s (Fig. 22), which was again confirmed by Hariskos et al. (2015), who observed photoinhibition at light intensities higher than 500 µmol/m^2/s and growth inhibition at higher irradiances was also observed in *E. huxleyi*. Nonetheless, optimal light conditions should be individually determined for each strain due to strain-specific light requirements (Hariskos et al. 2015; Jakob et al. 2018).

Because of the similar results obtained among different PFDs, the optimal light intensity was defined as 900 µmol/m^2/s, because the CC at day 7 reached its highest value (Fig. 21).

5.1.4. STANDARD CONDITIONS *VS* OPTIMIZED CONDITIONS

Finally, the last trial performed using the Algem® PBRs was the "standard" conditions (control) *vs.* optimized conditions (Table V). The standard conditions were chosen based on the recommended conditions provided by the RCC. Light intensity was selected based on the mean intensity on the month of April at Necton's facilities, provided by the Algem® software. The conditions under which *E. huxleyi* showed better growth performance were selected as the optimized conditions (Fig. 23).

Throughout the experiment, the duplicates of each condition showed a similar response (Fig. 23) and, as expected, the cultures exposed to the optimized conditions showed a higher growth performance. At the end of the experiment, it was possible to see that the controls had turned whitish (Fig. 24), suggesting that they had started the calcification process.

Regarding CC, there was a decrease in the growth performance of the cultures exposed to the standard conditions after day 7 (Fig. 25), consistent with what takes place with the OD.

Table V: Set of conditions (culture media, temperature and light intensity) used for each culture in the Algem® PBRs.

	Standard conditions	Optimized conditions
Culture Media	K/2	NB^+
Temperature	17ºC	23ºC
Light intensity	1219 µmol/m^2/s	900 µmol/m^2/s

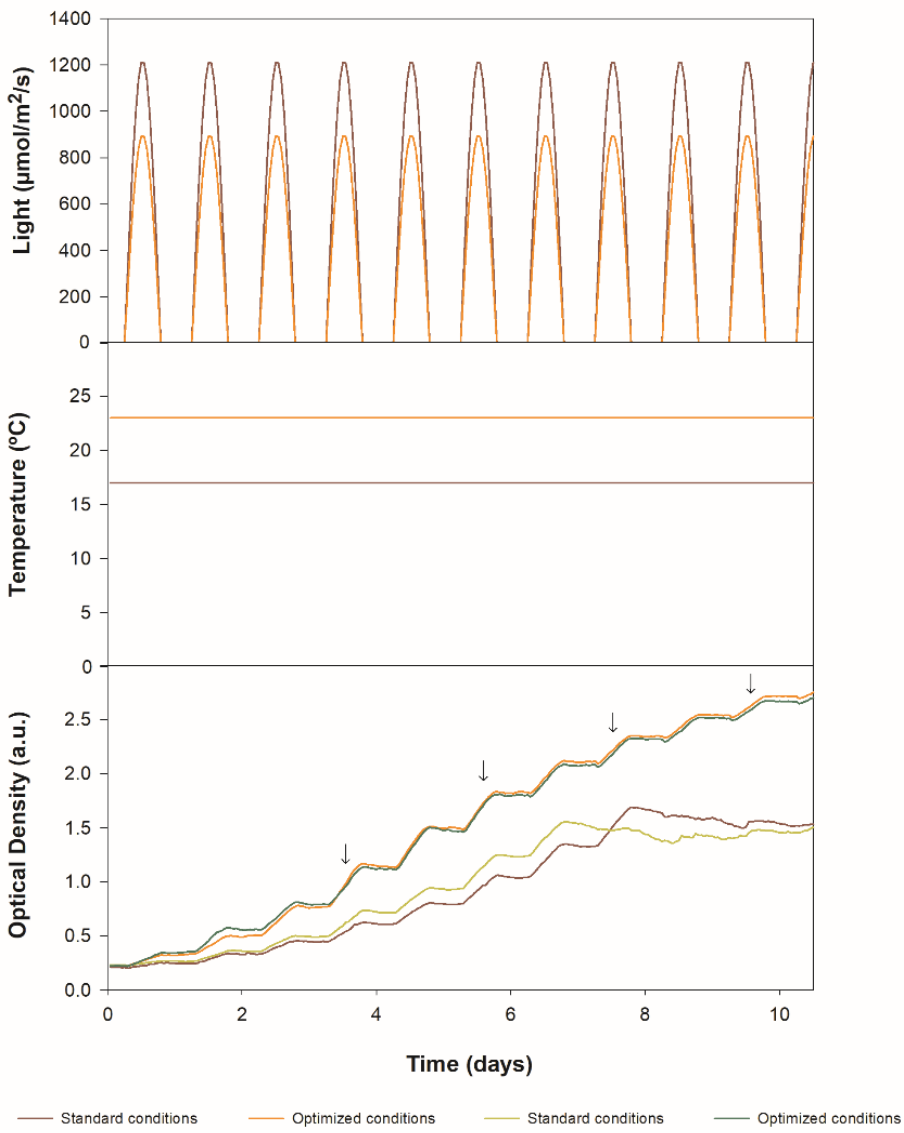

Figure 23 – Growth performance of Emiliania huxleyi when exposed to standard and optimized conditions. Arrows represent the replenishment of culture media.

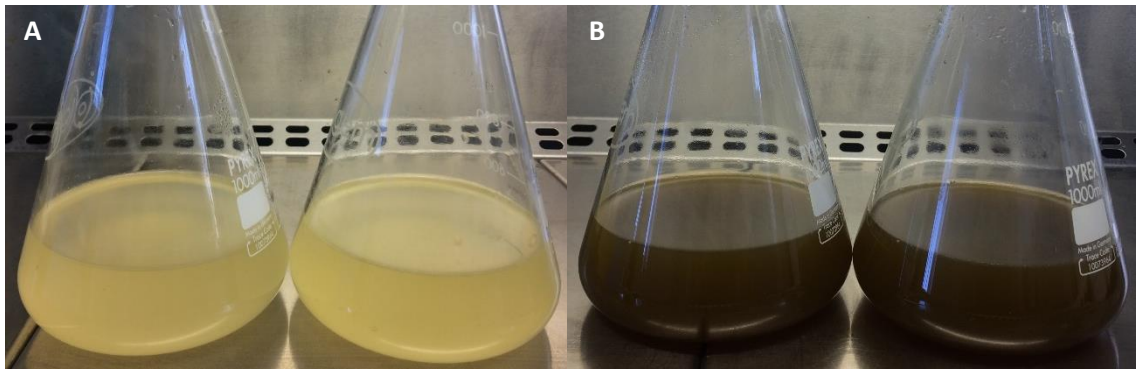

Figure 24 – Cultures at the end of the experiment (day 11) exposed to standard (A) and optimized conditions (B).

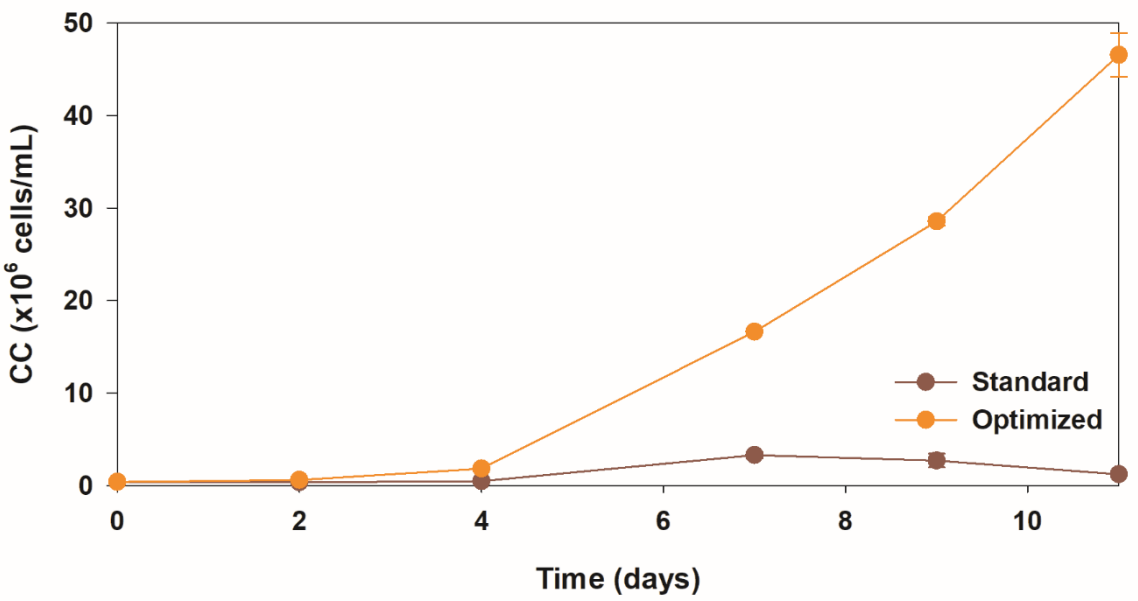

Figure 25 – Cellular concentration of the cultures exposed to standard and optimized conditions.

Fluorescence monitoring showed, at day 0, an OJIP curve with no inflections. This suggests a high level of electron acceptor reduction and a slow electron transport that may be explained by the low CC of the cultures. At day 4, the cultures exposed to the optimized conditions possessed a higher A_0 than the standard conditions (Table VI; Fig. 26B). The correspondent OJIP curves for the optimized conditions showed a slight J and I inflection, probably caused by a reduction of the PQ pool acceptors and a culture photosynthetically competent and growing well (Malapascua et al. 2014). At day 7 and 9, the same cultures presented a higher A_0 and a more typical OJIP curve (Table VI; Fig. 26C-26D) than the ones exposed to the standard conditions, suggesting a better response to the optimal conditions. Conversely, the algae grown under "standard" conditions had a smaller A_0 since day 4, which implies that the conditions to which the cultures were exposed were not optimal.

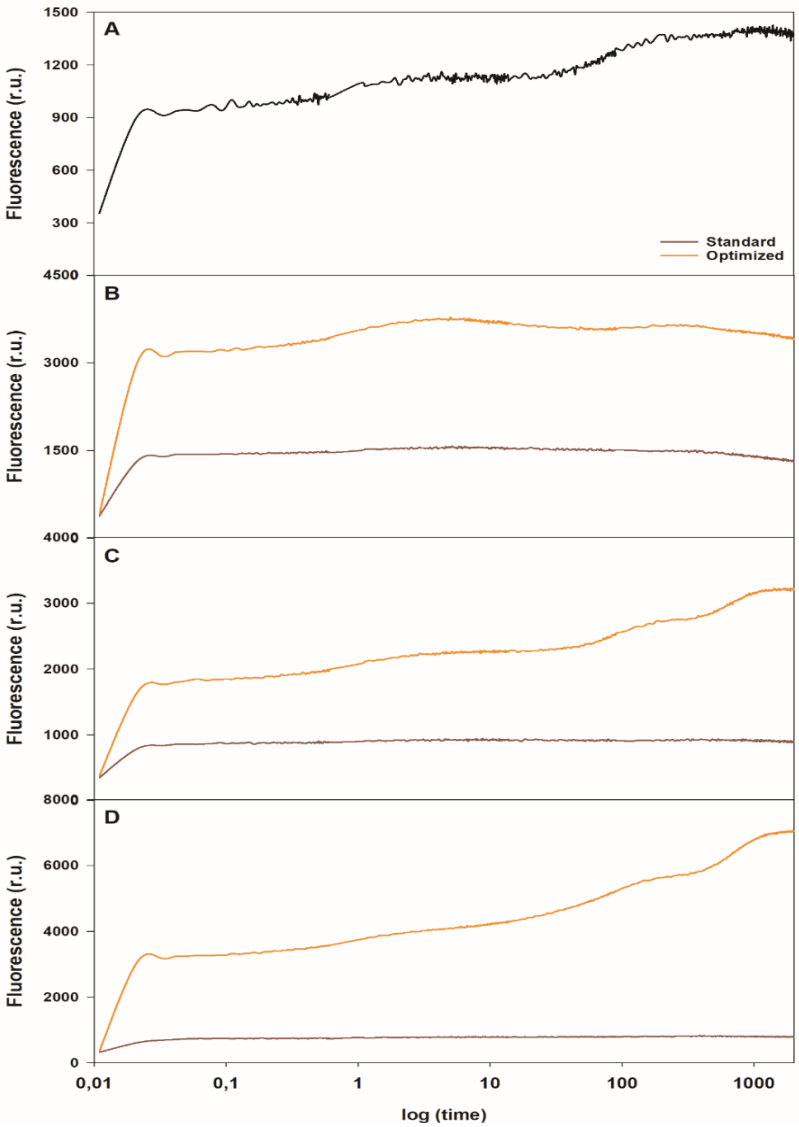

Figure 26 – Rapid fluorescence induction kinetics (OJIP test) of *Emiliania huxleyi* cultures in the trial of optimized conditions, at mid-day (12:00h) at day 0 (A), day 4 (B), day 7(C) and day 9 (D).

Table VI: Averaged areas (A_0) between the fluorescence curve and F_m of the OJIP test performed on the standard *vs* optimization trial and respective standard deviation.

	Standard conditions	Optimized conditions
Day 0	1.42×10^{6}	1.42×10^{6}
Day 4	$5.11\times10^{5} \pm 3.81\times10^{5}$	$1.86\times10^{6} \pm 1.17\times10^{6}$
Day 7	$2.64\times10^{5} \pm 1.38\times10^{4}$	$4.43\times10^{6} \pm 2.24\times10^{5}$
Day 9	$1.86\times10^{5} \pm 5.54\times10^{4}$	$1.11\times10^{7} \pm 2.93\times10^{5}$

NPQ values can reveal an activation of photoprotection mechanisms as a response to excess light (Lambrev et al. 2012). From day 0 to day 2, NPQ values decreased under both the standard and optimized conditions, showing that the cultures were able to use a great part of the energy to which they were exposed. Over the course of this experiment, NPQ values increased from day 2 to day 4 (Table VII). This increment revealed a higher need of the cells to cope with excess light by its dissipation in the form of heat (Malapascua et al. 2014). After day 4, NPQ values of the cultures exposed to the optimized conditions decreased until the end of the experiment. This suggests that the cells were able to use all the energy to which they were exposed, thereby not needing to dissipate it in the form of heat. On the other hand, the cultures exposed to the standard conditions had an increase in NPQ after day 7, which may have been due to light energy absorption exceeding the capacity for light utilization. This can lead to photodamage and, if persistent over time, photoinhibition (Muller et al. 2001; Lambrev et al. 2012).

The cultures that were exposed to the standard conditions had a decline in growth as shown in Fig. 23 and Fig. 25. Microscopic observations, showed that at day 7, a high percentage of cells presented coccoliths in their surface or detached from the cells (Fig. 27). Conversely, the cultures exposed to the optimized conditions, only started showing the formation of coccoliths at day 11 (Fig. 28).

Table VII: Averaged non-photochemical quenching (NPQ) values performed in the standard *vs* optimized conditions trial, and respective standard deviation.

	Standard conditions	Optimization conditions
Day 0	0.250	0.250
Day 2	0.070 ± 0.050	0.070 ± 0.070
Day 4	0.145 ± 0.055	0.085 ± 0.025
Day 7	0.070 ± 0.040	0.050 ± 0.010
Day 9	0.080	0.010
Day 11	0.085 ± 0.005	0

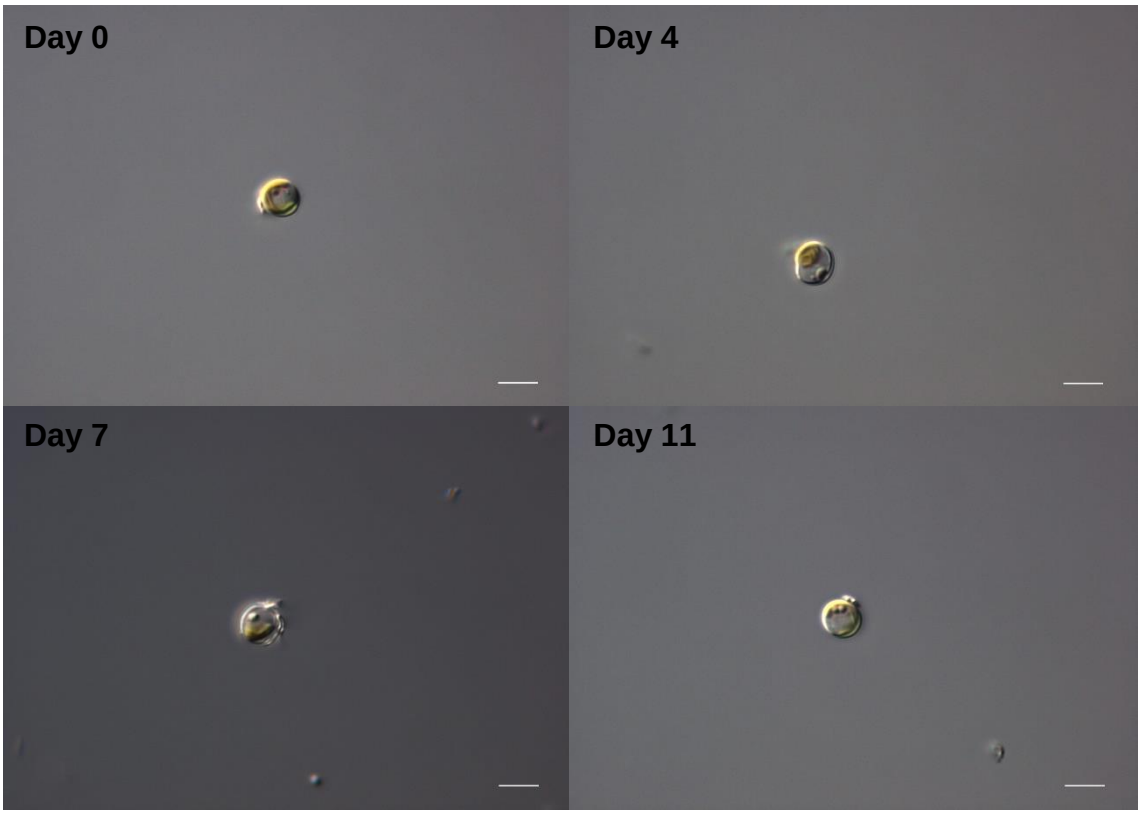

Figure 27 – Microscopic observations of *Emiliania huxleyi* under standard conditions, using DIC and a 100 × lens with an additional 1.6 × amplification provided by an Optovar module. Scale bar = 5 µm.

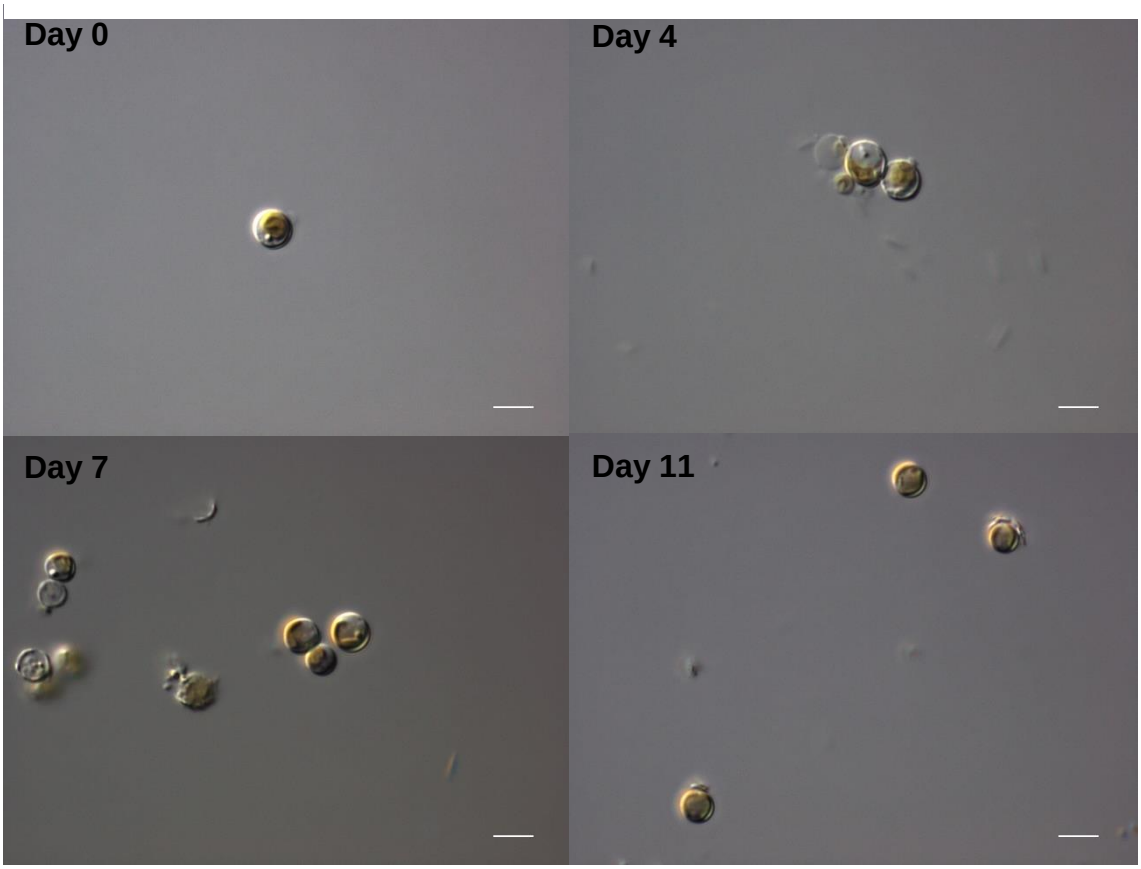

Figure 28 – Microscopic observations of *Emiliania huxleyi* under optimized conditions, using DIC and a 100 × lens with an additional 1.6 × amplification provided by an Optovar module. Scale bar = 5 µm.

5.2. BIOCHEMICAL COMPOSITION

5.2.1. PROTEINS

The total protein content was determined for the standard *vs* optimized conditions trial. The cultures exposed to the optimized conditions had a significantly higher protein content ($p < 0.05$) when compared to the cultures grown in the standard conditions (Table VIII). It has been shown that calcified cultures of *E. huxleyi* possess a lower protein content when compared to non-calcified cultures (Nanninga & Tyrrell 1996). In this work, the cultures exposed to the standard conditions had a higher calcification degree (Fig. 27 and 28). Because coccoliths were still present in the analysed biomass, protein content could be lower as calcium carbonate is present in higher amounts. Another hypothesis is that the protein content difference between both culture conditions may have been caused by the differences in light and culture media between the two treatments, specifically the amount of nitrate present in the medium and the duration of the L:D cycle (Myklestad 1974; van Liere et al. 1979; Fabregas et al. 1984).

Table VIII: Percentage of the protein content of *Emiliania huxleyi* cultures in the standard *vs* optimized conditions trial. Standard and optimized conditions are significantly different ($p < 0.05$) Given values are expressed as mean ± standard deviation.

	Protein content (%)
Standard conditions	22.10 ± 1.36
Optimized conditions	32.69 ± 3.79

5.2.2. LIPIDS

The total lipid content was analysed in all trials carried out in the Algem® PBRs and ranged from 16.8% to 32% of the biomass DW. The highest lipid content was obtained in the light intensity optimization trial, in the culture exposed to 1200 µmol/m^2/s, whereas the lowest lipid content was measured in the culture media optimization trial in the culture growing in NB^+ supplemented with a 0.3 mM NO_3^- (Table IX). It was not possible to identify a clear trend in the effect of culture media, temperature and light intensity on the lipid content. Regarding the standard *vs.* optimized conditions trial, the cultures exposed to the latter settings had a significantly higher lipid content when compared with those under standard conditions ($p < 0.05$). This difference seems to be related with the growth phase in which the cultures were analysed (Lombardi &

Table IX: Percentage of total lipid content of *Emiliania huxleyi* cultures throughout the culture conditions optimization. Standard and optimized conditions are significantly different ($p < 0.05$). Given values are expressed as mean ± standard deviation.

	Lipid content (%)
Culture media optimization[a]	
K/2 0.3 mM NO_3^-	30.91 ± 7.03
K/2 0.6 mM NO_3^-	20.38 ± 3.23
NB^+ 0.3 mM NO_3^-	16.82 ± 0.11
NB^+ 0.6 mM NO_3^-	23.47 ± 1.03
Temperature optimization[b]	
17ºC	25.34 ± 0.33
20ºC	16.96 ± 2.34
23ºC	26.16 ± 6.11
26ºC	28.22 ± 2.00
Light intensity optimization[c]	
600 µmol/m^2/s	26.89 ± 2.46
900 µmol/m^2/s	23.36 ± 0.84
1200 µmol/m^2/s	31.98 ± 1.69
1500 µmol/m^2/s	25.31 ± 2.05
Standard conditions[d]	21.73 ± 0.65
Optimized conditions[e]	26.15 ± 0.91

[a] 17 ºC, 1219 µmol/m^2/s

[b] NB^+ 0.3 and 0.6 mM NO_3^-, 1219 µmol/m^2/s

[c] NB^+ 0.3 and 0.6 mM NO_3^-, 23 ºC

[d] K/2 0.3 and 0.6 mM NO_3^-, 17 ºC, 1219 µmol/m^2/s

[e] NB^+ 0.3 and 0.6 mM NO_3^-, 23 ºC, 900 µmol/m^2/s

Wangersky 1995; Fiorini et al. 2010). Under the optimized conditions, the cultures were still in the exponential phase (Fig. 23 and Fig. 25), while the cultures exposed to the standard conditions had already entered in the decline phase. Another factor that can also significantly increase total lipid content is the culture conditions, since stress conditions are known to induce lipid production (Ren et al. 2013; Pereira et al. 2013; Zhu et al. 2016).

5.2.3. FATTY ACIDS COMPOSITION

In general, the FA composition of *E. huxleyi* RCC1250 was mainly composed of myristic (C14:0), palmitic (C16:0), oleic (C18:1), OPA (C18:5n-3), OTA (C18:4n-3) and DHA (C22:6n-3) acids. Moreover, palmitoleic (C16:1), linoleic (LA, C18:2n-6),

EPA (C20:5n-3) and behenic (C22:0) acids were also detected at relevant amounts. The FA profile of *E. huxleyi* has been extensively described and are in accordance with the results here reported (Pond & Harris 1996; Riebesell et al. 2000; Evans et al. 2009; Fiorini et al. 2010; Khozin-Goldberg et al. 2011; Kotajima et al. 2014). Culture conditions are known to alter the composition of the FA profile. For instance, under stress conditions, microalgae tend to accumulate saturated (SFA) and monounsaturated FAs (MUFA) as a survival mechanism when under unfavourable conditions. On the other hand, structural lipids (PUFAs) are found at a higher amount under optimal growth conditions, since PUFAs are essential for effectively maintaining membrane functions (Paliwal et al. 2017). In this context, a brief overview of the effect of different parameters on the FA profile of strain RCC1250 is given below.

In the culture media optimization trial, the concentration of nitrates seems to have a major impact on FA composition. In the cultures supplemented with 0.3 mM of NO_3^-, SFA and MUFAs were present at a higher percentage than PUFAs, with myristic, palmitic and oleic acids as major components (Table X). However, the cultures supplemented with 0.6 mM of NO_3^- had a higher amount of PUFAs detected, with DHA and OPA as the most abundant components. The latter represents a biomarker for *Haptophyta* microalgae (Volkman et al. 1998).

Table X: Fatty acid profile of *Emiliania huxleyi* on the culture media optimization trial. Given values are expressed as mean of total FAME percentages ± standard deviation. n.d., not detected.

Fatty acid (%)	**K/2 0.3 mM NO_3^-**	**K/2 0.6 mM NO_3^-**	**NB^+ 0.3 mM NO_3^-**	**NB^+ 0.6 mM NO_3^-**
C14:0	22.66 ± 0.75	23.73 ± 1.74	20.39 ± 0.41	15.88 ± 0.32
C15:0	2.49 ± 0.02	0.98 ± 0.03	1.68 ± 0.07	1.09 ± 0.01
C16:0	18.38 ± 0.18	9.07 ± 0.18	14.55 ± 0.22	6.03 ± 0.16
C18:0	5.43 ± 0.20	1.84 ± 0.25	4.16 ± 1.16	1.05 ± 0.02
C22:0	4.84 ± 0.39	1.90 ± 0.16	3.18 ± 0.50	1.51 ± 0.02
Σ SFA	53.81 ± 1.55	37.52 ± 2.36	43.96 ± 2.37	25.55 ± 0.53
C16:1	6.19 ± 1.03	2.00 ± 0.57	4.08 ± 0.64	1.27 ± 0.11
C18:1	24.33 ± 1.51	17.90 ± 0.28	20.48 ± 0.18	13.72 ± 0.02
Σ MUFA	30.52 ± 2.54	19.90 ± 0.85	24.56 ± 0.82	14.99 ± 0.13
C18:5*n*-3	3.84 ± 0.28	15.27 ± 0.27	10.66 ± 0.18	20.55 ± 0.47
C18:4*n*-3	3.95 ± 0.30	6.86 ± 0.09	6.19 ± 0.16	10.69 ± 0.12
C18:3*n*-3	n.d.	n.d.	n.d.	0.39 ± 0.03
C18:2*n*-6	1.93 ± 0.07	1.17 ± 0.02	1.92 ± 0.003	2.45 ± 0.06
C20:5*n*-3	3.31	1.14 ± 0.21	1.38	1.14 ± 0.09
C22:6*n*-3	4.29 ± 0.29	18.14 ± 0.46	12.01 ± 0.96	24.25 ± 0.14
Σ PUFA	17.33 ± 0.94	42.58 ± 1.04	32.17 ± 1.30	59.46 ± 0.92

In the temperature optimization trial, microalgae at the lowest and highest temperatures (17ºC and 26ºC, respectively) accumulated a higher amount of SFA and a lower amount of PUFAs, when compared to those growing at 20ºC and 23ºC (Table XI). Myristic, palmitic and oleic acids were the most abundant FA on all temperatures, in accordance with the previous trial. The culture exposed to 17ºC showed the highest amount of MUFAs, which is in disagreement with Kotajima et al. (2014), who showed evidence for a decrease in SFA and an increase in MUFAs under low temperature conditions in *E. huxleyi* cultures transferred from 25ºC into 15ºC.

Wei et al. (2014) also presented evidence for a decrease in PUFAs with the consequent rise of SFA and MUFAs contents in *Nannochloropsis oculata* and *Tetraselmis subcordiformis* cultivated at higher temperatures. These contradictory results may be explained by the different metabolic mechanisms present within different groups of microalgae.

Among the PUFAs detected in *E. huxleyi*, DHA was still the major component, followed by OPA at 17º and 20ºC and OTA at 23º and 26ºC. The latter was not a major component of PUFAs in the previous trial. Because linolenic acid (18:3*n*-3) is a precursor

Table XI: Fatty acid profile of *Emiliania huxleyi* on the temperature optimization trial. Given values are expressed as mean of total FAME percentages ± standard deviation. n.d., not detected.

Fatty acid (%)	**17ºC**	**20ºC**	**23ºC**	**26ºC**
C14:0	33.04 ± 13.02	19.17 ± 0.18	20.28 ± 0.57	29.20 ± 0.96
C15:0	1.96 ± 0.82	1.47 ± 0.001	1.51 ± 0.00	1.53 ± 0.02
C16:0	9.79 ± 1.72	5.58 ± 0.52	6.75 ± 0.58	8.41 ± 0.13
C18:0	1.57	1.36 ± 0.50	0.97 ± 0.27	0.19
C22:0	2.29	1.29 ± 0.04	1.32 ± 0.14	0.77 ± 0.002
Σ SFA	48.64 ± 15.56	28.88 ± 1.24	30.83 ± 1.55	40.10 ± 1.11
C16:1	2.70 ± 0.98	1.17 ± 0.05	1.07 ± 0.04	0.71 ± 0.14
C18:1	6.73 ± 4.33	10.66 ± 0.15	10.91 ± 0.11	10.69 ± 0.07
Σ MUFA	9.43 ± 5.31	11.83 ± 0.19	11.98 ± 0.15	11.40 ± 0.21
C18:5*n*-3	14.81 ± 6.16	20.95 ± 0.45	10.57 ± 0.08	5.81 ± 0.17
C18:4*n*-3	11.07 ± 2.74	12.71 ± 0.30	17.84 ± 0.18	18.45 ± 0.02
C18:3*n*-3	0.83	0.43 ± 0.003	0.62 ± 0.19	0.09
C18:2*n*-6	2.56 ± 0.20	1.59 ± 0.01	1.98 ± 0.03	2.18 ± 0.13
C20:5*n*-3	0.99	1.04	0.97 ± 0.14	0.47 ± 0.02
C22:6*n*-3	14.50 ± 9.33	23.09 ± 0.53	25.21 ± 0.55	21.64 ± 0.84
Σ PUFA	44.77 ± 18.42	59.81 ± 1.30	57.19 ± 1.16	48.64 ± 1.17

for other *n*-3 and *n*-6 PUFA (Pereira et al. 2012), it is possible that it was used for the biosynthesis of OTA.

Regarding the light intensity trial, the amount of SFA and MUFAs increased with the light intensity, myristic, palmitic and oleic acids being the predominant FA. Although OTA and DHA were detected at a higher amount at 600 µmol/m^2/s, both PUFAs decreased with the light intensity (Table XII). These results are consistent with experiments performed with *Nannochloropsis sp.* (Sukenik & Carmeli 1989), *N. gaditana* (Mitra et al. 2015) and *N. salina* (Van Wagenen et al. 2012), which show that PUFA content is inversely related to PFD (Paliwal et al. 2017).

Finally, in the standard *vs*. optimization trial, the cultures exposed to the standard conditions had a higher amount of SFA and MUFAs, indicating a higher level of stress (Paliwal et al. 2017). In the cultures grown at standard conditions, temperature and light intensity had most probably a major impact on the FA composition, as previously discussed (Table XIII). The cultures exposed to the optimized conditions had a higher amount of PUFAs, achieving the highest quantity of DHA (30.36 ± 0.52%) and OTA (18.81 ± 0.59%) in the present study. The FA content of cultures growing under optimized conditions are significantly different from the FA content of the standard conditions: myristic ($p < 0.01$), palmitic ($p < 0.0001$) and oleic ($p < 0.001$) were the major SFA and

Table XII: Fatty acid profile of *Emiliania huxleyi* on the light intensity optimization trial. Given values are expressed as mean of total FAME percentages ± standard deviation. n.d., not detected.

Fatty acid (%)	600 µmol photons/m^2/s	900 µmol photons/m^2/s	1200 µmol photons/m^2/s	1500 µmol photons/m^2/s
C14:0	23.13 ± 0.34	30.69 ± 0.43	30.62 ± 0.08	35.35 ± 0.47
C15:0	0.95 ± 0.03	1.27 ± 0.04	1.43 ± 0.01	1.92 ± 0.04
C16:0	6.85 ± 0.24	9.86 ± 0.22	11.12 ± 0.14	12.58 ± 0.12
C18:0	0.17 ± 0.14	1.01 ± 0.03	1.03 ± 0.03	1.39 ± 0.11
C22:0	1.27 ± 0.23	1.67 ± 0.21	1.77 ± 0.05	1.76 ± 0.02
Σ SFA	32.38 ± 0.98	44.49 ± 0.94	45.98 ± 0.32	52.99 ± 0.75
C16:1	1.40 ± 0.14	1.81 ± 0.20	2.10 ± 0.02	1.85 ± 0.01
C18:1	13.38 ± 0.25	17.25 ± 0.22	17.68 ± 0.02	18.06 ± 0.43
Σ MUFA	14.78 ± 0.39	19.06 ± 0.42	19.79 ± 0.04	19.91 ± 0.44
C18:5*n*-3	7.91 ± 0.10	6.38 ± 0.04	5.37 ± 0.04	5.02 ± 0.07
C18:4*n*-3	18.39 ± 0.15	12.06 ± 0.05	12.42 ± 0.12	8.64 ± 0.07
C18:3*n*-3	0.11	n.d.	n.d.	n.d.
C18:2*n*-6	1.34 ± 0.18	1.04 ± 0.04	1.09 ± 0.03	0.93 ± 0.07
C20:5*n*-3	0.57 ± 0.01	0.46 ± 0.07	n.d.	n.d.
C22:6*n*-3	24.58 ± 0.62	16.51 ± 0.35	15.36 ± 0.002	12.51 ± 0.02
Σ PUFA	52.89 ± 1.06	36.46 ± 0.55	34.23 ± 0.19	27.10 ± 0.23

Table XIII: Fatty acid profile of *Emiliania huxleyi* on the standard *vs.* optimization trial. Given values are expressed as mean of total FAME percentages ± standard deviation. n.d., not detected.

Fatty acid (%)	Standard conditions	Optimized conditions
C14:0	32.99 ± 4.56	21.21 ± 0.75
C15:0	0.84 ± 0.10	1.03 ± 0.15
C16:0	16.50 ± 1.13	5.67 ± 0.48
C18:0	5.57 ± 0.34	0.44 ± 0.30
C22:0	2.17 ± 0.11	1.08 ± 0.34
Σ SFA	58.07 ± 6.24	29.42 ± 2.02
C16:1	2.60 ± 0.54	0.86 ± 0.32
C18:1	23.17 ± 3.01	9.56 ± 0.61
Σ MUFA	25.76 ± 3.55	10.42 ± 0.93
C18:5*n*-3	3.31 ± 0.29	9.37 ± 0.78
C18:4*n*-3	4.20 ± 0.60	18.81 ± 0.55
C18:3*n*-3	0.47 ± 0.06	0.35 ± 0.30
C18:2*n*-6	0.75 ± 0.09	1.29 ± 0.07
C20:5*n*-3	n.d.	0.48 ± 0.02
C22:6*n*-3	7.67 ± 0.99	30.36 ± 0.66
Σ PUFA	16.40 ± 2.03	60.67 ± 2.39

MUFAs, while OTA ($p < 0.0001$) and DHA ($p < 0.0001$) were the major PUFAs detected. In minor amounts, EPA (C20:5*n*-3) was detected in the cultures under optimized conditions.

The production of high-value *n*-3 PUFA was successfully optimized in the course of this work, with an increase of DHA and OTA production by 4- and 5-fold, respectively.

Microalgae are a great source of numerous compounds with commercial interest (pharmaceutical and nutraceutical for example), with the production of LC-PUFAs being one of them (Khozin-Goldberg et al. 2011). *E. huxleyi* is a major source of essential FA for marine ecosystems (Pond & Harris 1996), thus representing a new source of FA as feed supplement in aquaculture (Spolaore et al. 2006). This species also shows great potential as a source of high-value LC-PUFAs, namely DHA and OPA, which are considered an essential element in animal and human nutrition (Boelen et al. 2013).

5.2.4. PIGMENT AND CAROTENOID COMPOSITION

One of the most abundant pigment present in *E. huxleyi* is an acyloxy derivative of fucoxanthin called 19'-hexanoyloxyfucoxanthin (Haxo 1985; Garrido & Zapata 1998; Cook et al. 2011; Garrido et al. 2016). The contents of 19'-hexanoyloxyfucoxanthin and

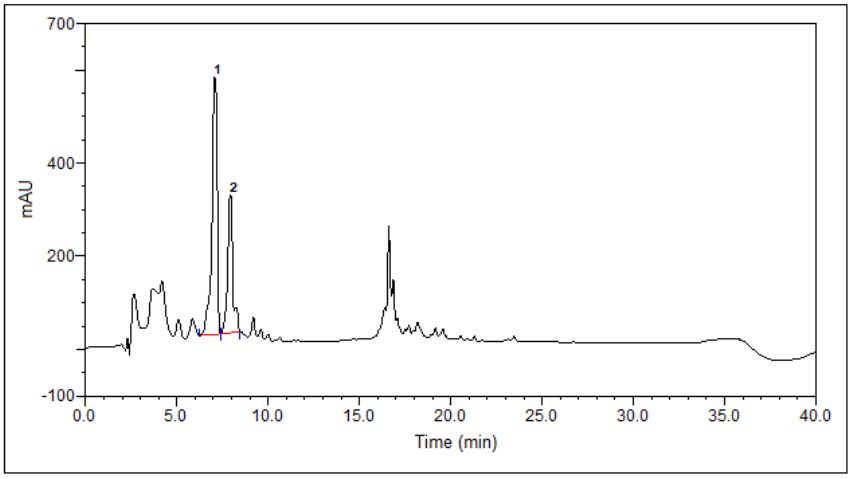

Figure 29 – Example of a chromatogram obtained by HPLC when analysing a sample from the culture exposed to optimized conditions, with the peaks for fucoxanthin (1) and 19'-hexanoyloxyfucoxanthin (2).

fucoxanthin were determined by HPLC in the standard *vs* optimization trial (Fig. 29). and were approximately determined using a fucoxanthin calibration curve and a comparison to previously published chromatograms (Garrido & Zapata 1998; Zapata et al. 2004; Garrido et al. 2016). At the end of the trial, the cultures exposed to different conditions had a very distinct brownish colour, suggesting the increase of fucoxanthin in microalgal cultures (Fig. 22; Cook et al. 2011).

The cultures under standard conditions had a concentration of fucoxanthin of 2.57 ± 0.003 mg/g (Table XIV). The concentration of fucoxanthin more than triplicated ($p < 0.001$) in the cultures exposed to the optimized conditions (8.10 ± 1.37 mg/g). Garrido et al. (2016) showed a higher concentration of 19'-hexanoyloxyfucoxanthin with cultures under low light. The concentration of 19'-hexanoyloxyfucoxanthin was also significantly increased under optimized conditions ($p < 0.0001$), more than doubling from its non-optimal concentration (2.81 ± 0.10 mg/g) to 6.37 ± 0.40 µg/g (Table XIV).

Pigment changes are a mechanism used by *E. huxleyi* and other microalgae to maintain photosynthetic performance linked to variations in light, where they cope with light harvesting and photoprotective capacity (Garrido et al. 2016).

The demand for natural colorants is increasing due to the association of synthetic colorants to several health issues (Mulders et al. 2014). One source for natural pigments is, in fact, microalgae, which may contain concentrations of said pigments in much higher concentrations than those found on higher plants (Mulders et al. 2014). Fucoxanthin is one of those pigments and occurs abundantly in the marine ecosystems (Haxo 1985; Peng et al. 2011; Kim et al. 2012), being produced mainly by *Haptophyta* (Mulders et al. 2014).

Table XIV: Fucoxanthin and 19'-hexanoyloxyfucoxanthin concentration (mg/g) of *Emiliania huxleyi* under standard and optimized conditions. Given values are in mean ± standard deviation.

	Fucoxanthin (mg/g)	19'-hexanoyloxyfucoxanthin (mg/g)
Standard conditions	2.57 ± 0.003	2.81 ± 0.10
Optimized conditions	8.10 ± 1.37	6.37 ± 0.40

This carotenoid is viewed as a valuable pigment (Min et al. 2012), contributing to more than 10% of the estimated total carotenoid production found in nature (Dembitsky & Maoka 2007; Peng et al. 2011). Fucoxanthin can also be used in the pharmaceutical and nutraceutical market because of its physiological and biological properties (such as antiobesity, antitumor, antidiabetes, antioxidant and anticancer activities; Abidov et al. 2010; Woo et al. 2010; Peng et al. 2011; D'Orazio et al. 2012; Zhang et al. 2015).

Besides high-value LC-PUFAs, *E. huxleyi* also represents a source of fucoxanthin, which increases the value of the overall biomass.

5.3. OSTEOGENIC ACTIVITY

The osteogenic activity was assessed *in vivo*, by exposing zebrafish larvae (until 6 dpf) to four concentrations (0.1, 1, 10 and 100 µg/mL) of ethanol, EA and water extracts of *E. huxleyi*. It is noteworthy to highlight that the extracts used in this section did not affect the area of the head of the larvae, and that this was the parameter used to correct the operculum area (Supplementary Data 3).

At the highest concentration tested of ethanolic extract (100 µg/mL), a high toxicity was observed, leading to the death of all zebrafish larvae, at 5 dpf. Conversely, at the lowest concentration (0.1 µg/mL), the extract had no effect on the operculum formation, showing an area similar to the negative control (Fig. 30A). When the larvae were exposed to 1 and 10 µg/mL of ethanolic extract, the operculum formation was significantly increased when compared to the negative control ($p < 0.01$), namely, 10.78 ± 15.03% and 19.54 ± 12.81%, respectively. Interestingly, at 10 µg/mL, the operculum formation showed a similar response ($p < 0.05$) to the positive control (23.64 ± 23.08%).

Regarding the EA extract, larvae exposed to 0.1, 1 and 10 µg/mL had an operculum formation response similar to the negative control ($p < 0.05$), increasing 2.53 ± 11.79%, 2.23% ± 9.48% and 5.30% ± 13.45%, respectively (Fig. 30B). On the other hand, at 100 µg/mL, an increase of 12.17% ± 14.05% in the operculum area led to significant differences ($p < 0.01$) when compared to the negative control (Fig. 25B).

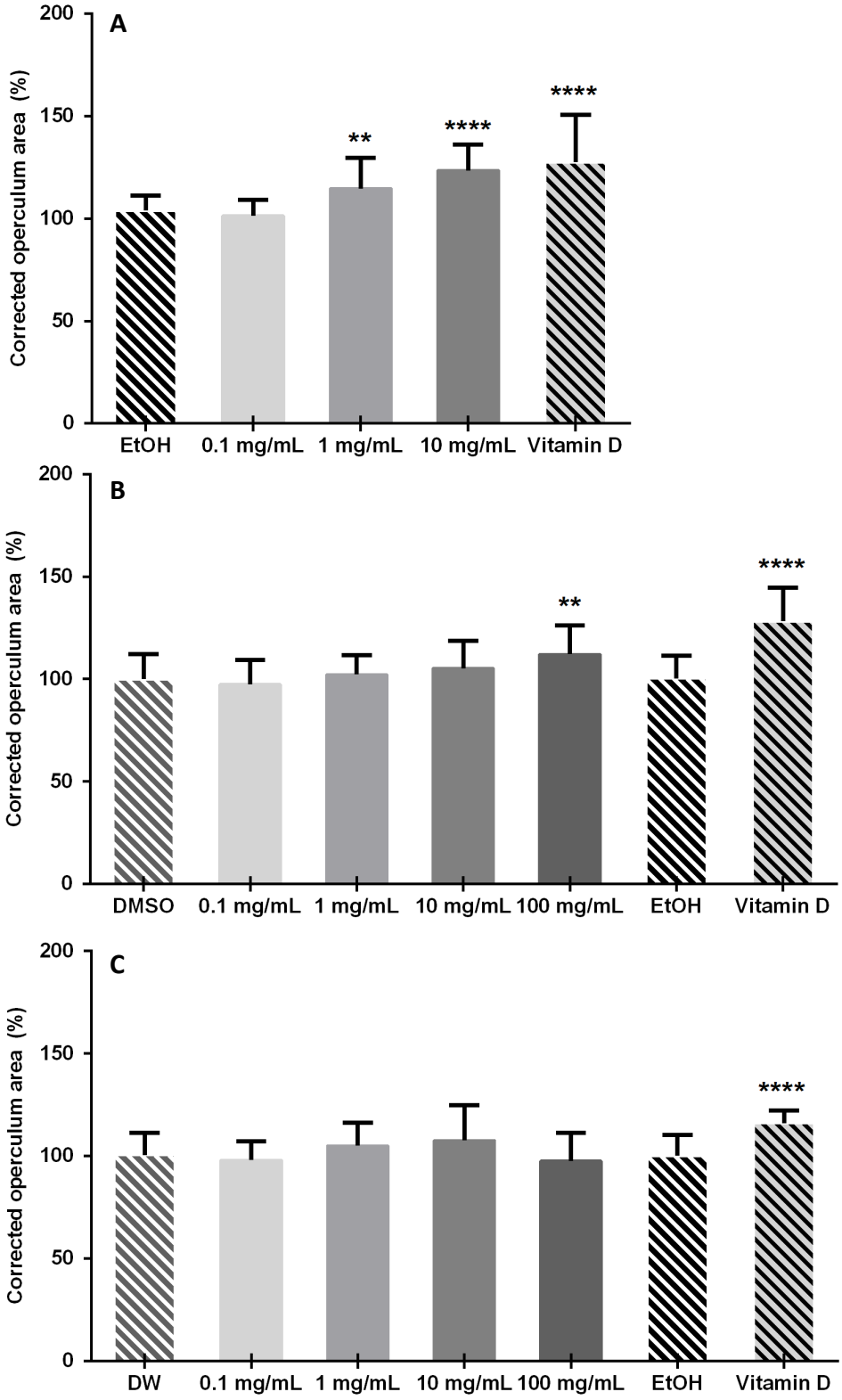

Figure 30 – Effect of ethanol (A), ethyl acetate (B) and water extract (C) on the osteogenic development of zebrafish' operculum (corrected operculum area). Ethanol, DMSO and distilled water (DW) were used as negative controls and vitamin D as a positive control (lined columns). Values are presented as the mean ± standard deviation. Asterisks represent statistically different values according to one-way ANOVA test (**$p < 0.01$; ****$p < 0.05$).

For the water extract, even though small increases (2.51 ± 9.14% at 0.1 µg/mL and 2.89 ± 13.78% at 100 µg/mL) and decreases in the operculum area were found (4.58 ± 11.20% at 1 µg/mL and 7.14 ± 17.20% at 10 µg/mL), none of them showed significant differences in the operculum formation (Fig. 30C). It is therefore possible to conclude that the water extract had no effect on operculum formation at these concentrations.

Zebrafish was chosen to evaluate the osteogenic activity because of several inherent advantages of this model organism, namely, reduced size, high fecundity, short generation time, easy to manipulate and rapid development (Kalueff et al. 2013; Laizé et al. 2014). In addition, zebrafish are sensitive to pharmacological factors, and the operculum represents a reliable system that allows for rapid detection of potential osteogenic activity (Tarasco et al. 2017; Carson et al. 2018).

From all extracts under study, the ethanolic extract showed the highest *in vivo* activity, followed by the EA extract, both causing a significant increase in the operculum area. On the other hand, the water extracts did not display any activity. Overall, it is possible to conclude that the ethanol extract apparently showed a dose-dependent response in the operculum formation. In fact, concentrations of 10 µg/mL and 100 µg/mL for the ethanol and EA extracts, respectively, were enough to cause an increase in the operculum area, suggesting the presence of pro-mineralogenic compounds that are able to stimulate cell proliferation. Nevertheless, the ethanol extract is apparently the most promising one, since the response was as high as the positive control, therefore demonstrating its ability to promote bone growth.

The potential for osteogenic activity has not been tested in microalgae, but rather in macroalgae. Extracts of *Plocamium lyngbyanum* and *Ceramium secundatum* were used for *in vitro* and *in vivo* assays. *P. lyngbyanum* increased the growth of human bone marrow stromal cells *in vitro*, the highest at a concentration of 135 µg/mL and had a greater *in vitro* mineralisation potential. *C. secundatum* promoted osteogenic differentiation at a concentration of 70 µg/mL (Carson et al. 2018).

The identification of the bioactive compounds present in these extracts could be important for the development of novel drug leads to treat osteoporosis or bone fractures. Moreover, the use of the whole biomass or extracts of *E. huxleyi* could also be beneficial as feed or food supplements to treat the aforementioned conditions, or for the pharmaceutical market after the identification of the compound responsible for the bioactivity.

VI CONCLUSIONS

The present study provides novel insights as to how abiotic factors impact the growth performance of *Emiliania huxleyi* RCC1250 in photobioreactors. Overall, the results obtained revealed that the composition of the culture medium is crucial for the optimal growth of this strain. One major conclusion is that high concentrations of NO_3^- during the first days of culture, when the cultures are still diluted, can inhibit growth. However, during the exponential growth phase, the concentration of NO_3^- needs to be increased to ensure optimal growth conditions. Apart from NO_3^- concentration, the overall culture media composition also had a great impact on growth, as cultures cultured in NB^+ showed better growth performance as compared to *E. huxleyi* cultivated in K/2 growth medium. Moreover, temperature and light intensity also influenced the growth performance of *E. huxleyi*. Optimal temperature for the RCC1250 strain was 23ºC, even though it was able to grow at 26 ºC as well. This adequate response to higher temperatures has led to a later onset of the calcification process as compared to other temperatures tested. The optimal light intensity was defined at 900 µmol photons/m^2/s, as higher light intensities promoted photoinhibition of this strain.

The production of high-value compounds was also improved. Under optimized conditions, cultures of *E. huxleyi* showed a greater increase on growth performance, with a correspondent increase on protein content, *n*-3 LC-PUFAs and pigment concentration. In this context, compared to the standard growth conditions, the production of *n*-3 PUFA was successfully optimized with an increase of DHA and OTA production by 4- and 5-fold, respectively. The same pattern was observed for the concentration of fucoxanthin and 19'-hexanoyloxyfucoxanthin, which also increased by 3- and 2-fold, respectively.

Finally, *E. huxleyi* was tested for osteogenic activity, using three different biomass extracts. Ethanolic and EA extracts showed a significant increase on zebrafish' operculum formation, at concentrations of 10 µg/mL and 100 µg/mL, respectively. The ethanolic extract demonstrated a similar response as the positive control. In conclusion, both extracts present pro-osteogenic compounds with possible potential for new drug development.

Overall, *E. huxleyi* shows great potential for the production of biomass for different biotechnological purposes. Because this biomass is rich in high-value *n*-3 PUFAs (mainly DHA and OTA) and fucoxanthin, it could potentially be included in the

maintenance of commercial animal feeds and in food or feed supplements. Moreover, because this species also produces calcium carbonate, this can be used as a substitute for industrial calcite or even used for nanotechnological applications. However, the production protocols are still far from large-scale industrial production. Although there are still several abiotic factors to optimize, the effective production of *E. huxleyi* in industrial facilities, as seen in open ocean (as the major bloom-forming microalgae), can be a breakthrough in microalgal biotechnology.

Abidov, M., Ramazanov, Z., Seifulla, R. & Grachev, S. 2010. The effects of Xanthigen™ in the weight management of obese premenopausal women with non-alcoholic fatty liver disease and normal liver fat. *Diabetes, Obesity and Metabolism*, 12, pp.72–81.

Adl, S. M., Simpson, A.G.B., Lane, C.E., Lukeš, J., Bass, D., Bowser, S.S., Brown, M.W., Burki, F., Dunthorn, M., Hampl, V., Heiss, A., Hoppenrath, M., Lara, E., Gall, L.L., Lynn, D.H., McManus, H., Mitchell, E.A.D., Mozley-Stanridge, S.E., Parfrey, L.W., Pawlowski, J., Rueckert, S., Shadwick, L., Schoch, C.L., Smirnov & A., Spiegel, F.W., 2012. The revised classification of eukaryotes. *Journal of Eukaryotic Microbiology*, 59, pp.429–493.

Aluwihare, L.I. & Repeta, D.J., 1999. A comparison of the chemical characteristics of oceanic DOM and extracellular DOM produced by marine algae. *Marine Ecology Progress Series*, 186, pp.105–117.

Aluwihare, L.I., Repeta, D.J. & Chen, R.F., 1997. A major biopolymeric component to dissolved organic carbon in surface sea water. *Nature*, 387, pp.166–169.

Andersen, R.A., 2004. Biology and systematics of heterokont and haptophyte algae. *American Journal of Botany*, 91, pp.1508–1522.

Andrades, J.A., Becerra, J. & Fernández-Llebrez, P., 1996. Skeletal deformities in larval, juvenile and adult stages of cultured gilthead sea bream (*Sparus aurata* L .). *Aquaculture*, 141, pp.1–11.

APHA, 2000. 4500-NO3- Nitrogen (Nitrate). *Standard Methods for the Examination of Water and Wastewater*, pp.120–129.

Babayan, V.K., 1987. Medium chain triglycerides and structured lipids. *Lipids*, 22(6), pp.417–420.

Bachvaroff, T.R., Puerta, M.V.S. & Delwiche, C.F., 2005. Chlorophyll c-containing plastid relationships based on analyses of a multigene data set with all four chromalveolate lineages. *Molecular Biology and Evolution*, 22, pp. 1772-1782.

Backiel, T., B, K. & Ogorzalek, A., 1984. High incidence of skeletal anomalies in carp, *Cyprinus carpio*, reared in cages in flowing water. *Aquaculture*, 43, pp.369–380.

Balch, W.M., Kilpatrick, K., Holligan, P.M. & Cucci, T., 1993. Coccolith Production and Detachment By *Emiliania huxleyi* (Prymnesiophyceae). *Journal of Phycology*,

29, pp.566–575.

Balch, W.M., 2018. The Ecology, Biogeochemistry, and Optical Properties of Coccolithophores. *Annual Review of Marine Science*, 10, pp.71–98.

Balch, W.M., Fritz, J. & Fernandez, E., 1996. Decoupling of calcification and photosynthesis in the coccolithophore *Emiliania huxleyi* under steady-state light-limited growth. *Marine Ecology Progress Series*, 142, pp.87–97.

Ball, S., Colleoni, C., Cenci, U., Rag, J.N. & Tirtiaux, C., 2011. The evolution of glycogen and starch metabolism in eukaryotes gives molecular clues to understand the establishment of plastid endosymbiosis. *Journal of Experimental Botany*, 62, pp.1775–1801.

Barcelos e Ramos, J., Muller, M.N. & Riebesell, U., 2010. Short-term response of the coccolithophore *Emiliania huxleyi* to an abrupt change in seawater carbon dioxide concentrations. *Biogeosciences*, 7, pp.177–186.

Barreira, L., Resek, E., Rodrigues, M.J., Rocha, M.I., Pereira, H., Bandarra, N., Moreira da Silva, M., Varela, J. & Custódio, L., 2017. Halophytes: Gourmet food with nutritional health benefits? *Journal of Food Composition and Analysis*, 59, pp.35–42.

Bartal, R., Shi, B., Cochlan, W.P. & Carpenter, E.J., 2015. A model system elucidating calcification functions in the prymnesiophyte *Emiliania huxleyi* reveals dependence of nitrate acquisition on coccoliths. *Limnology and Oceanography*, 60, pp.149–158.

Beattie, A., Hirst, E.L. & Percival, E., 1961. Studies on the metabolism of the Chrysophyceae. Comparative structural investigations on leucosin (chrysolaminarin) separated from diatoms and laminarin from the brown algae. *The Biochemical journal*, 79, pp.531–7.

Beaufort, L., Probert, I., Bendif, E.M., Metzl, N., Goyet, C., Buchet, N., Coupel, P., Grelaud, M., Rost, B., Rickaby, R.E.M. & de Vargas, C., 2011. Sensitivity of coccolithophores to carbonate chemistry and ocean acidification. *Nature*, 476, pp.80–83.

Bell, M. V & Pond, D., 1996. Lipid composition during growth of motile and coccolith forms of *Emiliania huxleyi*. *Phytochemistry*, 41, pp.465–471.

Bengtsson, B.-E. & Larsson, A., 1986. Vertebral deformities and physiological effects in fourhorn sculpin (*Myoxocephalus quadricornis*) after long-term exposure to a simulated heavy-metal containing effluent. *Aquatic Toxicology*, 9, pp.215–229.

Bensimon-Brito, A., Cardeira, J., Dionísio, G., Huysseune, A., Cancela, M.L.& Witten, P.E., 2016. Revisiting in vivo staining with alizarin red S - a valuable approach to analyse zebrafish skeletal mineralization during development and regeneration. *BMC Developmental Biology*, 16, pp.1–9.

Berillis, P., 2017. Skeletal deformities in seabreams. Understanding the genetic origin can improve production? *Journal of FisheriesSciences.com*, 11, pp.57–59.

Bernabei, R., Martone, A.M., Ortolani, E., Landi, F. & Marzetti, E., 2014. Screening diagnosis and treatment of osteoporosis: a brief review. *Clinical Cases in Mineral and Bone Metabolism*, 11, pp.201–207.

Bidle, K.D., Haamaty, L., Barcelos e Ramos, J.& Falkowski, P., 2007. Viral activation and recruitment of metacaspases in the unicellular coccolithophore, *Emiliania huxleyi*. *Proceedings of the National Academy of Sciences*, 104, pp.6049–6054.

Biersmith, A. & Benner, R., 1998. Carbohydrates in phytoplankton and freshly produced dissolved organic matter. *Marine Chemistry*, 63, pp.131–144.

Billard C. & Inouye I., 2004. What is new in coccolithophore biology? *In* Coccolithophores - from molecular processes to global impact. Chief Eds.: Thierstein, H.R. & Young, J.R., Springer, pp 1-29.

van Bleijswijk, J.D.L., Kempers, R.S., Veldhuis, M.J. & Westbroek, P., 1994. Cell and growth characteristics of types a and b of *Emiliania huxleyi* (Prymnesiophyceae) as determined by flow cytometry and chemical analyses. *Journal of Phycology*, 30, pp.230–241.

Bligh, E.G. & Dyer, W.J., 1959. A rapid method of total lipid extraction and purification. *Canadian Journal of Biochemistry and Physiology*, 37, pp.911–917.

De Bodt, C., Van Oostende, N., Harlay, J., Sabbe, K. & Chou, L., 2010. Individual and interacting effects of pCO2 and temperature on *Emiliania huxleyi* calcification: Study of the calcite production, the coccolith morphology and the coccosphere size. *Biogeosciences*, 7, pp.1401–1412.

Boelen, P., van Dijk, R., Damsté, J.S.S., Rijpstra, W.I.C. & Buma, A.G.J., 2013. On the potential application of polar and temperate marine microalgae for EPA and DHA production. *AMB Express*, 3, p.26.

Boglione, C., Gagliardi, F., Scardi, M. & Cataudella, S., 2001. Skeletal descriptors and quality assessment in larvae and post-larvae of wild-caught and hatchery-reared gilthead sea bream (*Sparus aurata* L. 1758). *Aquaculture*, 192, pp.1–22.

Borchard, C. & Engel, A., 2012. Organic matter exudation by *Emiliania huxleyi* under

simulated future ocean conditions. *Biogeosciences*, 9, pp.3405–3423.

Borchard, C. & Engel, A., 2015. Size-fractionated dissolved primary production and carbohydrate composition of the coccolithophore *Emiliania huxleyi*. *Biogeosciences*, 12, pp.1271–1284.

Borman, A.H., de Jong, E.W., Huizinga, M., Kok, D.J., Westbroek, P. & Bosch, L., 1982. The role in CaCO3 crystallization of an acid Ca2+-binding polysaccharide associated with coccoliths of *Emiliania huxleyi*. *Eur. J. Biochem*, 129, pp.179–183.

Børsheim, K.Y., Myklestad, S.M. & Sneli, J.A., 1999. Monthly profiles of DOC, mono- and polysaccharides at two locations in the Trondheimsfjord (Norway) during two years. *Marine Chemistry*, 63, pp.255–272.

Brown, C.I. & Núñez, J.M., 1998. Disorders of development. *In* Fish diseases and disorders, Volume 2 - Non-infectious diseases, Chief Eds.: Leatherland, J.F. & Woo, P.T.K., CABI pubisinhg, pp.1-17.

Brown, C.W. & Yoder, J.A., 1994. Coccolithophorid blooms in the global ocean. *Journal of Geophysical Research*, 99, pp.7467–7482.

Bruhn, A., LaRoche, J. & Richardson, K., 2010. *Emiliania Huxleyi* (Prymnesiophyceae): Nitrogen-metabolism genes and their expression in response to external nitrogen sources. *Journal of Phycology*, 46, pp.266–277.

Burki, F., Kaplan, M., Tikhonenkov, D.V., Zlatogursky, V., Minh, B.Q., Radaykina, L.V., Smirnov, A., Mylnikov, A.P. & Keeling, P.J., 2016. Untangling the early diversification of eukaryotes: a phylogenomic study of the evolutionary origins of Centrohelida, Haptophyta and Cryptista. *Proceedings of the Royal Society B: Biological Sciences*, 283, p.20152802.

Carlucci, A.F. & Bowes, P.M., 1970. Production of vitamin B12, thiamine and biotin by phytoplankton. *J Phycol*, 6, pp.351–357.

Carson, M.A., Nelson, J.m Cancela, M.L., Laizé, V., Gavaia, P.J., Rae, M., Heesch, S., Verzin, E., Maggs, C., Gilmore, B.F. & Clarke, S.A., 2018. Red algal extracts from *Plocamium lyngbyanum* and *Ceramium secundatum* stimulate osteogenic activities in vitro and bone growth in zebrafish larvae. *Scientific Reports*, 8, pp.1–12.

Chandra, R., Goswami, D. & Biotech, E., 2011. *Scenedesmus dimorphus* and *Scenedesmus quadricauda*: two potent indigenous microalgae strains for biomass production and CO2 mitigation - A study on their growth behavior and lipid productivity under different concentration of urea as nitrogen source. *Journal of Algal Biomass Utilization*, 2, pp.42–49.

Chau, Y.K., Chuecas, L. & Riley, J.P., 1967. The component combined amino acids of some marine phytoplankton species. *Journal of the Marine Biological Association of the UK*, 47, pp.543–554.

Chisti, Y., 2001. Hydrodynamic Damage to Animal Cells, *Critical Reviews in Biotechnology*, 21, pp.67-110.

Chisti, Y., 2007. Biodiesel from microalgae. *Biotechnology Advances*, 25, pp.294–306.

Coesel, S.N., Baumgartner, A.C., Teles, L.M., Ramos, A.A., Henriques, N.M., Cancela, L. & Varela, J.C.S., 2008. Nutrient limitation is the main regulatory factor for carotenoid accumulation and for Psy and Pds steady state transcript levels in *Dunaliella salina* (Chlorophyta) exposed to high light and salt stress. *Marine Biotechnology*, 10, pp.602–611.

Coleman, R.E., 2006. Clinical features of metastatic bone disease and risk of skeletal morbidity. *Clinical Cancer Research*, 12, pp.6243–6250.

Conte, M.H., Thompson, A., Lesley, D. & Harris, R.P., 1998. Genetic and physiological influences on the alkenone/alkenoate versus growth temperature relationship in emiliania huxleyi and gephyrocapsa oceanica. *Geochimica et Cosmochimica Acta*, 62, pp.51–68.

Conte, M.H., Volkman, J.K. & Eglinton, G., 1994. Lipid biomarkers of the Prymnesiophyceae. *The Haptophyte Algae*, 51, pp.351–377.

Cook, S.S., Whittock, L., Wright, S.W. & Hallegraeff, G.M., 2011. Photosynthetic pigment and genetic differences between two southern ocean morphotypes of *Emiliania huxleyi* (Haptophyta). *Journal of Phycology*, 47, pp.615–626.

Cunningham, M.E., Markle, D.F., Watral, V.G., Kent, M.L. & Curtis, L.R., 2005. Patterns of fish deformities and their association with trematode cysts in the Willamette River, Oregon. *Environmental Biology of Fishes*, 73, pp.9–19.

Custódio, L., Soares, F., Pereira, H., Barreira, L., Vizetto-Duarte, C., Rodrigues, M.J., Rauter, A.P., Alberício, F. & Varela, J., 2014. Fatty acid composition and biological activities of *Isochrysis galbana* T-ISO, *Tetraselmis sp.* and *Scenedesmus sp.*: Possible application in the pharmaceutical and functional food industries. *Journal of Applied Phycology*, 26, pp.151–161.

Custódio, L., Justo, T., Silvestre, L., Barradas, A., Duarte, C.V., Pereira, H., Barreira, L., Rauter, A.P., Alberício, F. & Varela, J., 2012. Microalgae of different phyla display antioxidant, metal chelating and acetylcholinesterase inhibitory activities. *Food Chemistry*, 131, pp.134–140.

D'Orazio, N., Gemello, E., Gammone, M.A., de Girolamo, M., Ficoneri, C. & Riccioni, G., 2012. Fucoxantin: A Treasure from the Sea. *Marine Drugs*, 10, pp.604–616.

Dabrowski, K., Hinterleitner, S., Sturmbauer, C., El-Fiky, N. & Wieser, W., 1988. Do carp larvae require vitamin C? *Aquaculture*, 72, pp.295–306.

Dashiell, C., 2010. A review of the Prymnesiophyta, emphasizing the morphology and systematics of Hymenomonas Stein (1878) and Pleurochrysis Pringsheim (1955). Thesis for the Degree of Master of Science, University of North Carolina Wilmington, pp. 4-5.

von Dassow, P., Ogata, H., Probert, I., Wincker, P., Da Silva, C., Audic, S., Claverie, J. & de Vargas, C., 2009. Transcriptome analysis of functional differentiation between haploid and diploid cells of *Emiliania huxleyi*, a globally significant photosynthetic calcifying cell. *Genome Biology*, 10, p.R114.

Dembitsky, V.M. & Maoka, T., 2007. Allenic and cumulenic lipids. *Progress in Lipid Research*, 46, pp.328–375.

Department of Health and Human Services, U.S., 2004. *Bone Health and Osteoporosis: A Report of the Surgeon General*,

Didymus, J.M., Oliver, P., Mann, S., DeVries, A.L., Hauschka, P.V. & Westbroek, P., 1993. Influence of low-molecular-weight and macromolecular organic additives on the morphology of calcium carbonate. *Journal of the Chemical Society, Faraday Transactions*, 89, p.2891.

Drews-Jr, P., Colares, R.G., Machado, P., de Faria, M., Detoni, A. & Tavano, V., 2013. Microalgae classification using semi-supervised and active learning based on Gaussian mixture models. *Journal of the Brazilian Computer Society*, 19, pp.411–422.

Eissa, A.E., Moustafa, M., El-Husseiny, I.N., Saeid, S., Saleh, O. & Borhan, T., 2009. Identification of some skeletal deformities in freshwater teleosts raised in Egyptian aquaculture. *Chemosphere*, 77, pp.419–425.

Eltgroth, M.L., Watwood, R.L. & Wolfe, G. V., 2005. Production and cellular localization of neutral long-chain lipids in the haptophyte algae *Isochrysis galbana* and *Emiliania huxleyi*. *Journal of Phycology*, 41, pp.1000–1009.

van Emburg, P.R., de Jong, E.W. & Daems, W.T., 1986. Immunochemical localization of a polysaccharide from biomineral structures (coccoliths) of *Emiliania huxleyi*. *Journal of Ultrastructure Research and Molecular Structure Research*, 94, pp.246–259.

Engel, A., Händel, N., Wohlers, J., Lunau, M., Grossart, H.P., Sommer, U. & Riebesell, U., 2011. Effects of sea surface warming on the production and composition of dissolved organic matter during phytoplankton blooms: Results from a mesocosm study. *Journal of Plankton Research*, 33, pp.357–372.

Engel, A., Szlosek, J., Abramson, L., Liu, Z. & Lee, C., 2009. Investigating the effect of ballasting by CaCO3 in *Emiliania huxleyi*: I. Formation, settling velocities and physical properties of aggregates. *Deep-Sea Research II*, 56, pp.1396–1407.

Evans, C., Pond, D.W. & Wilson, W.H., 2009. Changes in *Emiliania huxleyi* fatty acid profiles during infection with *E. huxleyi* virus 86: Physiological and ecological implications. *Aquatic Microbial Ecology*, 55(3), pp.219–228.

Fabregas, J., Abalde, J., Herrero, C., Cabezas, B. & Veiga, M., 1984. Growth of the marine microalga *Tetraselmis suecica* in batch cultures with different salinities and nutrient concentrations. *Aquaculture*, 42, pp.207–215.

Feng, X. & McDonald, J.M., 2011. Disorders of Bone Remodeling. *Annual Review of Pathology: Mechanisms of Disease*, 6(1), pp.121–145.

Fernandez, E., Balch, W.M., Marañon, E. & Holligan, P., 1994. High rates of lipid biosynthesis in cultured, mesocosm and coastal populations of the coccolithophore *Emiliania huxleyi*. *Marine Ecology Progress Series*, 114, pp.13–22.

Fichtinger-Schepman, A.M.J., Kamerling, J.P., Versluis, C. & Vliegenthart, J.F.G., 1981. Structural analysis of acidic oligosaccharides derived from the methylated, acidic polysaccharide associated with coccoliths of *Emiliania huxleyi* (lohmann) kamptner. *Carbohydrate Research*, 93, pp.105–123.

Fiorini, S., Gattuso, J.P., van Rijswijk, P. & Middelburg, J., 2010. Coccolithophores lipid and carbon isotope composition and their variability related to changes in seawater carbonate chemistry. *Journal of Experimental Marine Biology and Ecology*, 394, pp.74–85.

Flynn, K.J., 1990. Composition of intracellular and extracellular pools of amino-acids, and amino-Acid utilization of microalgae of different sizes. *Journal of Experimental Marine Biology and Ecology*, 139, pp.151–166.

Frada, M., Probert, I., Allen, M.J., Wilson, W.H., de Vargas, C., 2008. The " Cheshire Cat " escape strategy of the coccolithophore *Emiliania huxleyi* in response to viral infection. *PNAS*, 105, pp.15944–15949.

Frada, M.J., Bidle, K.D., Probert, I. & de Vargas, C., 2012. In situ survey of life cycle phases of the coccolithophore *Emiliania huxleyi* (Haptophyta). *Environmental*

Microbiology, 14, pp.1558–1569.

Garrido, J.L., Bruner, C. & Rodriguez, F., 2016. Pigment variations in *Emiliania huxleyi* (CCMP370) as a response to changes in light intensity or quality. *Environmental Microbiology*, 18(12), pp.4412–4425.

Garrido, J.L. & Zapata, M., 1998. Detection of new pigments from *Emiliania huxleyi* (Prymnesiophyceae) by high-performance liquid chromatography, liquid chromatography-mass spectrometry, visible spectroscopy, and fast atom bombardment mass spectrometry. *J. Phycol.*, 34, pp.70–78.

Gordon, H.R. & Du, T., 2001. Light scattering by nonspherical particles: Application to coccoliths detached from *Emiliania huxleyi*. *Limnology and Oceanography*, 46(6), pp.1438–1454.

Gouveia, L., Batista, A.P., Sousa, I., Raymundo, A. & Bandarra, N.M., 2008. Microalgae in novel food products. *In* Papadoupoulos, K. - Food Chemistry Research Developments. Nova Science Publishers. pp. 75-112

Green, J.C., Course, P.A. & Tarran, G.A., 1996. The life-cycle of *Emiliani huxleyi*: A brief review and a study of relative ploidy levels analysed by flow cytometry. *Journal of Marine Systems*, 9, pp.33–44.

Guedes, A.C., Amaro, H.M. & Malcata, F.X., 2011. Microalgae as sources of high added-value compounds-a brief review of recent work. *Biotechnology Progress*, 27(3), pp.597–613.

Hagino, K., Young, J.R. & Probert, I., 2011. New evidence for morphological and genetic variation in the cosmopolitan coccolithophore *Emiliania huxleyi* (Prymnesiophyceae) from the COX1b-ATP4 genes. *J. Phycol*, 47, pp.1164–1176.

Haiduc, A.G., Brandenberger, M., Suquest, S., Vogel, F., Bernier-Latmani, R. & Ludwig, C., 2009. SunCHem: an integrated process for the hydrothermal production of methane from microalgae and CO2 mitigation. *J Appl Phycol*, 21, pp.529–541.

Hariskos, I., Rubner, T. & Posten, C., 2015. Investigation of cell growth and chlorophyll a content of the coccolithophorid alga *Emiliania huxleyi* by using simple bench-top flow cytometry. *Journal of Bioprocessing & Biotechniques*, 5, pp.1–8.

Harris, R.P., 1994. Zooplankton grazing on the coccolithophore *Emiliania huxleyi* and its role in inorganic carbon flux. *Marine Biology*, 119, pp.431–439.

Haxo, F.T., 1985. Photosynthetic action spectrum of the coccolithphorid, *Emiliania*

huxleyi (Haptophyceae): 19'hexanoyloxyfucoxanthin as antenna pigment. *Journal of Phycology*, 21, pp.282–287.

Helliwell, K.E., Wheeler, G.L., Leptos, K.C., Goldstein, R.E. & Smith, A.G., 2011. Insights into the evolution of vitamin B 12 auxotrophy from sequenced algal genomes. *Molecular Biology and Evolution*, 28, pp.2921–2933.

Hemaiswarya, S., Raja, R., Ravikumar, R. & Carvalho, I.S., 2013. Microalgae Taxonomy and Breeding. *Biofuel Crops: Production, Physiology and Genetics*, pp.44–53.

Henriksen, K., Stipp, S.L.S., Young, J.R., Marsh, M.E., 2004. Biological control on calcite crystallization: AFM investigation of coccolith polysaccharide function. *American Mineralogist*, 89, pp.1709–1716.

Holligan, P.M., Fcrmindcz, E., Balch, W.M., Boyd, P., Peter, H., Finch, M., Groom, B., Muller, K., Putdie, D.A., Trees, C.C. & Turner, S.M., 1993. A biogeochemical study of the coccolithophore, *Emiliania huxleyi*, in the north Atlantic. *Global Biogeochemical Cycles*, 7, pp.879–900.

Hu, B., Min, M., Zhou, W., Li, Y., Mohr, M., Cheng, Y., Lei, H., Liu, Y., Lin, X., Chen, P. & Ruan, R., 2012. Influence of exogenous CO2 on biomass and lipid accumulation of microalgae *Auxenochlorella protothecoides* cultivated in concentrated municipal wastewater. *Applied Biochemistry and Biotechnology*, 166, pp.1661–1673.

Hu, Q., Sommerfeld, M., Jarvis, E., Ghirardi, M., Posewitz, M., Seibert, M. & Darzins, A., 2008. Microalgal triacylglycerols as feedstocks for biofuel production: Perspectives and advances. *Plant Journal*, 54, pp.621–639.

Hussain, F., Shah, S.Z., Zhou, W., Iqbal, M., 2017. Microalgae screening under CO2 stress: Growth and micro-nutrients removal efficiency. *Journal of Photochemistry and Photobiology B: Biology*, 170, pp.91–98.

Huycke, T.R., Eames, B.F. & Kimmel, C.B., 2012. Hedgehog-dependent proliferation drives modular growth during morphogenesis of a dermal bone. *Development*, 139, pp.2371–2380.

Ietswaart, T., Schneider, P.J. & Prins, R.A., 1994. Utilization of organic nitrogen sources by two phytoplankton species and a bacterial isolate in pure and mixed cultures. *Applied and Environmental Microbiology*, 60, pp.1554–1560.

Iglesias-Rodriguez, M.D., Schofield, O.M., Batley, J., Medlin, L.K. & Hayes, P.K., 2006. Intraspecific genetic diversity in the marine coccolithophore *Emiliania*

huxleyi (Prymnesiophyceae): The use of microsatellite analysis in marine phytoplankton population studies. *Journal of Phycology*, 42, pp.526–536.

Jakob, I., Chairopoulou, M.A., Vucak, M., Posten, C. & Telpel, U., 2017. Biogenic calcite particles from microalgae—Coccoliths as a potential raw material. *Engineering in Life Sciences*, 17, pp.605–612.

Jakob, I., Weggenmann, F. & Posten, C., 2018. Cultivation of *Emiliania huxley*i for coccolith production. *Algal Research*, 31, pp.47–59.

Jeffrey, S.W., 1976. The occurrence of chlorophyll c1 and c2 in algae. *Journal of Phycology*, 12, pp.349–354.

Jones, B.M., Edwards, R.J., Skipp, P.J., O'Connor, C.D. & Iglesias-Rodriguez, M.D., 2011. Shotgun proteomic analysis of *Emiliania huxleyi*, a marine phytoplankton species of major biogeochemical importance. *Marine Biotechnology*, 13, pp.496–504.

De Jong, E.W., Bosch, L. & Westbroek, P., 1976. Isolation and characterization of a ca2+-binding polysaccharide association with coccoliths of *Emiliania huxleyi* (Lohmann) Kamptner. *Eur. J. Biochem.*, 70, pp.611–621.

Jordan, R.W.R. & Chamberlain, A.H.L., 1997. Biodiversity among haptophyte algae. *Biodiversity & Conservation*, 6(1), pp.131–152.

Kalaji, H.M., Schansker, G., Ladle, R.J., Goltsev, V., Bosa, K., Allakhverdiev, S.I., Brestic, M., Bussotti, F., Calatayud, A., Dąbrowski, P., Elsheery, N.I., Ferroni, L., Guidi, L., Hogewoning, S.W., Jajoo, A., Misra, A.N., Nebauer, S.G., Pancaldi, S., Penella, C., Poli, D., Pollastrini, M., Romanowska-Duda, Z.B., Rutkowska, B., Serôdio, J., Suresh, K., Szulc, W., Tambussi, E., Yanniccari, M., & Zivcak, M., 2014. Frequently asked questions about in vivo chlorophyll fluorescence: Practical issues. *Photosynthesis Research*, 122, pp.121–158.

Kalin, M., Wheeler, W.N. & Meinrath, G., 2005. The removal of uranium from mining waste water using algal/microbial biomass. *Journal of Environmental Radioactivity*, 78, pp.151–177.

Kalueff, A.V., Gebhardt, M., Stewart, A.M., Cachat, J.M., Brimmer, M., Chawla, J.S., Craddock, C., Kyzar, E.J., Roth, A., Landsman, S., Gaikwad, S., Robinson, K., Baatrup, E., Tierney, K., Shamchuk, A., Norton, W., Miller, N., Nicolson, T., Braubach, O., Gilman, C.P., Pittman, J., Rosemberg, D.B., Gerlai, R., Echevarria, D., Lamb, E., Neuhauss, S.C.F., Weng, W., Bally-Cuif, L. & Schneider, H., 2013. Towards a comprehensive catalog of zebrafish behavior 1.0 and beyond. *Zebrafish*,

10, pp.70–86.

Kawachi, M., Inouye, I., Maeda, O., Chihara, M. 1991. The haptonema as a food-capturing device: observations on *Chrysochromulina hirta* (Prymnesiophyceae). *Phycologia*, 30, pp.563–573.

Kawai, H. & Inouye, I., 1989. Flagellar autofluorescence in 44 chlorophyll c-containing algae. *Phycologia*, 28(2), pp.222–227.

Kayano, K., Saruwatari, K., Kogure, T. & Shiraiwa, Y., 2011. Effect of coccolith polysaccharides isolated from the coccolithophorid, *Emiliania huxleyi*, on calcite crystal formation in in vitro CaCO3 crystallization. *Marine Biotechnology*, 13, pp.83–92.

Kayano, K. & Shiraiwa, Y., 2009. Physiological regulation of coccolith polysaccharide production by phosphate availability in the coccolithophorid *Emiliania huxleyi*. *Plant and Cell Physiology*, 50, pp.1522–1531.

Keeling, P.J., 2009. Chromalveolates and the evolution of plastids by secondary endosymbiosis. *Journal of Eukaryotic Microbiology*, 56, pp.1–8.

Keeling, P.J., 2010. The endosymbiotic origin, diversification and fate of plastids. *Philosophical Transactions of the Royal Society B: Biological Sciences*, 365, pp.729–748.

Keeling, P.J., 2013. The number, speed, and impact of plastid endosymbioses in eukaryotic evolution. *Annual Review of Plant Biology*, 64(1), pp.583–607.

Keller, M.D., Selvin, R.C., Claus, W. & Guillard, R.R.L., 1987. Media for the culture of oceanic ultraphytoplankton. *Journal of Phycology*, 23, pp.633–638.

Khan, M., Cheung, A.M. & Khan, A.A., 2017. Drug-Related Adverse Events of Osteoporosis Therapy. *Endocrinology and Metabolism Clinics of North America*, 46, pp.181–192.

Khozin-Goldberg, I., Iskandarov, U. & Cohen, Z., 2011. LC-PUFA from photosynthetic microalgae: Occurrence, biosynthesis, and prospects in biotechnology. *Applied Microbiology and Biotechnology*, 91, pp.905–915.

Kim, S.M., Jung, Y. & Kwon, O., 2012. A potential commercial source of fucoxanthin extracted from the microalga *Phaeodactylum tricornutum*. *Appl Biochem Biotechnol*, 166, pp.1843–1855.

Klaveness, D., 1972a. *Coccolithus huxleyi* (Lohm .) Kamptn II. The flagellate cell, aberrant cell types, vegetative propagation and life cycles. *Br. phycol. J.*, 7, pp.309–318.

Klaveness, D., 1972b. *Coccolithus huxleyi* (Lohmann) Kamptner I. - Morphological investigations on the vegetative cell and process of coccolith formation. *Protistologica*, 8, pp.335–346.

Kooistra, W.H.C.F., Gersonde, R., Medlin, L.K. & Mann, D.G., 2007. The origin and evolution of the diatoms: their adaptation to a planktonic existence. *In* Evolution of primary producers in the sea, Chief Eds.: Falkowski, P.G. & Knoll, A.H., Elsevier, pp.207-249.

Kotajima, T., Shiraiwa, Y. & Suzuki, I., 2014. Functional screening of a novel Δ15 fatty acid desaturase from the coccolithophorid *Emiliania huxleyi*. *Biochimica et Biophysica Acta (BBA) - Molecular and Cell Biology of Lipids*, 1841, pp.1451–1458.

Laguna, R., Romo, J., Read, B.A. & Wahlund, T.M., 2001. Induction of phase variation events in the life cycle of the marine coccolithophorid *Emiliania huxleyi*. *Applied and Environmental Microbiology*, 67, pp.3824–3831.

Laizé, V., Gavaia, P.J. & Cancela, M.L., 2014. Fish: A suitable system to model human bone disorders and discover drugs with osteogenic or osteotoxic activities. *Drug Discovery Today: Disease Models*, 13, pp.29–37.

Lambrev, P.H., Miloslavina, Y., Jahns, P. & Holzwarth, A.R., 2012. On the relationship between non-photochemical quenching and photoprotection of Photosystem II. *Biochimica et Biophysica Acta - Bioenergetics*, 1817, pp.760–769.

Lepage, G. & Roy, C.C., 1984. Improved recovery of fatty acid through direct transesterification without prior extraction or purification. *Journal of Lipid Research*, 25, pp.1391–1396.

van Liere, L., Mur, L.R., Gibson, C.E. & Herdman, M., 1979. Growth and physiology of *Oscillatoria agardhii* gomont cultivated in continuous culture with a light-dark cycle. *Archives of Microbiology*, 123, pp.315–318.

Lim, C. & Lovell, R.T., 1978. Pathology of the vitamin C deficiency syndrome in channel catfish (*Ictalurus punctatus*). *Journal of Nutrition*, 108, pp.1137–1146.

Linschooten, C., van Bleijswijk, J.D.l., van Emburg, P.R., de Vrind, J.P.M., Kempers, E.S., Westbroek, P. & de Vrind-de Jong, E.W., 1991. Role of the light-dark cycle and medium composition on the production of coccoliths by *Emiliania huxleyi* (Haptophyceae). *J Phycol*, 27, pp.82–86.

Lombardi, A.T. & Wangersky, P.J., 1995. Particulate lipid class composition of three marine phytoplankters *Chaetoceros gracilis*, *Isochrysis galbana* (Tahiti) and

Dunaliella tertiolecta grown in batch culture. *Hydrobiologia*, 306, pp.1–6.

Longwell, A.C., Chang, S., Hebert, A., Hughes, J.B. & Perry, D., 1992. Pollution and developmental abnormalities of Atlantic fishes. *Environmental Biology of Fishes*, 35, pp.1–21.

Mair, G.C., 1992. Caudal deformity syndrome (CDS): an autosomal recessive lethal mutation in the tilapia, *Oreochromis niloticus* (L.). *Journal of Fish Diseases*, 15, pp.71–75.

Malapascua, J.R.F., Jerez, C.G., Sergejevová, M., Figueroa, F.L. & Masojidek, J., 2014. Photosynthesis monitoring to optimize growth of microalgal mass cultures: Application of chlorophyll fluorescence techniques. *Aquatic Biology*, 22, pp.123–140.

Malik, N., 2002. Biotechnological potential of immobilised algae for wastewater N, P and metal removal: a review. *BioMetals*, 15, pp.377–390.

Marlowe, I.T., Green, J.C., Neal, A.C., Brassell, S.C., Eglinton, G. & Course, P.A., 1984. Long chain (n-C37–C39) alkenones in the Prymnesiophyceae. Distribution of alkenones and other lipids and their taxonomic significance. *Br. phycol. J.*, 19, pp.203–216.

Mayers, T.J., Bramucci, A.R., Yakimovich, K.M. & Case, R.J., 2016. A bacterial pathogen displaying temperature-enhanced virulence of the microalga *Emiliania huxleyi*. *Frontiers in Microbiology*, 7, pp.1–15.

McClung, M., Harris, S.T., Miller, P.D., Bauer, D.C., Davison, K.S., Dian, L., Hanley, D.A., Kendler, D.L., Yuen, C.K. & Lewiecki, E.M., 2013. Bisphosphonate therapy for osteoporosis: Benefits, risks, and drug holiday. *American Journal of Medicine*, 126, pp.13–20.

McKew, B.A., Metodieva, G., Raines, C.A., Metodiev, M.V. & Geider, R.J., 2015. Acclimation of *Emiliania huxleyi* (1516) to nutrient limitation involves precise modification of the proteome to scavenge alternative sources of N and P. *Environmental microbiology*, 17, pp.4050–4062.

Mendes, R.L., Nobre, B.P., Cardoso, M.T., Pereira, A.P. & Palavra, A.F., 2003. Supercritical carbon dioxide extraction of compounds with pharmaceutical importance from microalgae. *Inorganica Chimica Acta*, 356, pp.328–334.

Merico, A., Tyrrell, T., Brown, C.W., Groom, S.B. & Miller, P.I., 2003. Analysis of satellite imagery for *Emiliania huxleyi* blooms in the Bering Sea before 1997. *Geophysical Research Letters*, 30, pp.1–4.

Miller, P.D., 2009. Denosumab: Anti-RANKL Antibody. *Current Osteoporosis Reports*, 7, pp.18–22.

Milliman, J.D., 1993. Production and accumulation of calcium carbonate in the ocean: budget of a nonsteady state. *Global Biogeochemical Cycles*, 7, pp.927–957.

Min, S., Kang, S., Kwon, O., Chung, D. & Pan, C., 2012. Fucoxanthin as a major carotenoid in isochrysis aff . Galbana : characterization of extraction for commercial application. *J Korean Soc Appl Biol Chem*, 55, pp.477–483.

Mitra, M., Patidar, S.K., George, B., Shah, F. & Mishra, S., 2015. A euryhaline *Nannochloropsis gaditana* with potential for nutraceutical (EPA) and biodiesel production. *Algal Research*, 8, pp.161–167.

Mizoguchi, T., Kimura, Y., Yoshitomi, T. & Tamiaki, H., 2011. The stereochemistry of chlorophyll-c3 from the haptophyte *Emiliania huxleyi*: The (132R)-enantiomers of chlorophylls-c are exclusively selected as the photosynthetically active pigments in chromophyte algae. *Biochimica et Biophysica Acta - Bioenergetics*, 1807, pp.1467–1473.

Moheimani, N.R., Isdepsky, A., Lisee, J., Raes, E. & Botowitzka, M.A., 2011. Coccolithophorid algae culture in closed photobioreactors. *Biotechnology and Bioengineering*, 108, pp.2078–2087.

Moheimani, N.R., 2005. The culture of coccolithophorid algae for carbon dioxide bioremediation. Thesis for the degree of Doctor of Philosophy, Murdoch University.

Van Mooy, B.A.S., Fredricks, H.F., Pedler, B.E., Dyhrman, S.T., Karl, D.M., Koblížek, M., Lomas, M.W., Mincer, T.J., Moore, L.R., Moutin, T., Rappé, M.S. & Webb, E.A., 2009. Phytoplankton in the ocean use non-phosphorus lipids in response to phosphorus scarcity. *Nature*, 458, pp.69–72.

Mulders, K.J.M., Lamers, P.P, Martens, D.E. & Wiffels, R.H., 2014. Phototrophic pigment production with microalgae: biological constraints and opportunities. *J. Phycol.*, 50, pp.229–242.

Müller, M.N., Antia, A.N. & Laroche, J., 2008. Influence of cell cycle phase on calcification in the coccolithophore *Emiliania huxleyi*. *Limnology and Oceanography*, 53, pp.506–512.

Müller, M.N., Trull, T.W. & Hallegraeff, G.M., 2017. Independence of nutrient limitation and carbon dioxide impacts on the Southern Ocean coccolithophore *Emiliania huxleyi*. *Nature Publishing Group*, 11, pp.1777–1787.

Muller, P., Li, X.-P. & Niyogi, K.K., 2001. Non-Photochemical Quenching. A response to excess light energy. *Plant Physiology*, 125, pp.1558–1566.

Muñoz, R. & Guieysse, B., 2006. Algal-bacterial processes for the treatment of hazardous contaminants: A review. *Water Research*, 40, pp.2799–2815.

Mutanda, T., Ramesh, D., Karthikeyan, S., Kumari, S., Anandraj, A. & Bux, F., 2011. Bioprospecting for hyper-lipid producing microalgal strains for sustainable biofuel production. *Bioresource Technology*, 102, pp.57–70.

Myklestad, S., 1974. Production of carbohydrates by marine planktonic diatoms. I. Comparison of nine different species in culture. *Journal of Experimental Marine Biology and Ecology*, 15, pp.261–274.

Myklestad, S.M., 2000. Dissolved organic carbon from phytoplankton. *Marine Chemistry*, 5, pp.112–144.

Nanninga, H.J., Ringenaldus, P. & Westbroek, P., 1996. Immunological quantitation of a polysaccharide formed by *Emiliania huxleyi*. *Journal of Marine*, 9, pp.67–74.

Nanninga, H.J. & Tyrrell, T., 1996. Importance of light for the formation of algal blooms by *Emiliania huxleyi. Marine Ecology Progress Series*, 136, pp.195–203.

Obata, T., Schoenefeld, S., Krahnert, I., Bergmann, S., Scheffel, A. & Fernie, A.R., 2013. Gas-chromatography mass-spectrometry (GC-MS) based metabolite profiling reveals mannitol as a major storage carbohydrate in the coccolithophorid alga *Emiliania huxleyi*. *Metabolites*, 3, pp.168–184.

Obata, T. & Shiraiwa, Y., 2005. A novel eukaryotic selenoprotein in the haptophyte alga *Emiliania huxleyi. Journal of Biological Chemistry*, 280(18), pp.18462–18468.

Van Oostende, N., Moerdijk-Poortvliet, T.C.W., Boschker, H.T.S., Vyverman, W. & Sabbe, K., 2012. Release of dissolved carbohydrates by *Emiliania huxleyi* and formation of transparent exopolymer particles depend on algal life cycle and bacterial activity. *Environmental Microbiology*, 15, pp.1514–1531.

Oura, T. & Kajiwara, S., 2010. *Candida albicans* sphingolipid C9-methyltransferase is involved in hyphal elongation. *Microbiology*, 156, pp.1234–1243.

Paasche, E., 2002. A review of the coccolithophorid *Emiliania huxleyi* (Prymnesiophyceae), with particular reference to growth, coccolith formation and calcification-photosyntheis interactions. *Phycologia*, 40, pp.503–529.

Paasche, E., 1968. Biology and physiology of coccolithophorids. *Annu. Rev. Microbiol*, 22, pp.71–86.

Paasche, E. & Klaveness, D., 1970. A physiological comparison of coccolith-forming and naked cells of *Coccolithus huxleyi*. *Arch. Mikrobiol*, 73, pp.143–152.

Pakulski, J.D. & Benner, R., 1994. Abundance and distribution of carbohydrates in the ocean. *Limnology and Oceanography*, 39, pp.930–940.

Paliwal, C., Mitra, M., Bhayani, K., Bharadwaj, V.S.V., Chosh, T., Dubey, S. & Mishra, S., 2017. Abiotic stresses as tools for metabolites in microalgae. *Bioresource Technology*, 244, pp.1216–1226.

Pasnik, D.J., Evans, J.J. & Klesius, P.H., 2007. Development of skeletal deformities in a Streptococcus agalactiae- challenged male Nile tilapia (*Oreochromis niloticus*) broodfish and in its offspring. *Bulletin of the European Association of Fish Pathologists*, 27, pp.169–176.

Patil, K.J., Patil, V.A., Mahajan, S.R. & Mahajan, R.T., 2011. Bio-activity of algae belonging to Bhusawal region , Maharashtra. *Current Botany*, 2, pp.29–31.

Peng, J., Yuan, J., Wu, C. & Wang, J., 2011. Fucoxanthin, a marine carotenoid present in brown seaweeds and diatoms: metabolism and bioactivities relevant to human health. *Marine Drugs*, 9, pp.1806–1828.

Pereira, H., Custódio, L., Rodrigues, M.J., de Sousa, C.B., Oliveira, M., Barreira, L., Neng, N.R., Nogueira, J.M.F., Mouffouk, F., Abu-Salah, K.M., Ben-Hamadou, R. & Varela, J., 2015. Biological activities and chemical composition of methanolic extracts of selected autochthonous microalgae strains from the Red Sea. *Marine Drugs*, 13, pp.3531–3549.

Pereira, H., Barreira, L., Custódio, L., Alrokayan, S., Mouffouk, F., Varela, J., Abu-Salah, K.M. & Ben-Hamadou, R., 2013. Isolation and fatty acid profile of selected microalgae strains from the red sea for biofuel production. *Energies*, 6, pp.2773–2783.

Pereira, H., Gangadhar, K.N., Schulze, P.S.C., Santos, T., de Sousa, C.B., Schueler, L.M., Custódio, L., Malcata, F.X., Gouveia, L., Varela, J.C.S. & Barreira, L., 2016. Isolation of a euryhaline microalgal strain, *Tetraselmis* sp. CTP4, as a robust feedstock for biodiesel production. *Scientific Reports*, 6, p.35663.

Pereira, H., Barreira, L., Mozes, A., Florindo, C., Polo, C., Duarte, C.V., Custódio, L. & Varela, J., 2011. Microplate-based high throughput screening procedure for the isolation of lipid-rich marine microalgae. *Biotechnology for Biofuels*, 4, p.61.

Pereira, H., Barreira, L., Figueiredo, F., Custódio, L., Vizetto-Duarte, C., Polo, C., Resek, E., Engelen, A. & Varela, J., 2012. Polyunsaturated fatty acids of marine

macroalgae : potential for nutritional and pharmaceutical applications. *Marine Drugs*, 10, pp.1920–1935.

Perrin, L., Probert, I., Langer, G. & Aloisi, G., 2016. Growth of the coccolithophore *Emiliania huxleyi* in light- and nutrient-limited batch reactors: relevance for the BIOSOPE deep ecological niche of coccolithophores. *Biogeosciences*, 13, pp.5983–6001.

Pisani, P., 2013. Screening and early diagnosis of osteoporosis through X-ray and ultrasound based techniques. *World Journal of Radiology*, 5, p.398.

Plaza, M., Herrero, M., Cifuentes, A. & Ibañez, E., 2009. Innovative natural functional ingredients from microalgae. *Journal of Agricultural and Food Chemistry*, 57, pp.7159–7170.

Pond, D.W. & Harris, R.P., 1996. The lipid composition of the coccolithophore *Emiliania huxleyi* and its possible ecophysiological significance. *Journal of the Marine Biological Association of the United Kingdom*, 76, pp.579–594.

Poulton, A.J., Charalampopoulou, A., Young, J.R., Tarran, G.A., Lucas, M.I. & Quartly, G.D., 2010. Coccolithophore dynamics in non-bloom conditions during late summer in the central Iceland Basin (July-August 2007). *Limnology and Oceanography*, 55, pp.1601–1613.

Poulton, A.J., Painter, S.C., Young, J.R., Bates, N.R., Bowler, B., Drapeau, D., Lyczsckowski, E. & Balch, W.M., 2013. The 2008 *Emiliania huxleyi* bloom along the Patagonian Shelf : Ecology , biogeochemistry , and cellular calci fi cation. *Global Biogeochemical Cycles*, 27, pp.1023–1033.

Promdaen, S., Wattuya, P. & Sanevas, N., 2014. Automated microalgae image classification. *Procedia Computer Science*, 29, pp.1981–1992.

Pulz, O. & Gross, W., 2004. Valuable products from biotechnology of microalgae. *Applied Microbiology and Biotechnology*, 65, pp.635–648.

Ragni, M., Airs, R.L., Leonardos, N. & Geider, R.J., 2008. Photoinhibition of PSII in *Emiliania huxleyi* (Haptophyta) under high light stress: The roles of photoacclimation, photoprotection, and photorepair. *Journal of Phycology*, 44, pp.670–683.

Read, B.A., Kegel, J., Klute, M.J., Kuo, A., Lefebvre, S.C., Maumus, F., Mayer, C., Miller, J., Monier, A., Salamov, A., Young, J., Aguilar, M., Claverie, J., Frickenhaus, S., Gonzalez, K., Herman, E.K., Lin, Y., Napier, J., Ogata, H., Sarno, A.F., Shmutz, J., Schroeder, D., de Vargas, C., Verret, F., von Dassow, P.,

Valentin, K., Peer, Y.V., Wheeler, G., Dacks, J.B., Delwiche, C.F., Dyhrman, S.T., Glockner, G., John, U., Richards, T., Worden, A.Z., Zhang, X. & Grigoriev, I.V., 2013. Pan genome of the phytoplankton *Emiliania* underpins its global distribution. *Nature*, 499, pp.209–213.

Ren, M., Ogden, K. & Lian, B., 2013. Effect of culture conditions on the growth rate and lipid production of microalgae *Nannochloropsis gaditana*. *Journal of Renewable and Sustainable Energy*, 5.

Richier, S. & Fiorini, S., 2011. Response of the calcifying coccolithophore *Emiliania huxleyi* to low pH / high pCO2 : from physiology to molecular level. *Mar Biol*, 3, pp.551–560.

Riebesell, U., 2004. Effects of CO2 enrichment on marine phytoplankton. *Journal of Oceanography*, 60, pp.719–729.

Riebesell, U., Revill, A.T., Holdsworth, D.G. & Volkman, J.K., 2000. The effects of varying CO2 concentration on lipid compositionand carbon isotope fractionation in *Emiliania huxleyi*. *Geochimica et Cosmochimica Acta*, 64, pp.4179–4192.

Riegman, R., Stolte, W., Noordeloos, A.A.M. & Slezak, D., 2000. Nutrient uptake and alkaline phosphatase (EC 3:1:3:1) activity of *Emiliania huxleyi* (Prymnesiophyceae) during growth under N and P limitation in continuous cultures. *J Phycol*, 96, pp.87–96.

Rokitta, S.D., de Nooijer, L.J., Trimborn, S., de Vargas, C., Rost, B. & John, U., 2011. Transcriptome analyses reveal differential gene expression patterns between the life-cycle stages of *Emiliania huxleyi* (Haptophyta) and reflect specialization to different ecological niches. *J.*, 47, pp.829–838.

Rokitta, S.D. & Rost, B., 2012. Effects of CO2 and their modulation by light in the life-cycle stages of the coccolithophore *Emiliania huxleyi*. *Limnology and Oceanography*, 57, pp.607–618.

Rontani, J.F., Jameson, I., Christodoulou, S. & Volkman, J.K., 2007. Free radical oxidation (autoxidation) of alkenones and other lipids in cells of *Emiliania huxleyi*. *Phytochemistry*, 68, pp.913–924.

Rosas-Navarro, A., Langer, G. & Ziveri, P., 2016. Temperature affects the morphology and calcification of *Emiliania huxleyi* strains. *Biogeosciences*, 13, pp.2913–2926.

Rose, S.L., Fulton, J.M., Brown, C.M., Natale, F., Van Mooy, B.A.S & Bidle, K.D., 2014. Isolation and characterization of lipid rafts in *Emiliania huxleyi*: A role for membrane microdomains in host-virus interactions. *Environmental Microbiology*,

16, pp.1150–1166.

Rost, B. & Riebesell, U., 2004. Coccolithophores and the biological pump: Responses to environmental changes. *In* Coccolithophores: From Molecular Processes to Global Impact, Chief Eds.: Thierstein, H.R. & Young, J.R., Springer, pp.99–125.

Sánchez, J.F., Fernández, F.G., Acién, F.G., Rueda, A., Pérez-Parra, J. & Molina, E., 2008. Influence of culture conditions on the productivity and lutein content of the new strain *Scenedesmus almeriensis*. *Process Biochemistry*, 43, pp.398–405.

Schroeder, D.C., Biggi, G.F., Hall, M., Davy, J., Richardson, A.J. & Wilson, W.H., 2005. A genetic marker to separate *Emiliania huxleyi* (Prymnesiophyceae) morphotypes. *J. Phycol.*, 41, pp.874–879.

Schulze, P.S.C., Barreira, L.A., Pereira, H.G.C., Perales, J.A. & Varela, J.C.S., 2014. Light emitting diodes (LEDs) applied to microalgal production. *Trends in Biotechnology*, 32, pp.422–430.

Schulze, P.S.C., Carvalho, C.F.M., Pereira, H., Gangadhar, K.N., Schüler, L.M., Santos, T.F., Varela, J.C.S. & Barreira, L., 2017. Urban wastewater treatment by Tetraselmis sp. CTP4 (Chlorophyta). *Bioresource Technology*, 223, pp.175–183.

Shemi, A., Schatz, D., Fredricks, H.F., Van Mooy, B.A.S., Porat, Z. & Vardi, A., 2016. Phosphorus starvation induces membrane remodeling and recycling in *Emiliania huxleyi*. *New Phytologist*, 211, pp.886–898.

Skau, L.F., Andersen, T., Thrane, J. & Hessen, D.O., 2017. Growth, stoichiometry and cell size; temperature and nutrient responses in haptophytes. *PeerJ*, 5, p.e3743.

Skeffington, A.W. & Scheffel, A., 2018. Exploiting algal mineralization for nanotechnology: bringing coccoliths to the fore. *Current Opinion in Biotechnology*, 49, pp.57–63.

Spolaore, P., Joannis-Cassan, C., Duran, E. & Isambert, A., 2006. Commercial applications of microalgae. *Journal of Bioscience and Bioengineering*, 101, pp.87–96.

Staunton, J. & Weissman, K.J., 2001. Polyketide biosynthesis: A millennium review. *Natural Product Reports*, 18, pp.380–416.

Steinke, M., Wolfe, G. V. & Kirst, G.O., 1998. Partial characterisation of dimethylsulfoniopropionate (DMSP) lyase isozymes in 6 strains of *Emiliania huxleyi*. *Marine Ecology Progress Series*, 175, pp.215–225.

Stevens, R., Kerans, B.L., Lemmon, J.C. & Rasmussen, C., 2001. The effects of Myxobolus cerebralis myxospore dose on triactinomyxon production and biology

of *Tubifex tubifex* from two geographic regions. *The Journal of parasitology*, 87, pp.315–21.

Stolte, W., Kraay, G.W., Noordeloos, A.A.M. & Riegman, R., 2000. Genetic and physiological variation in pigment composition of *Emiliania huxleyi* (Prymnesiophyceae) and the potential use of its pigment ratios as a quantitative physiological marker. *Journal of Phycology*, 36, pp.529–539.

Strom, S., Wolfe, G., Holmes, J., Stecher, H., Shimeneck, C., Lambert, S. & Moreno, E., 2003. Chemical defense in the microplankton I: Feeding and growth rates of heterotrophic protists on the DMS-producing phytoplankter *Emiliania huxleyi. Limnology and Oceanography*, 48, pp.217–229.

Sukenik, A. & Carmeli, Y., 1989. Regulation of fatty acid composition by irradiance level in the eustigmatophyte Nannochloropsis sp. *J. Phycol*, 25, pp.686–692.

Sumitra-Vijayaraghavan, 1976. Extracellular liberation of dissolved carbohydrates by *Cricosphaera carterae* and *Coccolithus huxleyi. Mahasagar*, 9, pp.71–74.

Surget, G., Roberto, V.P., Lann, K.L., Mira, S., Guérard, F., Laizé, V., Poupart, N., Cancela, M.L. & Stiger-Pouvreau, V., 2017. Marine green macroalgae: a source of natural compounds with mineralogenic and antioxidant activities. *Journal of Applied Phycology*, 29, pp.575–584.

Tarasco, M., Laizé, V., Cardeira, J., Cancela, M.L. & Gavaia, P.J., 2017. The zebrafish operculum: A powerful system to assess osteogenic bioactivities of molecules with pharmacological and toxicological relevance. *Comparative Biochemistry and Physiology, Part C*, 197, pp.45–52.

Taylor, A.R., Brownlee, C. & Wheeler, G., 2017. Coccolithophore cell biology: chalking up progress. *Annual Review of Marine Science*, 9, pp.283–310.

Thawechai, T., Cheirsilp, B., Louhasakul, Y., Boonsawanh, P. & Prasertsan, P., 2016. Mitigation of carbon dioxide by oleaginous microalgae for lipids and pigments production: Effect of light illumination and carbon dioxide feeding strategies. *Bioresource Technology*, 219, pp.139–149.

Thomas, D.M., Mechery, J. & Paulose, S. V., 2016. Carbon dioxide capture strategies from flue gas using microalgae: a review. *Environmental Science and Pollution Research*, 23, pp.16926–16940.

Tsuji, Y., Yamazaki, M., Suzuki, I. & Shiraiwa, Y., 2015. Quantitative analysis of carbon flow into photosynthetic products functioning as carbon storage in the marine coccolithophore, *Emiliania huxleyi. Marine Biotechnology*, 17, pp.428–

440.

Tyrell T & Merico A., 2004. *Emiliania huxleyi*: bloom observations and the conditions that induce them. *In* Coccolithophores - from molecular processes to global impact. Spring er-Verlag Berlin Heidelberg, Springer, pp 75-97.

Urey, H.C., 1952. The Planets: their origin and development. New Haven, Yale University Press.

Van Leening, K.V., Probert, I., Latasa, M., Estrada, M. & Young, J.R., 2004. Pigment diversity of coccolithophores in relation to taxonomy, phylogeny and ecological preferences *In* Coccolithophores - from molecular processes to global impact. Chief Eds.: Thierstein, H.R. & Young, J.R., Springer, pp 75-97.

Varela, J.C., Pereira, H., Vila, M. & León, R., 2015. Production of carotenoids by microalgae: Achievements and challenges. *Photosynthesis Research*, 125, pp.423–436.

de Vargas, C., Aubry, M., Probert, I. & Young, J., 2007. Origin and Evolution of Coccolithophores: From Coastal Hunters to Oceanic Farmers. *In* Evolution of primary producers in the sea, Chief Eds.: Falkowski, P.G. & Knoll, A.H., Elsevier, pp. 251-285.

Vasconcelos, M.T.S.D. & Leal, M.F.C., 2001. Antagonistic interactions of Pb and Cd on Cu uptake, growth inhibition and chelator release in the marine algae *Emiliania huxleyi*. *Marine Chemistry*, 75, pp.123–139.

Vasconcelos, M.T.S.D., Leal, M.F.C. & Van Den Berg, C.M.G., 2002. Influence of the nature of the exudates released by different marine algae on the growth, trace metal uptake and exudation of *Emiliania huxleyi* in natural seawater. *Marine Chemistry*, 77, pp.187–210.

Vogel, G., 2000. Zebrafish earns its stripes in genetic screens. *Science*, 288, pp.1160–1161.

Volkman, J.K., Barrett, S.M., Blackburn, S.I., Mansour, M.P., Sikes, E.L. & Gelin, F.O.I.S., 1998. Microalgal biomarkers : A review of recent research developments. *Org. Geochem*, 29, pp.1163–1179.

Volkman, J.K., Eglinton, G., Corner, E.D.S. & Sargent, J.R., 1980. Novel unsaturated straight-chain C37C39 methyl and ethyl ketones in marine sediments and a coccolithophore *Emiliania huxleyi*. *Physics and Chemistry of the Earth*, 12, pp.219–227.

Vrum, K.M., Kvam, B.J., Myklestad, S. & Paulsen, B.S., 1986. Structure of a food-reserve β-d-glucan produced by the haptophyte alga *Emiliania huxleyi* (lohmann) hay and mohler. *Carbohydrate Research*, 152, pp.243–248.

Van Wagenen, J., Miller, T.W., Hobbs, S., Hook, P., Crowe, B. & Huesemann, M., 2012. Effects of light and temperature on fatty acid production in *Nannochloropsis salina*. *Energies*, 5, pp.731–740.

Van Der Wal, P., Kempers, R.S. & Veldhuis, M.J.W., 1995. Production and downward flux of organic matter and calcite in a North Sea bloom of the coccolithophore *Emiliania huxleyi*. *Marine Ecology Progress Series*, 126, pp.247–265.

Walker, T.L., Purton, S., Becker, D.K. & Collet, C., 2005. Microalgae as bioreactors. *Plant Cell Reports*, 24, pp.629–641.

Wei, L., Huang, X. & Huang, Z., 2014. Temperature effects on lipid properties of microalgae *Tetraselmis subcordiformis* and *Nannochloropsis oculata* as biofuel resources. *Chinese Journal of Oceanology and Limnology*, 33, pp.99–106.

Westbroek, P., Brown, C.W., Bleijswijk, J.V., Brownlee, C., Jan, G., Conte, M., Fernfindez, E., Jordan, R., Knappertsbusch, M., Veldhuis, M. & Wal, P.V.D., 1993. A model system approach to biological climate forcing. The example of *Emiliania huxleyi*. *Global and Planetary Changes*, 8, pp.27–46.

Wilbur, K.M. & Watabe, N., 1963. Experimental studies on calcification in molluscs and the alga *Coccolithus huxleyi*. *Annals of the New York Academy of Sciences*, 109, pp.82–112.

Wilkinson, G.F. & Pritchard, K., 2015. In vitro screening for drug repositioning. *Journal of Biomolecular Screening*, 20, pp.167–179.

Wolfe, G.V. & Steinke, M., 1996. Grazing-activated production of dimethyl sulfide (DMS) by two clones of *Emiliania huxleyi*. *Limnology and Oceanography*, 41, pp.1151–1160.

Woo, M., Jeon, S., Kim, H., Lee, M., Shin, S., Shin, Y., Park, Y. & Choi, M., 2010. Fucoxanthin supplementation improves plasma and hepatic lipid metabolism and blood glucose concentration in high-fat fed C57BL / 6N mice. *Chemico-Biological Interactions*, 186, pp.316–322.

Wördenweber, R., Rokitta, S.D., Heidenreich, E., Corona, K., Kirschhöfer, F., Fahl, K., Klocke, J.L., Kottke, T., Brenner-Weiß, G., Rost, B., Mussgnug, J.H., Kruse, O., 2018. Phosphorus and nitrogen starvation reveal life-cycle specific responses in the metabolome of *Emiliania huxleyi* (Haptophyta). *Limnology and Oceanography*, 63,

pp.203–226.

Young, J.R., Davis, S.A., Bown, P.R. & Mann, S., 1999. Coccolith ultrastructure and biomineralisation. *Journal of Structural Biology*, 126, pp.195-215.

Young, J., Geisen, M., Cros, L., Kleijne, A., Sprengel, C., Probert, I. & Ostergaard, J., 2003. A guide to extant coccolithophore taxonomy. *Journal of Nannoplankton Research Special Issue*, 1, pp.8–9.

Young, J.R., Poulton, A.J. & Tyrrell, T., 2014. Morphology of *Emiliania huxleyi* coccoliths on the northwestern European shelf – is there an influence of carbonate chemistry? *Biogeosciences*, 2, pp.4771–4782.

Young, J.R. & Westbroek, P., 1991. Genotypic variation in the coccolithophorid species *Emiliania huxleyi*. *Marine Micropaleontology*, 18, pp.5–23.

Yun, H., Ji, M., Park, Y., Salama, E. & Choi, J., 2016. Microalga, *Acutodesmus obliquus* KGE 30 as a potential candidate for CO2 mitigation and biodiesel production. *Environmental Science and Pollution Research*, 23, pp.17831-17839.

Zapata, M., Jeffrey, S.W., Wright, S.W., Rodríguez, F., Garrido, J.L. & Clementson, L., 2004. Photosynthetic pigments in 37 species (65 strains) of Haptophyta: Implications for oceanography and chemotaxonomy. *Marine Ecology Progress Series*, 270, pp.83–102.

Zapata, M., Garrido, J.L. & Jeffrey, S.W., 2006. Chlorophyll c pigments: current status. *In* Chlorophylls and Bacteriochlorophylls, Volume 25 - Advances in photosynthesis and respiration, Chief Eds.: Grimm, B., Porra, R.J., Rüdinger, W. and Scheer, H., Springer, pp.39-53.

Zhang, H., Tang, Y., Zhang, Y., Zhang, S., Qu, J., Wang, X., Kong, R., Han, C. & Liu, Z., 2015. Fucoxanthin: a promising medicinal and nutritional ingredient. *Hindawi Publising Corporation*, 2015, pp.1–10.

Zhao, B. & Su, Y., 2014. Process effect of microalgal-carbon dioxide fixation and biomass production : A review. *Renewable and Sustainable Energy Reviews*, 31, pp.121–132.

Zhu, L.D., Li, Z.H. & Hiltunen, E., 2016. Strategies for lipid production improvement in microalgae as a biodiesel feedstock. *BioMed Research International*, 2016, pp.7–9.

Zondervan, I., Rost, B. & Riebesell, U., 2002. Effect of CO2 concentration on the PIC/POC ratio in the coccolithophore *Emiliania huxleyi* grown under light-limiting conditions and different daylengths. *Journal of Experimental Marine Biology and*

Ecology, 272(1), pp.55–70.

Supplementary Data 1: Compilation of experimental data from research made on *Emiliania huxleyi*, including strains used, culture medium, growth temperature, pH, light cycle, irradiance, salinity, duration and sampling and growth rate.

Species and strain	Culture medium	Modifications to the Medium Composition	Growth temperature (ºC)	pH	Light cycle (L:D)	PFD (µmol photons/m^2/s)	Salinity	Initial inoculum (cell/ml)	Duration and Sampling	Growth rate (d^{-1})	Main Results and Observations	References
Emiliania huxleyi	f/2	Standard	20	NA	NA	56-70	NA	NA	15 days incubation	NA	Dissolved carbohydrates (0.4 to 3.5µg/ml) accumulate when the culture of *E. huxleyi* reaches stationary and declining phases	(Sumitra-Vijayaragha van 1976)
Emiliania huxley AC481	Surface post-bloom SW	32 µM NO_3^-, 1 µM PO_4^{3-}	13 and 18	NA	14:10	150	35.6	NA	10 days, monitored 44-57 days	Higher growth rate at 18ºC and present CO2: 0.15	Effects of increased pCO_2 and temperature during exponential growth phase of *E. huxleyi*; Increase of POC from the present to the future pCO_2 at 13ºC and significant effect of pCO_2 and temperature on calcification through lower cellular production rate of PIC at 18ºC; reduction of coccosphere particles with increased temperature and [CO_2]; malformed coccoliths with increasing pCO_2	(De Bodt et al. 2010)
Emiliania huxleyi BOF92	Eppley and f/25	Standard	18	NA	15:9	45	NA	NA	18 days incubation	NA	Quantitative measurement of an extracellular polysaccharide produced by *E. huxleyi*: concentration was determined in the supernatant of actively growing cells; maximum concentration was reached in the late stationary phase; this polysaccharide makes a significant contribution to the pool of DOC	(Nanninga et al. 1996)
Emiliania huxleyi BOF92	Eppley and f/25	Standard	18	8.1	24:0	200	NA	NA	NA	2.6 and 2.8	*E. huxleyi* natural blooms suggest a connection between bloom formation, shallow mixed layers and high light intensities; a lack of photoinhibition may contribute to the species' dominance at high light intensities	(Nanninga & Tyrrell 1996)

Emiliania huxleyi B11	f/2	200µM NO_3^- and 40µM PO_4^{3-}	15	NA	14:10	30 and 300	NA	8×10^5	NA	0.11 - 0.45	The response of *E. huxleyi* to acute exposure to high photon flux densities showed that cells acclimated to low-light displayed more photoinhibition while cells acclimated to high-light were more susceptible to photodamage but more capable of compensating for it by performing a faster repair cycle	(Ragni et al. 2008)
Emiliania huxleyi B92/21, G1779Ga, M181[b], S.Africa, Van556	f/2	Standard	6, 9, 12, 15, 18, 21, 24, 27 and 30	NA	16:8	100-200	NA	$10\text{-}15 \times 10^3$	Different incubation days for different strains; Logarithmic and stationary growth phase	1.75 at 21ºC	*E. huxleyi* exhibited a controlled biochemical regulation of long-chain alkenones and alkyl alkenoates to growth temperatures: an increase in temperature reduces the unsaturation of the relative abundance of the alkyl alkenoates and alkenones; the physiological adjustment to temperature happens via biochemistry of the alkenones; subtropical strains didn't show growth at colder temperatures and cold-water strains failed to grow at 27ºC; Log phase was longest at <15ºC.	(Conte et al. 1998)
Emiliania huxleyi BT_6	D	Standard	NA	NA	NA	12	NA	NA	7-8 days	NA	19'-hexanoyloxyfucoxanthin is the major carotenoid of the photosynthetic apparatus of *E. huxleyi* and is an efficient antenna pigment for photosynthesis and preferentially associated with photosystem II; other modifications of the fucoxanthin molecule will also have photoacessory pigment function	(Haxo 1985)
Emiliania huxleyi CCAP 920/2	ASW supplemented	200µM KNO_3/100µM NH_4Cl	18	NA	12:12	80	NA	NA	Stationary phase	2.6 days (doubling time)	Composition of intra- and extracellular pools of aminoacids in *E. huxleyi*: higher concentration of amino acids in N-deprived cultures; histidine is a major component of amino-N in exponentially growing cells; coccolith-bearing cells have higher intracellular AA content; *E. huxleyi* contained the highest concentration of extracellular AA, with histidine as the major component	(Flynn 1990)
Emiliania huxleyi CCMP 370	L1	Standard	15	NA	12:12	130	NA	1×10^6	6 days	NA	To maintain photosynthetic performance, *E. huxleyi* undergoes pigment changes in the pigment pools of the same basic structure or carries out an *ex novo* synthesis; changes are linked to variations in light quality or intensity; fucoxanthin dominated in green and red light and 19'-hexanoyloxyfucoxanthin dominated in blue light; this pigment diversity enhances photoacclimative capacity of *E. huxleyi*	(Garrido et al. 2016)

Emiliania huxleyi CCMP 370, 373, 374, 379	f/2 (-Si)	Standard	15	NA	14:10	100	NA	NA	4 days	NA	Investigation of the production of chemical defences produced by *E. huxleyi* against protist grazers: cleavage of DMSP, resulting in DMS and acrylate; lower feeding rates for several protists on strains with high DMSP lyase activity; exposure to high lyase *E. huxleyi* cells confers no harmful consequences in terms of ability to feed and grow on other phytoplankton prey	(Strom et al. 2003)
Emiliania huxleyi CCMP 371	f/2	Standard	23	NA	12:12 and 18:6	300; 350; 320 and 120-130	NA	1.5×10^5	15 days	0.99±0.06; dry weight productivity: 0.47±0.02 2 g/L/day	Growth of *E. huxleyi* in closed PBR: 6L plate PBR was the most promising closed system where *E. huxleyi* reached 5.9×10^5 cells/ml and highest specific growth rate of the species studied; *E. huxleyi* was also grown in 10L carboy PBR but had a slower growth rate; species showed no growth in the Biocoil	(Moheimani et al. 2011)
Emiliania huxleyi CCMP 371	f/50	35.2 µM NO_3^- and 1.44 µM PO_4^{3-}	21	NA	12:12	300	NA	NA	13 days; exponential growth phase	From 1.05 to 1.08	Calcification on *E. huxleyi* occurs during G1 phase of the cell cycle, when growth was N-limited, cells decreased in size and remained in the G1 phase with an increase in calcite content; P-limited growth caused an increase in cell size and cellular calcite; light limitation slowed down growth rate, prolonging the time the cells spent in the G1 phase, with increase in calcite content	(Muller et al. 2008)
Emiliania huxleyi CCMP 371 and CS-369	Pacific ASW in modified f/50 (CCMP371) and GSe/2 (CS-369)	f/50: 150g/L $NaNO_3$, 10g/L $NaH_2PO_4.H_2O$, 0.945g/L Na_2EDTA, 1.22g/L $FeCl_3.6H_2O$, 0.001g/L cyanocobalamin, 2g/L thiamine, 0.001g/L biotin, 0.0129g/L SeO_2, 0.0072g/L $MnCl_2.4H_2O$, 0.04g/L $ZnSO_4.7H_2O$,	18, 20 and 25	7.7-7.9 and 8.1-8.3	12:12	150-300	23.7-33.1	bubble column reactor and aerated flasks: $1\times10^5\pm3\times10^4$; concentric draught-tube airlift PBR: $1.5\pm0.4\times10^4$; carboy PBR: $1.5\pm0.4\times10^5$; raceway pond: $1.2\text{-}1.5\times10^5$	15 days	0.17±0.09 - 1.19±0.03; 1.38±0.09 at 23.7 ppt; 0.99±0.06 in plate PBR	*E. huxleyi* showed a highest specific growth rate (28ºC) when incubated in plate PBRs among all the coccolithophore species studied; at pH 7.7-7.9, *E. huxleyi* grew well in platePBR, when reduced to 7.2, cells started sticking to the photobioreactor; In 10L carboy PBRs, *E. huxleyi* reached 6.9×10^5 but had a slower growth rate; in outdoor raceway ponds, *E. huxleyi* cultures deteriorated in less than 2 weeks due to contaminations from another microalgae (due to constant medium pH of 8.1-8.2 that allow for microalgae growth) and ciliates	(Moheimani, 2005)

Emiliania huxleyi CCMP 371 and RCC 1216	ESW	Standard	21	NA	24:0	10, 20, 50, 100, 300, 400, 500, 800, 1500	NA	10^4	12 days	1.1	Investigation towards the impact of varying irradiance on growth and chl-*a* content in *E. huxleyi*: photoinhibition was observed at >500µmol m^{-2} s^{-1} for calcifying strains; haplontic cells required higher irradiance to reach maximum growth rate while being much more tolerant to photoinhibition; chl-*a* content is higher at lower irradiance	(Hariskos et al. 2015)
Emiliania huxleyi CCMP 373	f/2 (-Si)	10^{-8} M sodium selenite	23	NA	14:10	900	NA	NA	Harvested at late log phase	NA	*E. huxleyi* exude DOM rich in polysaccharides that closely resemble acyl heteropolysaccharides previously identified as major compounds of naturally occurring marine HMW DOM	(Aluwihare & Repeta 1999)
Emiliania huxleyi CCMP 373 and CCMP 370	f/2	Standard	15	NA	16:8	80-100	NA	NA	15 days	0.47-0.70; no production of coccoliths	For *E. huxleyi*, enzyme activity per cell was constant during exponential growth but little DMS was produced by healthy cells; DMS production was activated when cells were subjected to physical/chemical stresses that caused cell lysis; DMSP lyase and DMSP are segregated in these cells only under conditions that result in cell stress or damage	(Wolfe & Steinke 1996)
Emiliania huxleyi CCMP 373 and CCMP 374	f/2 (-Si)	Standard	18	NA	14:10	450	NA	1×10^6	12 days; until stationary and death phases	0.9	Infection of *E. huxleyi* with a lytic virus resulted in a rapid internal degradation of cellular components, a reduction in photosynthetic efficiency and an up-regulation of metacaspase protein expression, facilitating viral lysis; virus activate and recruit host metacaspases as a replication strategy	(Bidle et al. 2007)
Emiliania huxleyi CCMP 1516	SW with f/2 metals and vitamins	Several media (e.g.38 µM PO_4^{3-}, 882 µM NO_3^-; 14 µM PO_4^{3-} and 200 µM NO_3^-)	20	NA	16:8	150	NA	NA	NA	From 0.67±0.05 to 1.25±0.04	Non-calcifying strains of *E. huxleyi* can outcompete the calcifyers in growth but, when both are exposed to several environmental stressors, coccoliths mitigate the stress imposed by mechanical perturbation, reducing cell lysis and supporting higher cell concentrations in the presence of turbulence	(Bartal et al. 2015)
Emiliania huxleyi CCMP 1516	f/2	Standard	15	NA	14:10	250	NA	NA	6 days; samples 4h into the light period	NA	Determination of FA profile: decrease in FA as cell numbers declined in virus-infected *E. huxleyi* cultures; shift from polyunsaturated to monosaturated and saturated FA; decreases were observed in major fatty acids 22:6(n-3) and 18:5(n-3) and increases in 18:1(n-9) and 22:0	(Evans et al. 2009)
Emiliania huxleyi CCMP 1516	ASW supplemented with Erd-Schreiber's SW	10nM sodium selenite	25	NA	24:0	100	NA	NA	NA	8.6±1.8 × 10^6 cells/mL	At 25ºC, *E. huxleyi* produces mainly 14:0, 18:4(n-3), 18:5(n-3) and 22:6(n-3); when transferred to 15ºC, unsaturated FA gradually increased; identification of a gene (EhDES15) involved in the production of (n-3) PUFA	(Kotajima et al. 2014)

Emiliania huxleyi CCMP 1516	f/50 or f/2	Standard	17-18	NA	24:0 or 12:12	600	NA	NA	12 days; late log-phase	NA	Laboratory method for inducing phase variation between *E. huxleyi* S cells and C cell: plating C cells on solid media induces phase switching from C to S cells; regeneration of C to S cells involves the formation of aggregations of S cells and the production of cultures primarily diploid	(Laguna et al. 2001)
Emiliania huxleyi CCMP 1516	ASW with f/8 trace metals and vitamins	1nM selenium; 150μM NH_4NO_3 and 20μM PO_4^{3-}; N-limiting: 25μM NH_4NO_3, 20μM PO_4^{3-}; P-limiting: 150μM NH_4NO_3, 7μM PO_4^{3-}	18	NA	16:8	300	NA	6×10^5	Exponential growth rate, 4h into the light phase	NA	Examination of the proteome of *E.huxleyi* responds to N and P limitation: changes in much of the proteome despite large physiological changes associated with nutrient limitation of growth rate; significant increases in the abundance of transporters for ammonium and nitrate under N limitation and for phosphate under P limitations; large increase in proteins involved in the acquisition of organic forms of N and P, including urea and AA/polyamine transporters and numerous C-N hydrolases under N limitation and large up-regulation of alkaline phosphatase under P limitation	(McKew et al. 2015)
Emiliania huxleyi CCMP 1516	f/2 (-Si)	Standard	18	NA	14:10	200	NA	NA	4 days; samples at each time point	2.5×10^6 cells/ml - cell abundance	Coccolithoviruses have a suite of glycosphingolipids to infect *E. huxley;* lipid rafts likely play a fundamental role in host-virus interactions; analysis showed flotilin as a major lipid raft protein along with several proteins affiliated with host defense, programmed cell death and innate immunity pathways	(Rose et al. 2014)
Emiliania huxleyi CCMP 1742, 1516, 370, 374	f/2 or f/20	NO_3^-/ PO_4^{3-} reduced 10% for limiting experiments	16	NA	16:8	80	NA	NA	NA	NA	*E. huxleyi* produce as neutral lipids several PULCA; they package their neutral lipid into cytoplasmic vesicles or lipid bodies that increase in abundance under nutrient limitation and disappear under prolonged darkness; purified lipid vesicles consist predominantly of PULCA that may be synthesized in chloroplasts and exported to cytoplasmic lipid bodies for storage or metabolism	(Eltgroth et al. 2005)
Emiliania huxleyi CCMP 2090	K/2	Standard	18	NA	16:8	100	NA	$10^7 – 10^8$	10 days	NA	Early phosphorus starvation-induced substitution of phospholipids in *E. huxleyi* membranes with galacto- and betaine lipids; lipid remodeling was rapid and reversible upon P resupply; P limitation enhanced the formation and acidification of membrane vesicles in the cytoplasm; long-term starvation was characterized by an increase in cell size and morphological alterations in cellular structure	(Shemi et al. 2016)

Emiliania huxleyi CCMP 3266, CCMP 3268 and CCMP 2090	L1 (-Si)	Standard	18	NA	16:8	NA	NA	10^4 - 10^5	5 days; Mid-point of the dark cycle	NA	Co-culture of *E. huxleyi* and *Ruegeria sp.*(pathogen); Rapid decline resulting in cell death for C and S cells at 25ºC but not for N cells, at either temperature; suggests *Ruegeria sp.*is a temperature-enhanced opportunistic pathogen of *E. huxleyi;* detection of caspase activity in dying C cells (programmed cell death)	(Mayers et al. 2016)
Emiliania huxleyi Ch24-90 and Ch25-90	f/2	1.5-3 µM ammonium, 30-39 µM NO_3^-, 0.2-0.4 µM PO_4^{3-}	10 and 15	7.98 - 8	16:8	70-155	NA	10^4	Exponential growth phase	0.8-0.9	In P-deprived *E. huxleyi* cultures, calcite carbon production exceeded organic carbon production; morphotype B showed a higher calcite carbon/organic carbon ratio than morphotype A; slow growing cultures produced calcite in the light and dark period; higher growth rate at 15ºC	(van Bleijswijk et al. 1994)
Emiliania huxleyi CS-57	f/2	Standard	20	NA	16:8	80	NA	NA	10-17 days; mid-log phase (10) and end of log phase (17)	NA	Growth of *E.huxleyi* under atmosphere of air + 0.5%CO_2 showed oxidative damage and major changes in lipid composition: FA was altered and lacked amounts of PUFA (18:5, 18:3 and 22:6); monounsaturated FA proved to be a good indicative of oxidative processes; degradation of oleic acid involved mainly free radical oxidation processes; large amounts of degradation products of the oxidation product 9,10-epoxyoctadecanoic acid including diols, methosyhydrins and chlorohydrins found in all lipid classes examined; alkenone content per cell was much higher in the presence of 0.5%CO_2 due to carbon storage under these conditions	(Rontani et al. 2007)
Emiliania huxleyi DWN 61/81/5	f/2	Standard	15	NA	12:12	100	NA	NA	18 days; samples at log and stationary phases	NA	Coccolith-forming *E. huxleyi* cells show higher levels of neutral lipids than flagellate cells; methyl and ethyl ketones were present in both cell types; phospholipids and glycolipids increase during log-phase and neutral lipids achieve highest levels in the late stationary-phase; in sulphoquinovosylglycerol and phosphatidylethanolamine, 18:3(n-3) and 18:4(n-3) were the predominant FA and 18:5(n-3) was the main FA in digalactosyldiacylglycerols and monogalactosydiacylglycerols; phosphatidylcholine was dominated by 22:6(n-3)/22:6(n-3) and 14:0/22:6(n-3)	(Bell & Pond 1996)
Emiliania huxleyi EHSO 5.14	f/20 or f/80	5.3 µM NO_3^- and 0.32 µM PO_4^{3-}	14	7.48-8.06	24:0	100-115	35	90-130	6-10 days; exponential phase	0.2	Nutrient limitations decreases per cell photosynthesis in *E. huxleyi* (POC production) and calcification (PIC production) rates for all pCO_2 levels, with more than 50% reductions under nitrogen limitation	(Müller et al. 2017)

Emiliania huxleyi EHSO 5.30, 5.25, 5.28, 5.11, 6.17, 8.15	K	290 µM NO_3^- and 4 µM PO_4^{3-}	16	NA	12:12	70	NA	NA	28 days	1.04 and 0.86	Differences between *E. huxleyi* morphotype A and B/C (type A has a bigger width of coccolith distal shield elements); The ratio 19'hexanoyloxyfucoxanthin:chl-a was higher in type B/C than type A	(Cook et al. 2011)
Emiliania huxleyi F	Eppley (-Si)	Standard	21	NA	24:0	196	30	NA	NA	1.42 (C-cells) and 1.68 (N-cells)	Naked cells and coccolith-forming cells of *E. huxleyi* do not differ significantly in regard of cell volume and protein content; smaller content of chl-a in naked cells caused by a lowering photosynthetic rate at all light intensities; deoxyribonucleic acid was the same in naked and coccolith-forming cells	(Paasche & Klaveness 1970)
Emiliania huxleyi F61, F63, G4	IMR/2	Standard	17	NA	NA	42 or 196	30	NA	NA	NA	*E. huxleyi'* morphological investigation: no presence of flagella nor haptonema, coccoliths are formed one at a time inside the cell and a primary coccolith vesicle is formed outside the nuclear envelope. This vesicle grows and assumes the shape of a coccolith and, at the same time, a matrix membrane is formed inside the coccolith vesicle that determines the final shape of the coccolith	(Klaveness 1972)
Emiliania huxleyi F61 and 92	Droop and Eppley (-Si)	Standard	19	NA	NA	70	NA	NA	NA	NA	Development of a new method for isolating *E. huxleyi* coccoliths; a polyssacharide was obtained from the coccoliths that contain two monobasic acid groups (one being uronic acid) in a total amount of 1.8µmol/mg; this polyssacharide can bind to Ca^{2+}	(Jong et al. 1976)
Emiliania huxleyi isolated	f/2 pre-culture and f/20 for experiment	f/20: 88 µM NO_3^- and 3.6 µM PO_4^{3-}	15	7.47 - 8.36	14:10	150	34	3.5×10^4	During the first light phase	1.01	*E. huxleyi* acclimation to rising CO_2 within 24h suggests that this cellular adjustment is independent of cell division; *E. huxleyi* rapidly changes the rates of essential metabolical processes in response to changes in the seawater chemistry, acclimating in a matter of hours.	(Barcelos e Ramos et al. 2010)
Emiliania huxleyi isolated	MNK	Standard	18	NA	18:6	NA	NA	NA	Exponential growth phase	NA	Analysis of the morphology of *E. huxleyi* coccoliths and of the partial mitochondrial sequences of the cytochrome oxidase 1b through adenosine triphosphate synthase 4; coccolith morphology showed a new morphotype (Type O) with an open central area; molecular analysis revealed that *E. huxleyi* consists of 2 mitochondrial sequence groups with different temperature preferences/tolerance	(Hagino et al. 2011)
Emiliania huxleyi isolated	IMR ½	Addition of 10nM selenite; P-limited: 1 µM PO_4^{3-}; high	13 and 19	NA	14:10	170	30	50 000	NA	Higher growth rate at high P:	High temperatures increased growth rate in *E. huxleyi* cultures with high P as well as cell volume-specific C, N and P; under P-limitation, P and RNA concentrations were lower at both temperatures	(Skau et al. 2017)

		P: 12.5 µM PO_4^{3-}								0.855-1.045		
Emiliania huxleyi L	f/50 or Eppley's	Standard	18	8	16:8	90	NA	NA	Experiment started with cells in the exponential growth phase	0.8 - 1.1 div/cell/4h (0.034 - 1.1)	During light period, about 8 coccoliths per cell were formed at a rate of 1 coccolith per 2h with the species *E. huxleyi*; cells divided during the first half of the dark period and there were no coccolith production during dark period; cells grown on enriched seawater tend to produce coccoliths that cover the cell in a single layer; when stationary phase is reached, coccolith production ceases; cells grown in a medium with 2% N and P produce coccoliths in the stationary phase, with the formation of multiple coccolith layers	(Linschooten et al. 1991)
Emiliania huxleyi L	Prepared from SSW	P limitation: 300µM NaNO3 and 1µM NaH_2PO_4; N limitation: 25µM $NaNO_3$ and 25µM NaH_2PO_4; 24.5g NaCl, 9.8g $MgCl_2.6H_20$, 0.53g $CaCl_2.2H_2O$, 3.22g Na_2SO_4, 0.85g K_2SO_4; H_3BO_3, 0.36µmol RbCl	15	8	24:0	200	NA	NA	6 days	0.14 - 0.63	Under P limitation, *E. huxleyi* expressed 2 different types of alkaline phosphatase enzyme kinetics: one type was synthesized constitutively and the other was induced and has higher activity at lowest growth rates; N-limited cells were smaller than P-limited and contained 50% less organic and inorganic carbon; *E. huxleyi* is expected to perform well in P-controlled ecosystems	(Riegman et al. 2000)
Emiliania huxleyi L and CCMP 370, 373, 374, 379 and 1516	f/2 (-Si)	5.8 µM Fe	15	NA	18:6	40	30	3000	14 days	0.62 - 0.82	Most of *E. huxleyi* cultures produced high concentrations of intracellular DMSP, constant over the growth cycle; DMSP lyases appeared constitutive; there are several structurally different DMSP lyase isozymes within *E. huxleyi*	(Steinke et al. 1998)
Emiliania huxleyi L, 92, 92D and MCH	f/50	10×10^{-6} molar KNO_3, 1×10^{-6} molar K_2HPO_4	19	NA	16:8	NA	NA	5% inoculum	8 days; late-log phase	NA	*E. huxleyi* coccoliths show variations that occur independently of each other and within each genotypic strain and are influenced by the environment	(Young & Westbroek 1991)

Emiliania huxleyi NIES-837	MNK	Standard	20	NA	12:12	20-30	NA	NA	NA	NA	Full characterization of *E. huxleyi* chl-c_3 was performed; the rigid planar structure of the acrylate causes an inhibition of DPOR reaction creating green chl pigments; presence of chl-c_2	(Mizoguchi et al. 2011)
Emiliania huxleyi NIES 873	Erd-Schreiber	10 nM sodium selenite	20	NA	24:0	100	NA	NA	5 days	NA	*E. huxleyi* possess 6 selenium-containing proteins, requiring selenium for growth; EhSEP2 protein is homologous to protein disulphide isomerase and contains a highly conserved thioredoxin domain	(Obata & Shiraiwa 2005)
Emiliania huxleyi PCC 92 and 92d	ESW	176µM NO_3^- and 7.26µM PO_4^{3-}	18	NA	24:0	NA	NA	0.5×10^6	10 days	NA	Study the effects of algal exudates on algal growth, uptake of metals and extent of exudation in *E. huxleyi*; improvement in final cell yield of *E. huxleyi* was caused by the addition of *Enteromorpha* exudates and growth inhibition was caused by the addition of *P. tricornutum* exudates; nature and concentration of organic compounds also influenced trace metal uptake and the concentration and composition of the exudates produced by *E. huxleyi*	(Vasconcelos et al. 2002)
Emiliania huxleyi PCC 92 and 92d	f/10	176µM NO_3^- and 7.26µM PO_4^{3-}	18	8	24:0	NA	35	0.5×10^6	10 days; Stationary phase	From 0.72 to 0.83	The addition of Pb to *E. huxleyi* cultures reduced growth rate but did not promote the liberation of organic ligands; cellular levels of Cu decreased or didn't change suggesting that Pb antagonised Cu uptake	(Vasconcelos & Leal 2001)
Emiliania huxleyi PML B92/11	Treated and supplemented SW with f/2 metals	29µM NO_3^- and 1.1µM PO_4^{3-}	14 and 18	7.97	16:8	300	32	3000	28 days	0.1 and 0.3	Under enhanced nutrient stress, *E. huxleyi* has higher concentrations of HMW-dCCHO, pCCHO and transparent exopolymer particles; at a growth rate of $0.3d^{-1}$, pCCHO increased with elevated CO_2 and temperature; at a growth rate of $0.1d^{-1}$, HMW-dCCHO was lower while pCCHO and transparent exopolymer particles were higher at the same conditions; CO_2 and temperature will increase exudation by *E. huxleyi*	(Borchard & Engel 2012)
Emiliania huxleyi PML B92/11	f/2	43µM NO_3^- and 1.5µM PO_4^{3-}	14	8.24	16:8	19	33	5000	44 days	0.2	ER is a mechanism used by *E. huxleyi*, and was characterized with distinct size classes; ER is low during steady-state growth and acidic sugars had a significantly share on pCCHO and HMW-dCCHO; pCCHO and the smaller size HMW-dCCHO had similar sugar composition (dominated by glucose), HMW-dCCHO of bigger classes had higher arabinose	(Borchard & Engel 2015)
Emiliania huxleyi PML B92/11	f/2	100µM NO_3^- and 6.25µM PO_4^{3-}	15	7.8 – 8.6	24:0 and 16:8	15, 30 and 80	NA	NA	During photoperiod and end of dark period;	1.11 (high [CO2])	With increasing [CO_2] in *E. huxleyi* culture, was observed a decrease in the PIC/POC ratio at all light intensities and light:dark cycles tested; the individual response in cellular PIC and POC to [CO_2] depended strongly on PFD; cell growth rate decreased with decreasing PFD but was independent of ambient [CO_2]	(Zondervan et al. 2002)

Emiliania huxleyi RCC 1216 and RCC 1217	K/2 (-Tris, -Si)	115 µM NO_3^-, 20 µM ammonium, 7.2 µM PO_4^{3-}, 1/2 K/2 trace metals, K/2 vitamins	17	NA	14:10	80	NA	NA	Mid-exponential phase	0.843 ± 0.028 and 0.851 ± 0.004	Identification of genes involved in diploid-specific biomineralization, haploid-specific motility and transcriptional control in *E. huxleyi*; greater transcriptome in diploid cells suggest more versatility to exploit several environments and haploid cells are more streamlined	(Dassow et al. 2009)
Emiliania huxleyi RCC 1216 and RCC 1217	K/2 (-Tris, -Si)	Standard	17	NA	14:10	150	38	50	8 days	control: 0.79±0.02; elevated pCO2: 0.76±0.02	Increased pCO_2 in *E. huxleyi* cultures does not affect calcification rate; elevated pCO_2 induces only limited changes in the transcription of several transporters; suggests that *E. huxleyi* is adapt to withsteand future ocean acidification	(Richier & Fiorini 2011)
Emiliania huxleyi RCC 1216 and RCC 1217	North Sea SW with f/2 vitamins and trace metals	100µM NO_3^- and 6.25µM PO_4^{3-}	15	7.7 – 8.2	18:6	50 and 300	32	NA	4-6 days; midexponential growth phase	From 0.63±0.14 to 1.18±0.20	Diploid *E. huxleyi* cells responded to elevated pCO_2 by shunting resources from the production of PIC toward organic C, keeping the production of total particulate C constant; haploid cells maintained elemental composition and production rates under elevated pCO_2	(Rokitta & Rost 2012)
Emiliania huxleyi RCC 1216 and RCC 1217	f/2	100µM NO_3^- and 6.25µM PO_4^{3-}	15	8.1 – 8.2	16:8	50 and 300	32.2	NA	Harvested at exponential growth phase	From 0.87±0.12 to 1.18±0.20	Haploid and diploid *E. huxleyi* stages exhibit different properties of regulating genome expression, proteome maintenance and metabolic processing (pronounced primary metabolism and motility in haploid cells and calcification in diploid); higher abundances of transcripts related to endocytotic and digestive machinery in diploid cells; both cell types are capable of particle uptake in late-stationary growth phase	(Rokitta et al. 2011)
Emiliania huxleyi RCC 1216, 1249 and 1213	K/2 (-Tris, -Si)	Standard	18	NA	12:12	85	NA	2×10^6	60 days	NA	Haploid phase of *E. huxleyi* is resistant to viruses that kill the diploid phase: when diploid cells are exposed to the virus, transition to the haploid phase is induced; this resistance in the haploid phase provides an escape mechanism that involves separation of the meiosis from sexual fusion, ensuring that genes of dominant diploid clones are passed to the next generation	(Frada et al. 2008)
Emiliania huxleyi RCC 1266	Oligotrophic SSW	32µM NO_3^- and 1µM PO_4^{3-}	16	NA	14:10	60	NA	0.5	20 days	diploid: 0.75±0.03 (axenic) and 0.76±0.01 (non-axenic); haploid: 0.98±0.05	Analysis of photosynthetically fixed carbon during P-limited stationary growth of *E. huxleyi*: bacteria enhanced the accumulation of dissolved polyssacharides and altered the composition of dissolved HMW NAld, and stimulated the formation of transparent exopolymer particles containing high densities of charged polyssacharides in diploid cells; in haploid cells, there is an accumulation of dissolved carbohydrates with a different composition of NAld than the one present in diploid cells; Diploid cultures present a high level of extracellular release of organic carbon, mainly particulate	(Van Oostende et al. 2012)

Emiliania huxleyi RuG collection	f/2	Standard	16	NA	16:8	75	35	35 μm^3 (biovolume)	Exponential growth phase	0.34±0.08	Highest production of DHA by *E.huxleyi* between the observed species (164µg L^{-1} d^{-1}) even though growth rate and maximal biomass were relatively low; between species, *E.huxleyi* had minimal amounts of EPA; ALA is present in substancial amounts	(Boelen et al. 2013)
Emiliania huxleyi 88E	K	Standard	19	NA	14:10	51	NA	5-7 × 10^5	11 days	NA	Accumulation of coccoliths was maximum at the end of the logarithmic growth with 50-80 coccoliths/cell (3-5 complete layers of coccoliths); net growth rates of coccoliths were about 7 coccoliths $cell^{-1}$ d^{-1} and net detachment rate as high as 15 coccoliths $cell^{-1}d^{-1}$ for stationary phase cells	(Balch et al. 1993)
Emiliania huxleyi 88E	K	400 µM NO_3^- and 20 µM phosphorus	17	7.93 - 8.74	NA	75	NA	NA	Continuous culture at steady-state	From 0.24 to 0.99	The ratio of calcification to photosynthesis increased as the *E. huxleyi* growth rate increased, but later decreased as the growth rate reached about 1 d^{-1}; as growth becames more light-limited, there is a decoupling of photosynthesis from calcification	(Balch et al. 1996)
Emiliania huxleyi 88E	K	75% reduction in the final concentrations	16	NA	16:8	200	NA	2-3 × 10^4	12 days; Logarithmic and stationary phase	0.49±0.01 for low irradiance and 0.81±0.04 for high irradiance	In *E. huxleyi*, the flows of carbon incorporated through photosynthesis were mainly directed towards the synthesis of lipids whereas carbon incorporation for proteins was low; actively dividing cells showed higher rates of incorporation into protein during darkness; under energy-limited growing, proteins produced during the light period were catabolized during darkness	(Fernandez et al. 1994)
Emiliania huxleyi 92D	f/2	Standard	15	NA	12:12	50-100	NA	NA	Exponential growth phase	0.9	Analysis of copepod (*Calanus helgolandicus* and *Pseudocalanus elongatus*) grazing on *E. huxleyi*and the role in the inorganic carbon flux; equivalent ingestion rates for both copepods; only 27-50% of the ingested calcite was egested in the faecal pellets	(Harris 1994)
Emiliania huxleyi 92d	1:1:1 Erd-Schreiber, ASP2 and Miquel-Allen	Mixture of 3 media	15	NA	12:12	NA	NA	NA	Exponential phase	NA	Presence of n-alkenones in *E. huxleyi* (mainly C37:3Me); *E. huxleyi* shows a different distribution pattern, having significant proportions of di-unsaturated components (C38:2Et ester and C37:2Me ester); it also has two sterols: 24-methylcholesta-5,22-dien-3β-ol and cholest-5-en-3β-ol	(Marlowe et al. 1984)
Emiliania huxleyi (several strains)	f/2	Standard	15	NA	12:12	100	NA	NA	20 days; Logarithmic and stationary phases	NA	In *E. huxleyi* lipid composition, methyl and ethyl ketones were the dominant lipid classes; levels of total FA per cell decreased between logarithmic and stationary phases due to reduction of saturated and monounsaturated FA; major FA were 14:0, 16:0, 18:1(n-9), 18:4(n-3), 18:5(n-3) and 22:6(n-3); stationary phase cultures contained highest proportions of polyunsaturated FA, with DHA being the most abundant (38.4% of total FA)	(Pond & Harris 1996)

*Emiliania huxleyi (*16 different strains)	Nutrients added to nutrient-poor SW	N-limitation: 25µM $NaNO_3$ and 25µM NaH_2PO_4; P-limitation: 300µM $NaNO_3$ and 1µM NaH_2PO_4	15	NA	16:8	70	NA	3-5 × 10^5	NA	From 0.13 to 0.70	Use of individual pigments as a taxonomic marker at the species level; 19'hexanoyloxyfucoxanthin is synthesized from fucoxanthin with light as a modulating factor; the rate of diatoxanthin depends on the concentration of diadinoxanthin and light	(Stolte et al. 2000)
Emiliania huxleyi (34 different strains)	f/2	Standard	15	NA	14:10	200	NA	10^4	Exponential growth phase	NA	Presence of different *E. huxleyi* genotypes on a global scale that allow for adaptation to changing environment	(Iglesias-Rodriguez et al. 2006)

Glossary: AA - Amino acids; ALA - Alpha-linolenic acid; ASW - Artificial seawater; DHA - Docosahexaenoic acid; DMS - Dimethyl sulfide; DMSP - Dimethylsulfoniopropionate; DOC - Dissolved organic carbon; DOM - Dissolved organic matter; DPOR - Dark operative protochlorophyllide oxidoreductase; EPA - Eicosapentaenoic acid; ESW - Enriched seawater; ER - Extracellular release; FA - Fatty acid; HMW dCCHO - High molecular weight dissolved carbohydrates; HMW DOM - High molecular weight dissolved organic matter; HMW NAld - High molecular weight neutral aldoses; L:D - Light:Dark; NA - Not available; PBR - Photobioreactors; pCCHO - Particulated carbohydrates; PIC - Particulate inorganic carbon; PFD - Photon flux density; POC - Particulate organic carbon; PUFA - Polyunsaturated fatty acid; PULCA - Polyunsaturated long-chain alkenones, alkenoates and alkenes; SW - Seawater; SSW - Synthetic seawater.

Supplementary Data 2: Compilation of commercially available strains of *Emiliania huxleyi*, including growth temperature, culture medium, if produces coccoliths, region, price, isolation date, cryopreservation and the institution where it is available.

Strain	Growth Temperature (ºC)	Culture Medium	Coccoliths	Region	Price	Isolation Date	Cryopreservation	Institution
Emiliania huxleyi AC335	17	K/5	Yes	Sorth Africa	Starter 30 ml - 50€	2000	No	Algobank Caen
Emiliania huxleyi AC472	17	K/5	Yes	New Zeland	Starter 30 ml - 50€	1998	No	Algobank Caen
Emiliania huxleyi AC474	17	K/5	ND	Spain	Starter 30 ml - 50€	1998	No	Algobank Caen
Emiliania huxleyi AC477	17	K/5	ND	Sorth Africa	Starter 30 ml - 50€	1999	No	Algobank Caen
Emiliania huxleyi AC481	17	K/5	ND	France	Starter 30 ml - 50€	2003	No	Algobank Caen
Emiliania huxleyi AC795	16	f/2	Yes	France	Starter 30 ml - 50€	2009	No	Algobank Caen
Emiliania huxleyi AC840	16	K/5	Yes	France	Starter 30 ml - 50€	2010	No	Algobank Caen
Emiliania huxleyi AC848	16	ES	Yes	France	Starter 30 ml - 50€	2009	No	Algobank Caen
Emiliania huxleyi AC906	16	K/2	ND	France	Starter 30 ml - 50€	2009	No	Algobank Caen
Emiliania huxleyi CCAC 1890 B	15	f/2 - Si	Yes	Germany	2x 10 ml - 40€	2001	No	CCAC
Emiliania huxleyi CCAC 1912 B	15	f/2 - Si	Yes	Germany	2x 10 ml - 40€	2001	No	CCAC
Emiliania huxleyi CCAP 920/8	15	f/20 or L1 dil	Yes	Norway	2x 10 ml - 50£	n.a.	No	CCAP
Emiliania huxleyi CCAP 920/9	15	f/20 or L1 dil	Yes	England	2x 10 ml - 50£	n.a.	No	CCAP
Emiliania huxleyi CCAP 920/12	15	f/20 or L1 dil	Yes	Scotland	2x 10 ml - 50£	n.a.	No	CCAP
Emiliania huxleyi YOKSN80	ND	f/2	ND	United Kingdom		n.a.		EGEMACC
Emiliania huxleyi NIVA-7/82	16	ES	ND	Norway	1x 20 ml - 50€	1981	No	NIVA
Emiliania huxleyi UIO 139	20	L1	Yes	Spain	1x 20 ml - 50€	n.a.	No	NIVA
Emiliania huxleyi UIO 371	10	L1	ND	Norway	1x 20 ml - 50€	n.a.	No	NIVA
Emiliania huxleyi UIO 372	10	L1	ND	Norway	1x 20 ml - 50€	n.a.	No	NIVA
Emiliania huxleyi UIO 373	10	L1	ND	Norway	1x 20 ml - 50€	n.a.	No	NIVA
Emiliania huxleyi 33.90	16	SWES	ND	United Kingdom	40€ + 10€portes	1950	No	EPSAG

Emiliania huxleyi RCC 868	17	K/2	Yes	Sorthern Pacific	30 ml - 50€	2004	Yes	Roscoff Culture Collection
Emiliania huxleyi RCC 904	17	K/2	Yes	Mediterranean Sea	30 ml - 50€	1999	No	Roscoff Culture Collection
Emiliania huxleyi RCC 911	17	K/2	Yes	Pacific Ocean	30 ml - 50€	2004	No	Roscoff Culture Collection
Emiliania huxleyi RCC 914	17	K/2	Yes	Pacific Ocean	30 ml - 50€	2004	Yes	Roscoff Culture Collection
Emiliania huxleyi RCC 921	17	K/2	Yes	Pacific Ocean	30 ml - 50€	2004	Yes	Roscoff Culture Collection
Emiliania huxleyi RCC 948	17	K/2	Yes	Sorthern Pacific	30 ml - 50€	2004	No	Roscoff Culture Collection
Emiliania huxleyi RCC 955	17	K/2	Yes	Pacific Ocean	30 ml - 50€	2004	No	Roscoff Culture Collection
Emiliania huxleyi RCC 956	17	K/2	Yes	Pacific Ocean	30 ml - 50€	2004	Yes	Roscoff Culture Collection
Emiliania huxleyi RCC 958	17	K/2	Yes	Pacific Ocean	30 ml - 50€	2004	No	Roscoff Culture Collection
Emiliania huxleyi RCC 962	17	K/2	Yes	Pacific Ocean	30 ml - 50€	2004	No	Roscoff Culture Collection
Emiliania huxleyi RCC 963	17	K/2	Yes	Pacific Ocean	30 ml - 50€	2004	No	Roscoff Culture Collection
Emiliania huxleyi RCC 1208	17	K/2	Yes	Mediterranean Sea	30 ml - 50€	1999	Yes	Roscoff Culture Collection
Emiliania huxleyi RCC 1210	17	K/2	Yes	Sweden	30 ml - 50€	1998	No	Roscoff Culture Collection
Emiliania huxleyi RCC 1212	17	K/2	Yes	Sorth Atlantic	30 ml - 50€	2000	No	Roscoff Culture Collection
Emiliania huxleyi RCC 1215	17	K/2	Yes	Spain	30 ml - 50€	2001	Yes	Roscoff Culture Collection
Emiliania huxleyi RCC 1216	17	K/2	Yes	Tasman Sea	30 ml - 50€	1998	Yes	Roscoff Culture Collection
Emiliania huxleyi RCC 1218	17	K/2	Yes	Tasman Sea	30 ml - 50€	1998	Yes	Roscoff Culture Collection
Emiliania huxleyi RCC 1219	17	K/2	Yes	Tasman Sea	30 ml - 50€	1998	No	Roscoff Culture Collection
Emiliania huxleyi RCC 1220	17	K/2	Yes	Tasman Sea	30 ml - 50€	1998	Yes	Roscoff Culture Collection
Emiliania huxleyi RCC 1223	17	K/2	Yes	Mediterranean Sea	30 ml - 50€	1999	No	Roscoff Culture Collection
Emiliania huxleyi RCC 1231	17	K/2	Yes	Tasman Sea	30 ml - 50€	1998	Yes	Roscoff Culture Collection
Emiliania huxleyi RCC 1232	17	K/2	Yes	France	30 ml - 50€	n.a.	Yes	Roscoff Culture Collection
Emiliania huxleyi RCC 1233	17	K/2	Yes	France	30 ml - 50€	n.a.	Yes	Roscoff Culture Collection
Emiliania huxleyi RCC 1234	17	K/2	Yes	France	30 ml - 50€	n.a.	Yes	Roscoff Culture Collection
Emiliania huxleyi RCC 1235	17	K/2	Yes	France	30 ml - 50€	n.a.	Yes	Roscoff Culture Collection
Emiliania huxleyi RCC 1236	17	K/2	Yes	France	30 ml - 50€	n.a.	Yes	Roscoff Culture Collection

Emiliania huxleyi RCC 1237	17	K/2	Yes	France	30 ml - 50€	n.a.	Yes	Roscoff Culture Collection
Emiliania huxleyi RCC 1239	17	K/2	Yes	Japan	30 ml - 50€	2002	Yes	Roscoff Culture Collection
Emiliania huxleyi RCC 1240	17	K/2	Yes	Japan	30 ml - 50€	2002	Yes	Roscoff Culture Collection
Emiliania huxleyi RCC 1241	17	K/2	Yes	Japan	30 ml - 50€	2002	Yes	Roscoff Culture Collection
Emiliania huxleyi RCC 1245	17	K/2	Yes	France	30 ml - 50€	1999	Yes	Roscoff Culture Collection
Emiliania huxleyi RCC 1246	17	K/2	Yes	Spain	30 ml - 50€	1999	Yes	Roscoff Culture Collection
Emiliania huxleyi RCC 1247	17	K/2	Yes	Spain	30 ml - 50€	1999	Yes	Roscoff Culture Collection
Emiliania huxleyi RCC 1249	17	K/2	Yes	Spain	30 ml - 50€	1998	Yes	Roscoff Culture Collection
Emiliania huxleyi RCC 1250	17	K/2	Yes	Mediterranean Sea	30 ml - 50€	1999	No	Roscoff Culture Collection
Emiliania huxleyi RCC 1251	17	K/2	Yes	Portugal	30 ml - 50€	1999	Yes	Roscoff Culture Collection
Emiliania huxleyi RCC 1252	17	K/2	Yes	Japan	30 ml - 50€	2002	Yes	Roscoff Culture Collection
Emiliania huxleyi RCC 1253	17	K/2	Yes	Japan	30 ml - 50€	2002	Yes	Roscoff Culture Collection
Emiliania huxleyi RCC 1254	17	K/2	Yes	Mediterranean Sea	30 ml - 50€	1999	Yes	Roscoff Culture Collection
Emiliania huxleyi RCC 1258	17	K/2	Yes	Portugal	30 ml - 50€	1998	Yes	Roscoff Culture Collection
Emiliania huxleyi RCC 1261	17	K/2	Yes	Spain	30 ml - 50€	1999	Yes	Roscoff Culture Collection
Emiliania huxleyi RCC 1322	17	K/2	Yes	Mediterranean Sea	30 ml - 50€	1998	No	Roscoff Culture Collection
Emiliania huxleyi RCC 1825	17	K/2	Yes	Mediterranean Sea	30 ml - 50€	2008	Yes	Roscoff Culture Collection
Emiliania huxleyi RCC 1812	17	K/2	Yes	Mediterranean Sea	30 ml - 50€	2008	Yes	Roscoff Culture Collection
Emiliania huxleyi RCC 1813	17	K/2	Yes	Mediterranean Sea	30 ml - 50€	2008	Yes	Roscoff Culture Collection
Emiliania huxleyi RCC 1814	17	K/2	Yes	Mediterranean Sea	30 ml - 50€	2008	Yes	Roscoff Culture Collection
Emiliania huxleyi RCC 1815	17	K/2	Yes	Mediterranean Sea	30 ml - 50€	2008	Yes	Roscoff Culture Collection
Emiliania huxleyi RCC 1816	17	K/2	Yes	Mediterranean Sea	30 ml - 50€	2008	Yes	Roscoff Culture Collection
Emiliania huxleyi RCC 1817	17	K/2	Yes	Mediterranean Sea	30 ml - 50€	2008	Yes	Roscoff Culture Collection
Emiliania huxleyi RCC 1818	17	K/2	Yes	Mediterranean Sea	30 ml - 50€	2008	Yes	Roscoff Culture Collection

Emiliania huxleyi RCC 1819	17	K/2	Yes	Mediterranean Sea	30 ml - 50€	2008	Yes	Roscoff Culture Collection
Emiliania huxleyi RCC 1820	17	K/2	Yes	Mediterranean Sea	30 ml - 50€	2008	Yes	Roscoff Culture Collection
Emiliania huxleyi RCC 1821	17	K/2	Yes	Mediterranean Sea	30 ml - 50€	2008	Yes	Roscoff Culture Collection
Emiliania huxleyi RCC 1822	17	K/2	Yes	Mediterranean Sea	30 ml - 50€	2008	Yes	Roscoff Culture Collection
Emiliania huxleyi RCC 1823	17	K/2	Yes	Mediterranean Sea	30 ml - 50€	2008	Yes	Roscoff Culture Collection
Emiliania huxleyi RCC 1824	17	K/2	Yes	Mediterranean Sea	30 ml - 50€	2008	Yes	Roscoff Culture Collection
Emiliania huxleyi RCC 1826	17	K/2	Yes	Mediterranean Sea	30 ml - 50€	2008	Yes	Roscoff Culture Collection
Emiliania huxleyi RCC 1827	17	K/2	Yes	Mediterranean Sea	30 ml - 50€	2008	Yes	Roscoff Culture Collection
Emiliania huxleyi RCC 1828	17	K/2	Yes	Mediterranean Sea	30 ml - 50€	2008	Yes	Roscoff Culture Collection
Emiliania huxleyi RCC 1829	17	K/2	Yes	Mediterranean Sea	30 ml - 50€	2008	Yes	Roscoff Culture Collection
Emiliania huxleyi RCC 1830	17	K/2	Yes	Mediterranean Sea	30 ml - 50€	2008	Yes	Roscoff Culture Collection
Emiliania huxleyi RCC 1831	17	K/2	Yes	Mediterranean Sea	30 ml - 50€	2008	Yes	Roscoff Culture Collection
Emiliania huxleyi RCC 1832	17	K/2	Yes	Mediterranean Sea	30 ml - 50€	2008	Yes	Roscoff Culture Collection
Emiliania huxleyi RCC 1833	17	K/2	Yes	Mediterranean Sea	30 ml - 50€	2008	Yes	Roscoff Culture Collection
Emiliania huxleyi RCC 1834	17	K/2	Yes	Mediterranean Sea	30 ml - 50€	2008	Yes	Roscoff Culture Collection
Emiliania huxleyi RCC 1838	17	K/2	Yes	Mediterranean Sea	30 ml - 50€	2008	Yes	Roscoff Culture Collection
Emiliania huxleyi RCC 1839	17	K/2	Yes	Mediterranean Sea	30 ml - 50€	2008	Yes	Roscoff Culture Collection
Emiliania huxleyi RCC 1840	17	K/2	Yes	Mediterranean Sea	30 ml - 50€	2008	Yes	Roscoff Culture Collection
Emiliania huxleyi RCC 1845	17	K/2	Yes	Mediterranean Sea	30 ml - 50€	2008	Yes	Roscoff Culture Collection
Emiliania huxleyi RCC 1846	17	K/2	Yes	Mediterranean Sea	30 ml - 50€	2008	Yes	Roscoff Culture Collection
Emiliania huxleyi RCC 1847	17	K/2	Yes	Mediterranean Sea	30 ml - 50€	2008	Yes	Roscoff Culture Collection
Emiliania huxleyi RCC 1848	17	K/2	Yes	Mediterranean Sea	30 ml - 50€	2008	Yes	Roscoff Culture Collection

Emiliania huxleyi RCC 3484	22	K/2	Yes	Japan	30 ml - 50€	2011	No	Roscoff Culture Collection
Emiliania huxleyi RCC 3485	22	K/2	Yes	Japan	30 ml - 50€	2011	No	Roscoff Culture Collection
Emiliania huxleyi RCC 3487	22	K/2	Yes	Japan	30 ml - 50€	2011	No	Roscoff Culture Collection
Emiliania huxleyi RCC 3488	22	K/2	Yes	Japan	30 ml - 50€	2011	No	Roscoff Culture Collection
Emiliania huxleyi RCC 3490	22	K/2	Yes	Japan	30 ml - 50€	2011	No	Roscoff Culture Collection
Emiliania huxleyi RCC 3491	22	K/2	Yes	Japan	30 ml - 50€	2011	No	Roscoff Culture Collection
Emiliania huxleyi RCC 3492	22	K/2	Yes	Japan	30 ml - 50€	2011	No	Roscoff Culture Collection
Emiliania huxleyi RCC 3493	22	K/2	Yes	Japan	30 ml - 50€	2011	No	Roscoff Culture Collection
Emiliania huxleyi RCC 3496	22	K/2	Yes	Japan	30 ml - 50€	2011	No	Roscoff Culture Collection
Emiliania huxleyi RCC 3497	22	K/2	Yes	Japan	30 ml - 50€	2011	No	Roscoff Culture Collection
Emiliania huxleyi RCC 3498	22	K/2	Yes	Japan	30 ml - 50€	2011	No	Roscoff Culture Collection
Emiliania huxleyi RCC 3499	22	K/2	Yes	Japan	30 ml - 50€	2011	No	Roscoff Culture Collection
Emiliania huxleyi RCC 3500	22	K/2	Yes	Japan	30 ml - 50€	2011	No	Roscoff Culture Collection
Emiliania huxleyi RCC 3716	17	K/2	Yes	Japan	30 ml - 50€	2011	No	Roscoff Culture Collection
Emiliania huxleyi RCC 3730	17	K/2	Yes	Japan	30 ml - 50€	2011	No	Roscoff Culture Collection
Emiliania huxleyi RCC 3731	17	K/2	Yes	Japan	30 ml - 50€	2011	No	Roscoff Culture Collection
Emiliania huxleyi RCC 3732	17	K/2	Yes	Japan	30 ml - 50€	2011	No	Roscoff Culture Collection
Emiliania huxleyi RCC 4097	20	K	Yes	Japan	30 ml - 50€	2013	No	Roscoff Culture Collection
Emiliania huxleyi RCC 4443	15	L1	Yes	Peru	30 ml - 50€	2014	No	Roscoff Culture Collection
Emiliania huxleyi RCC 4498	20	K	Yes	Japan	30 ml - 50€	2013	No	Roscoff Culture Collection
Emiliania huxleyi RCC 4534	17	K/2	Yes	Canary Islands	30 ml - 50€	2014	No	Roscoff Culture Collection
Emiliania huxleyi RCC 4535	17	K/2	Yes	Canary Islands	30 ml - 50€	2014	No	Roscoff Culture Collection
Emiliania huxleyi RCC 4536	17	K/2	Yes	Canary Islands	30 ml - 50€	2014	No	Roscoff Culture Collection
Emiliania huxleyi RCC 4537	17	K/2	Yes	Canary Islands	30 ml - 50€	2014	No	Roscoff Culture Collection
Emiliania huxleyi RCC 4538	17	K/2	Yes	Canary Islands	30 ml - 50€	2015	No	Roscoff Culture Collection
Emiliania huxleyi RCC 4539	17	K/2	Yes	Canary Islands	30 ml - 50€	2014	No	Roscoff Culture Collection

Emiliania huxleyi RCC 4540	17	K/2	Yes	Canary Islands	30 ml - 50€	2014	No	Roscoff Culture Collection
Emiliania huxleyi RCC 4541	17	K/2	Yes	Canary Islands	30 ml - 50€	2014	No	Roscoff Culture Collection
Emiliania huxleyi RCC 4542	17	K/2	Yes	Canary Islands	30 ml - 50€	2014	No	Roscoff Culture Collection
Emiliania huxleyi RCC 4543	17	K/2	Yes	Canary Islands	30 ml - 50€	2014	No	Roscoff Culture Collection
Emiliania huxleyi RCC 4544	17	K/2	Yes	Canary Islands	30 ml - 50€	2014	No	Roscoff Culture Collection
Emiliania huxleyi RCC 4545	17	K/2	Yes	Canary Islands	30 ml - 50€	2014	No	Roscoff Culture Collection
Emiliania huxleyi RCC 4546	17	K/2	Yes	Canary Islands	30 ml - 50€	2014	No	Roscoff Culture Collection
Emiliania huxleyi RCC 4547	17	K/2	Yes	Canary Islands	30 ml - 50€	2014	No	Roscoff Culture Collection
Emiliania huxleyi RCC 4549	20	K	Yes	Atlantic Ocean	30 ml - 50€	2014	No	Roscoff Culture Collection
Emiliania huxleyi RCC 4560	20	K	Yes	Atlantic Ocean	30 ml - 50€	2014	No	Roscoff Culture Collection
Emiliania sp. RCC 4567	20	K	Yes	Atlantic Ocean	30 ml - 50€	2014	No	Roscoff Culture Collection

Supplementary Data 3 – Effect of ethanol (A), ethyl acetate (B) and water extract (C) on the osteogenic development of zebrafish' head (corrected head area). Ethanol, DMSO and distilled water (DW) were used as negative controls and vitamin D as a positive control (lined columns). Values are presented as the mean ± standard deviation.